2011

Characterization of cyclic-di-GMP signaling with the Lyme spirochete, Borrelia burgdorferi

Jessica Kostick
Virginia Commonwealth University

CHARACTERIZATION OF CYCLIC-DI-GMP SIGNALING WITHIN THE LYME SPIROCHETE, *BORRELIA BURGDORFERI*

A dissertation submitted in partial fulfillment of the requirements for the degree of Doctor of Philosophy at Virginia Commonwealth University

by

JESSICA LYNN KOSTICK
Bachelor of Art, University of Delaware, 2006

Advisor: Richard T. Marconi, PhD
Professor
Department of Microbiology & Immunology

Virginia Commonwealth University
Richmond, Virginia
September, 2011

ACKNOWLEDGEMENT

I would like to recognize some of the individuals who have provided guidance and assistance throughout my graduate education. I would like to foremost acknowledge my advisor and mentor, Dr. Richard Marconi, for his guidance and support throughout this project. I especially am thankful for the freedom he provided me to independently explore and develop my work.

I also would like to thank my graduate committee: Drs. Kimberely Jefferson, Todd Kitten, Tomasz Kordula, and Masoud Manjili for contributing their time and scientific expertise for my scientific development.

I would like to thank the past and present members of the Marconi laboratory I had the distinct pleasure to work with over the course of my education at VCU: Dr. Christopher Earnhart, Lindy Fine, Dr. Jesse Frederick, John Courtland Freedman, Katherine Mallory, Dr. John McDowell, Daniel Miller, Emily Moser, Delacy LeBlanc Rhodes, Dr. Elizabeth Abdunnur, Juni Sarkar, Laura Shelton, Dr. Lee Szkotnicki, and Dr. Hongming Zhang. I especially want to thank Dr. Earnhart and Dr. Szkotnicki for their valued advice and assistance with this project, as well as thank Dr. Elizabeth Abdunnur for her all her work introducing this study into the Marconi laboratory.

Lastly, I would like to show appreciation to all my friends and family who have been my constant source of support during my graduate school journey. Thank you for your patience and understanding of my unyielding schedule, as well as much needed encouragement along the way. I am also deeply grateful for my friendship with Dr. Jill Callahan and Dr. Lisa Shock, as they have been my partners in crime throughout this experience.

Publisher permission has been granted for reuse of copyrighted figures and text utilized in this dissertation through the Copyright Clearance Center. The license numbers are as follows: 2746620818621, 2746601365090, 2746610964543, 2746611087934, 2746610054606, 2746610535309, 2746610336621.

TABLE OF CONTENTS

LIST OF TABLES

Page

LIST OF FIGURES

ABREVIATIONS

AA	amino acid
ABTS	2,2'-azino-bis(3-ethylbenzothiazoline-6-sulphonic acid)
ACA	Acrodermatitis chronicum atrophicans
ANOVA	Analysis of variance
B. afzelii	*Borrelia afzelii*
B. burgdorferi	*Borrelia burgdorferi*
B. garinii	*Borrelia garinii*
bp	base pair
BSK	Barbour-Stoenner-Kelly medium
CDC	Centers for Disease Control and Prevention
C-di-GMP	Bis-(3'-5')-cyclic-dimeric guanosine monophosphate
ºC	Degrees celcius
cDNA	Complementary DNA
DGC	Diguanylate cyclase
DIC	Differential interference contrast microscopy
DNA	deoxyribonucleic acid
ELISA	Enzyme-linked immunosorbent assay
EM	Erythema migrans
Eno	Enolase

FlaB	Flagellin protein
FlgB	Flagellar basal body rod protein
FRET	Fluorescence resonance energy transfer
GEMM	Genes for the environment, for membranes, and for motility
GTP	Guanosine-5'-triphosphate
hr	Hour
Hpk1	Histidine sensor kinase 1
HPLC	High-performance liquid chromatography
IgG	Immunoglobulin G
IPTG	isopropylthio-β-D-galactoside
Kan	Kanamycin
kb	Kilobase
µg	Microgram
µl	Microliter
µM	Micromolar
ml	Milliliter
mm	Millimeter
mM	Millimolar
min	Minute
mRNA	Messenger RNA
M	Molar
NAG	N-acetyl-D-glucosamine
NagA	NAG-6-phosphate deaminase

NagB	Glucosamine-6-phosphate-isomerase
ng	Nanogram
Ω	Ohms
OD	Optical density
ORF	Open reading frame
pmol	Picomolar
PBS	Phosphate buffered saline
PBS-T	Phosphate buffered saline-Tween 20
PCR	Polymerase chain reaction
PDE	Phosphodiesterase
PdeA	Phosphodiesterase A
PdeB	PhosphodiesteraseB
PlzA	PilZ domain-containing protein A
PlzB	PilZ domain-containing protein B
PtsG	PTS system, glucose-specific IIBC component
PVDF	Polyvinylidene difluoride
qPCR	Quantitative polymerase chain reaction
RBS	Ribosome binding site
rDNA	Ribosomal DNA
RNA	Ribonucleic acid
Rrp1	Response regulator protein 1
RT	Room temperature
RT-PCR	Reverse transcriptase polymerase chain reaction

SDS-PAGE	Sodium dodecyl sulfate-polyacrylamide gel electrophoresis
sec	Second
Spec	Spectinomycin
Strep	Streptomycin
V	Volts
wt/vol	Weight/volume

ABSTRACT

CHARACTERIZATION OF CYCLIC-DI-GMP SIGNALING WITHIN THE LYME SPIROCHETE, *BORRELIA BURGDORFERI*

By Jessica L. Kostick, Ph.D.

A dissertation submitted in partial fulfillment of the requirements for the degree of Doctor of Philosophy at Virginia Commonwealth University

Virginia Commonwealth University, 2011

Major Director: Richard T. Marconi, Ph.D.
Professor, Department of Microbiology and Immunology

Lyme disease is a tick-borne infection caused by *Borrelia burgdorferi, B. garinii,* and *B. afzelii.* These spirochetes experience environmental fluctuations as they are passed between mammalian and *Ixodes* tick hosts throughout their enzootic cycle. Recent studies have suggested cyclic diguanylate (c-di-GMP), a ubiquitous secondary messenger, is a key modulator of *B. burgdorferi* adaptive responses and may play a significant role in cycle progression. In this study, we examined the impact of the sole diguanylate cyclase (Rrp1), c-di-GMP binding proteins (PlzA and PlzB), and HD-GYP-containing phosphodiesterase (PdeB) in disease establishment of both murine and *Ixodes* tick systems. Strains harboring targeted gene deletions or plasmid-based constitutive gene expression constructs were generated.

Rrp1 was required for tick colonization, yet overexpression abolished murine disease, thus implicating the requirement of finely regulated c-di-GMP levels for enzootic cycle progression. Deletion of *rrp1* disrupted translational motion and swarming patterns by causing extended cell runs, eliminating stops/flexes, and reducing swarming capabilities. This was attributed to a defect in N-acetyl-D-glucosamine (NAG) metabolism and chemotaxis. NAG is a major source of nutrition for *B. burgdorferi* within the tick environment; therefore this defect would impede spirochete migration towards feeding ticks, as well as pathogen uptake and survival within the *Ixodes* vector.

In contrast, the downstream c-di-GMP effector, PlzA, was critical for murine disease but nonessential for survival within ticks nor functionally complemented by PlzB. Deletion of *plzA* altered strain motility and swarming similarly to the *rrp1* deletion mutant, yet had a distinct phenotype with significantly slower translational motion and no affect on NAG chemotaxis and metabolism. This indicates *B. burgdorferi* could possess alternate c-di-GMP effectors or Rrp1 could be directly influencing these cellular processes.

Uniquely, PdeB did not abolish murine infection via needle inoculation, but was required for natural transmission from ticks. This defect was linked to the decreased tick colonization efficiency upon *pdeB* deletion.

Together, these analyses indicate that c-di-GMP signaling is an important virulence mechanism of *Borrelia burgdorferi* and demonstrate the complexity of this signaling pathway in an arthropod-borne pathogen. The data presented here additionally provide significant new insight into the gene regulatory mechanisms of the Lyme disease spirochetes.

CHAPTER 1: INTRODUCTION & OVERVIEW

Lyme disease is an important emerging infection that plagues multiple continents throughout the world. Currently, it is the most common arthropod-borne illness in North America and Europe, but cases have also been reported in Asia (32). According to the Centers for Disease Control (CDC), this infection was named the 6th most common national notifiable disease in 2008 and the incidence continues to grow at a rapid pace. Approximately 39,000 cases were reported nationally in 2009, yet this estimate is believed to be an underrepresentation of the true number of cases due to misdiagnosis and lack of reporting (108). A United States incidence map schematic is depicted in Figure 1-1. Connecticut is the epicentre for contraction of Lyme disease but, as reported by the CDC, ninety-five percent of the total cases typically arise from twelve key states including: Connecticut, Delaware, Maine, Maryland, Massachusetts, Minnesota, New Hampshire, New Jersey, New York, Pennsylvania, Virginia, and Wisconsin.

The disease was first recognized in 1976 when juvenile rheumatoid arthritis symptoms plagued adolescent residents of the small town Lyme, Connecticut (92). It later became apparent that the symptoms were merely a late stage manifestation of a multi-system disorder initiated by a tick-transmitted disease (90). However, the cause of infection remained elusive until 1981, when Dr. Willy Burgdorfer and colleagues discovered spirochetes within *Ixodes* tick midguts isolated from Shelter Island, NY (13).

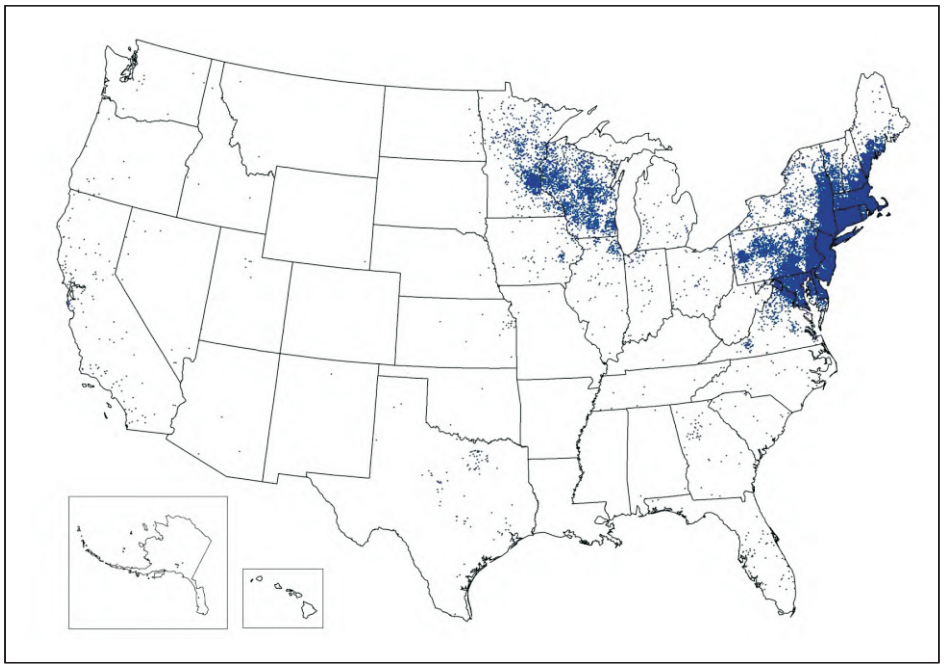

http://www.cdc.gov/lyme/stats/index.html

Figure 1-1. 2009 United States Lyme incidence map. Each dot represents a reported case of Lyme disease and is placed within the patient's county of residence. As evident by the dense clustering, Lyme disease is the most prevalent within the Northeastern United States and the Minnesota/Wisconsin region.

Ticks samples were cultured in media intended for the growth of relapsing fever spirochetes, but to the investigators' surprise, a new species of *Borrelia* appeared in the samples. The species, designated *Borrelia burgdorferi*, was thereafter identified in Lyme disease patient samples and concluded to be the disease-causing pathogen (10,13,91). Many patient symptoms, world-wide, were wrongfully misdiagnosed and symptoms ascribed to unknown viruses, etc. Therefore, this discovery represented a breakthrough in modern infectious disease medicine.

Many species related to *B. burgdorferi* have been identified to cause *Borreliosis*-like symptoms, including *B. garinii* and *B. afzelii,* which are broadly termed *B. burgdorferi sensu lato* (5). The main causative agent within the United States is the species *B. burgdorferi* specifically, which is referred to as *B. burgdorferi sensu stricto.* Acquisition of this pathogen occurs by the bite of an infected *Ixodes* tick, then spirochetes disseminate laterally through host tissues (72,90). Acute symptoms include the characteristic erythema migrans rash (EM) followed by fever, headache, arthralgia, and myalgia (88). Early treatment with oral antibiotics such as doxycycline, amoxicillin, or cefuroxime axetil is extremely effective and patients typically recover quickly and completely. Without antibiotics, the infection persists and disseminates into chronic stage Lyme disease with severe neurological, rheumatological, and dermatological complications such as *Borrelial* lymphocytoma, Bell's palsy, and Acrodermatitis chronica atrophicans (88). According to the CDC, prevention is solely based upon avoidance of tick habitat, wearing protective clothing, and early detection of symptoms followed by antibiotic administration. The lack of a commercially available vaccine, incidence climb, and low rate of prevention with current techniques demonstrate that more aggressive

methods of prevention and control are essential to combat the significant health risk imposed by Lyme disease. Complete analysis of the molecular mechanisms involved in the *Borrelia* enzootic cycle is a critical step to understanding and limiting infection.

The enzootic cycle of *Borrelia burgdorferi*

The Lyme species of *Borrelia* are maintained within an enzootic cycle consisting of ticks from the *Ixodes ricinus* complex and a wide range of animal hosts (Table 1-1) (52,90). The cycles for each of the respective species has evolved to be location specific based upon host and tick availability (45). The most notable tick vectors of the three main pathogenic Lyme species are *I. scapularis* (deer tick, northeastern and north central US), *I. pacificus* (western US), *I. ricinus* (sheep tick, Europe), and *I. persulcatus* (taiga tick, Asia) (90). Interestingly, Lyme disease is most prevalent in the Northeastern and North central United States where *Borrelia burgdorferi* is very efficiently transmitted between *I. scapularis* ticks and mammals, specifically the white-footed mouse, chipmunks, and white-tailed deer (51). This trend is not seen in the western portion of the nation where *I. spinipalpis* ticks do not bite humans and *I. pacificus* ticks are less often infected (12,83). Humans are also inefficiently infected in the southeastern US due to the *I. scapularis* ticks feeding readily on lizards which are resistant to infection by complement-mediated killing of the pathogen (43). As a result, research targeting the pathogenesis of *B. burgdorferi* is aimed at understanding the enzootic cycle consisting of *I. scapularis* ticks and mammals, which is most often associated with human disease in the United States.

Table 1-1. Putative and named Lyme spirochetes.

Species (c/p)[a] (type strain)	Distribution	Host range	Main vector
B. afzelii (c) (VS461)	Europe, Asia	*Apodemus* spp., *Myodes glareolus*, *Sorex* spp., *Sciurus* spp., *Erinaceus* spp., *Rattus* spp.	*Ixodes ricinus*, *I. persulcatus*, *I. hexagonus*
B. americana (p) (SCW-41)	North America	*Thryothorus ludovicianus*, *Pipilo erythrophthalmus*	*I. pacificus*, *I. minor*
B. andersonii (c) (21038)	North America	*Sylvilagus* spp., *(Passeriformes* spp.*)*	*I. dentatus*
B. bavariensis (p) (PBi)	Europe, Asia (?)	*Apodemus* spp., *Myodes* sp., *Microtus* spp.	*I. ricinus*, *I. persulcatus*(?)
B. bissettii (c) (DN127-cl9-2)	North America, Europe	*Neotoma* spp., *Peromyscus* spp., *Sigmodon* spp. EU: unknown	*I. pacificus*, *I. spinipalpis*, *I. affinis*, EU: unknown
B. burgdorferi (c) (B31)	North America, Europe	*Peromyscus* spp., *Tamias* spp., *Neatoma* spp., *Sorex* spp., *Sciurus* spp., *Sigmodon* spp. *Erinaceus* spp., *Rattus* spp., *Procyon lotor*, *Turdus migratorius*,	*I. ricinus*, *I. hexagonus*, *I. scapularis*, *I. pacificus*, *I. affinis*, *I. minor*, *I. spinipalpis*, *I. muris*
B. californiensis (c) (CA446)	Western US	*Dipodomys californensis*	Unknown
B. carolinensis (c) (SCW-22)	Southeast US	*P. gossypinus*, *N. floridana*	Unknown (*I. minor*?)
B. garinii (c) (20047)	Europe, Asia, Artic-Antartic circles	*Turdus merula*, *T. philomelos*, Parus major, seabirds (Puffin, Guillemot, Kittiwake, Razorbill)	*I. ricinus*, *I. persulcatus*, *I. uriae*
B. japonica (c) (HO14)	Japan	*Sorex unguiculatus*, *Apodemus* spp., *Eothenomys smithi*	*I. ovatus*
B. kurtenbachii (p) (25015)	Northamerica, (Europe?)	*Microtus pennsylvanicus*, *Zapus hudsonius Peromyscus*?	Unknown (*I. scapularis*?)
B. lusitaniae (c) (PoTiB2)	Mediterranean basin	*Lacertidae*	*I. ricinus*
B. sinica (c) (CMN3)	China	*Niviventer confucianus*	*I. ovatus*
B. spielmanii (c) (PC-Eq17N5)	Europe	Glis glis, *Eliomus quercinus*	*I. ricinus*
B. tanukii (c) (Hk501)	Japan	*Apodemus* sp., *Clethrionomys rufocanus*, *Eothenomys smithii*	*I. tanuki*
B. turdi (c) (Ya501)	Japan	*Turdus* spp.	*I. turdus*
B. valaisiana (c) (VS116)	Europe, Japan	*Turdus merula*, *T. philomelos*, Parus major	*I. ricinus*, *I. columnae*
B. yangtze (c) (nd)	China	*Niviventer fulvescens*, *Apodemus* sp.	*I. granulatus*, *I. nipponensis*
Genomospecies2	United States	Unknown	*I. spinipalpis*, *I. pacificus*

[a] c – confirmed; p – proposed; nd = not determined.

Table adapted from Margos, G., et al. Infection, Genetics, and Evolution. 2011.

The spirochetes are transmitted between hosts at multiple time points throughout the two year cycle (Figure 1-2) (51,90). Eggs are laid by adult female ticks in the early spring and hatched by summer for the larval stage feeding on small mammals and deer, followed by an autumn molt into nymphs and a dormancy period until spring. In the second year, the nymphal ticks feed on small mammals, birds, and humans in the late spring which initiates the final molt into adults by summer. In fall or the next spring, the adults feed on large mammals (particularly deer), mate, and lay eggs to complete the cycle.

During host transmission and spirochete acquisition, the bacteria are exposed to a diverse set of environmental cues (8,12,30,39,89). The pathogen possesses a minimalist genome consisting of a 0.91Mb linear chromosome which contains a relatively small set of housekeeping genes and only a few biosynthesis and metabolism open reading frames (26). As a result, *B. burgdorferi* is dependent on the rich host environments to provide nutrients for survival and, as a consequence, alter their gene expression profiles in accordance to host conditions (80). The *Borrelia* transcriptome is responsive to temperatures experienced in the tick (25º) and mammal (37º) along with alterations in pH, immune pressure, nutrient availability, etc (11,15,24,5961,68). Typically, bacteria utilize a variety of signalling and transducing mechanisms to respond to external stimuli, however *Borrelia* systems remain relatively uncharacterized.

Two-component systems and cellular signalling.

A prominent mechanism of bacterial adaptive responses is the two-component regulatory system (TCS). These regulators can have global or targeted effects

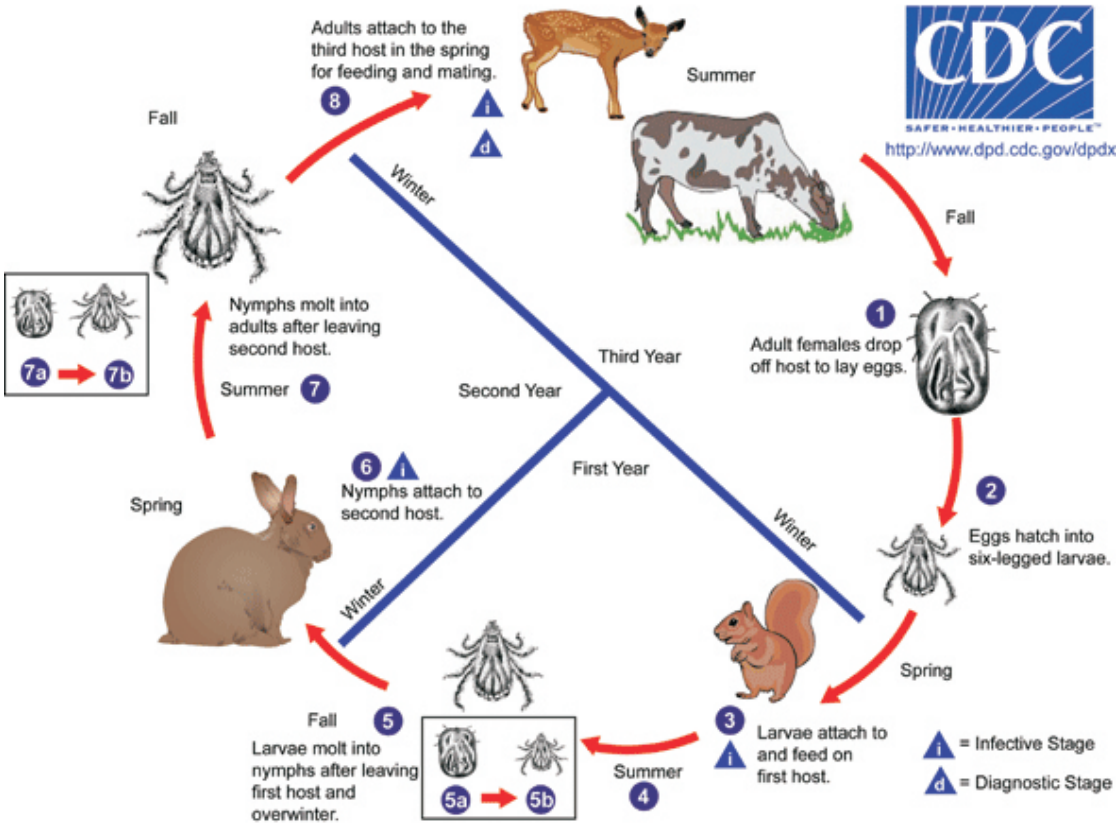

http://www.cdc.gov/lyme/stats/index.html

Figure 1-2. ***Borrelia burgdorferi*** **enzootic cycle.** The pathogen exists in a two year cycle involving the passage between a variety of hosts. Spirochete acquisition and transmission occurs through the bite of an infected *Ixodes* tick.

(16,70,105). Typically, TCS consist of a histidine kinase and a response regulator (94). The external stimuli are sensed through the N-terminal sensing domain of the histidine kinase to cause activation and ATP-dependent phosphorylation of the C-terminal cytoplasmic transmitter domain (106). The phosphoryl group of the transmitter domain is then transferred to the receiver domain of the response regulator. Upon transfer, the response regulator dimerizes and activates its output domain. Output domains can have a diverse range of functions including DNA-binding, RNA-binding, protein-binding, or enzymatic functions (29,48,85). Most bacteria contain numerous TCS such as *Vibrio cholera*, which alone encodes more than twenty-five (29). Genomic analysis of *B. burgdorferi* B31MI revealed approximately five TCS with only two holding global regulatory potential (70,107). The others have mainly motility and chemotaxis functionality (26,56,57). The systems demonstrated to have a role in global regulation are Hpk2-Rrp2 and Hpk1-Rrp1. The Hpk2-Rrp2 TCS was the first system characterized in *Borrelia*, consisting of the histidine protein kinase 2 (Hpk2) and response regulatory protein 2 (Rrp2) (107). Rrp2 contains a DNA-binding helix-turn-helix domain which regulates primarily plasmid-based genes including virulence factors such as OspC and DbpA (14,36).

In contrast, the Hpk1-Rrp1 TCS is not well understood. This system contains the histidine kinase-response regulator receiver protein 1(Hpk1; BB0420) and the response regulator protein 1(Rrp1; BB0419) (70). Hpk1 is the proposed activator of the system, but cooperation between these proteins has never been demonstrated. Unlike Rrp2, Rrp1 lacks a DNA-binding output domain but contains a GGD/EEF enzymatic domain which possesses diguanylate cyclase activity to convert two molecules of GTP to cyclic

diguanylate (c-di-GMP), an important bacterial secondary messenger (3,28,29,37). In vitro diguanylate cyclase activity of Rrp1 has been demonstrated using recombinant Rrp1 to produce c-di-GMP in a phosphorylation dependent manner (Figure 1-3) (27,77), but in vivo activity has never been investigated.

Cyclic-di-GMP.

C-di-GMP is a ubiquitious signaling molecule utilized in a variety of bacterial systems such as *Vibrio, Escherchia, Pseudomonas,* and *Salmonella* (9,11,49,53,65,99,102). Modifications of intracellular c-di-GMP pools impact many cellular processes including biofilm formation, virulence and persistence, motility/chemotaxis, quorum sensing, et cetera (Figure 1-4) (34). High intracellular c-di-GMP has generally been associated with increased biofilm production, sessility, and persistence as a result of increased expression of exopolysaccharide in *Vibrio* and adhesive fimbrae in *Pseudomonas* and *Salmonella* (38,42,101). In contrast, low intracellular c-di-GMP promotes motility and virulence (86,100).

The dinucleotide is highly regulated by two opposing activities: biosynthesis and hydrolysis. Synthesis is catalyzed by the diguanylate cyclase (DGC), while phosphodiesterases (PDE) harboring EAL and/or HD-GYP domains hydrolyze c-di-GMP via linear pGpG to two molecules of GMP (17,19,73,77,82,99). These proteins are typically functionally redundant in many pathogens and greatly complicate research schemes for understanding the full biological impact of c-di-GMP signaling (37). However, *Borrelia* possess only one genomic copy of each of the c-di-GMP network proteins including the diguanylate cyclase (Rrp1), EAL and HD-GYP

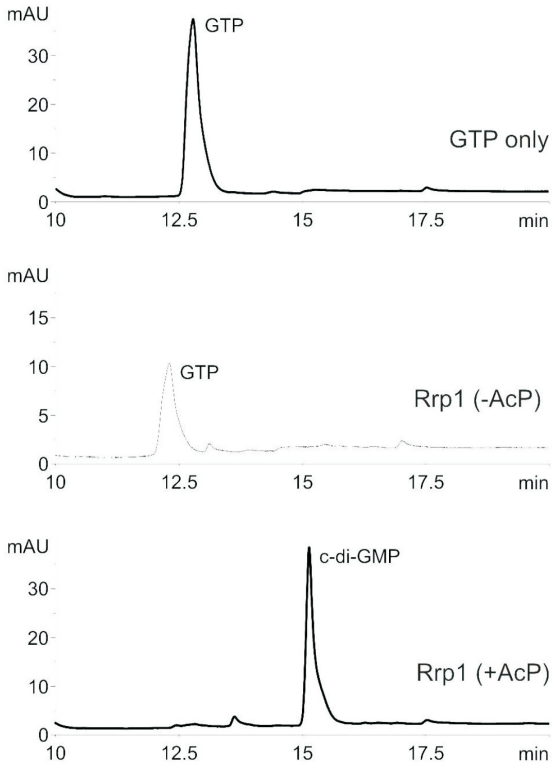

Figure 1-3. C-di-GMP synthesis by r-Rrp1. Recombinant Rrp1 was incubated with or without acetyl phosphate prior to the addition of GTP. Resulting nucleotides were analyzed by HPLC to assess Rrp1 activation and production of c-di-GMP.

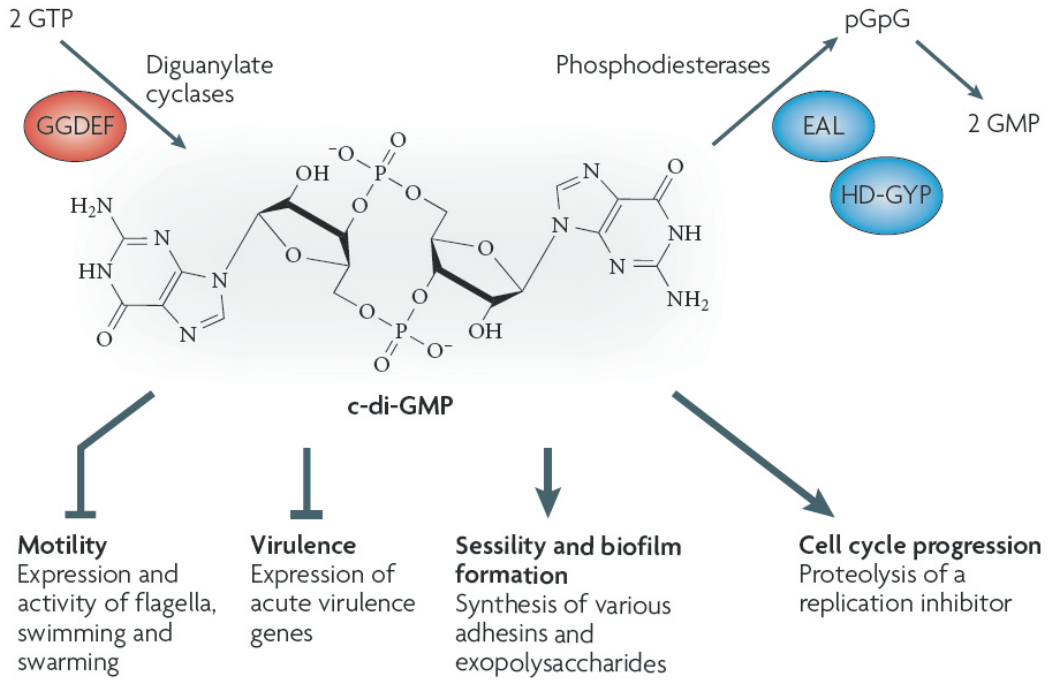

Figure 1-4. C-di-GMP regulation of bacterial cellular processes. Fluctuation of intracellular c-di-GMP levels has been demonstrated to inversely regulate cellular states by promoting sessility and biofilm formation in high c-di-GMP conditions and enhancing motility and virulence during low c-di-GMP levels.

phosphodiesterases (PdeA and PdeB, respectively), as well as one identified c-di-GMP-binding protein (PlzA) (27,41,63,70,96,97). The genes that encode each of these proteins are also universally distributed throughout Lyme spirochetes species (Figure 1-5). Consequently, these organisms provide a simplified and ideal model to study bacterial c-di-GMP signaling without redundancy complications. A representative schematic of the hypothesized *Borrelial* c-di-GMP network is presented in Figure 1-6.

Recent studies suggest that c-di-GMP is a key regulator of *B. burgdorferi* adaptive responses and may play an important role in the enzootic cycle (27,63,70,77,97). The global regulatory ability of Rrp1, and by extension c-di-GMP, was revealed through microarray analysis of an *rrp1* deletion mutant (70). The Rrp1 regulon, which consists of ~10% of the genome, includes genes that encode proteins spanning a wide range of functional categories with a concentration on motility, chemotaxis, and metabolism (Figure 1-7). Several of the Rrp1 regulated genes encode proteins that are likely to be in involved in the enzootic cycle. In addition, qRT-PCR analysis of infected flat and fed ticks revealed that *rrp1* expression is upregulated 6-fold in fed ticks, indicating that Rrp1 may have an important role in cycle progression particularly from *Ixodes* ticks to mammalian hosts (70).

As in other bacterial systems, c-di-GMP levels in *B. burgdorferi* are thought to be controlled by the opposing activities of diguanylate cyclases and phosphodiesterases. *Borrelia* strains encode an EAL domain phosphodiesterase (PdeA) and HD-GYP domain phosphodiesterase (PdeB) (70,77,97). Both proteins are active PDEs within *B. burgdorferi* and in vitro assays revealed the pathogen does not possess any other proteins which hydrolyze c-di-GMP (96). In vivo, PdeA and PdeB are necessary for

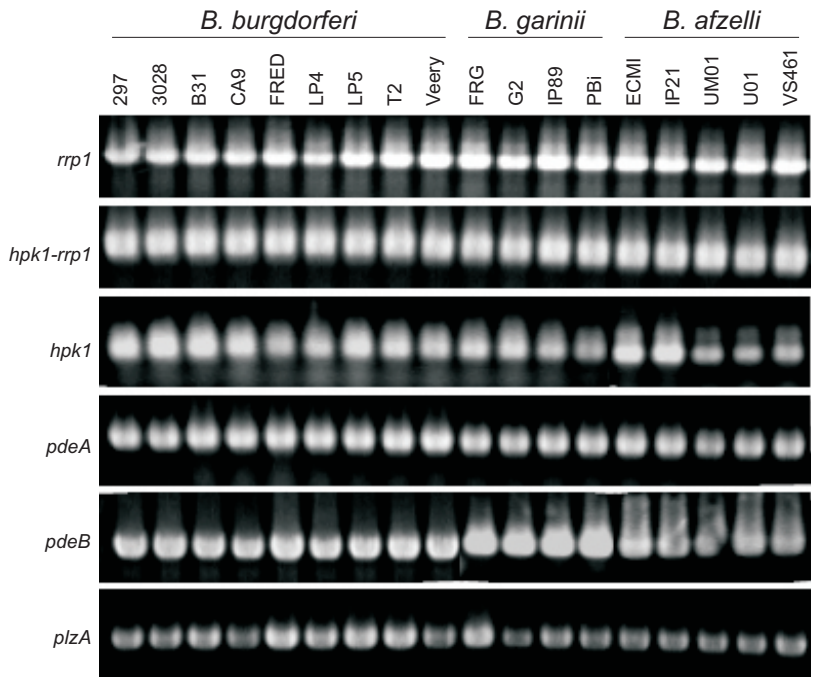

Figure 1-5. Universal distribution of the Lyme spirochete c-di-GMP network. Each component of the putative *Borrelia* c-di-GMP network was PCR amplified from various isolate samples of *B. burgdorferi sensu stricto* and *sensu lato* species. Isolate designations are listed immediately below species name and amplicon identification is located left of the panel.

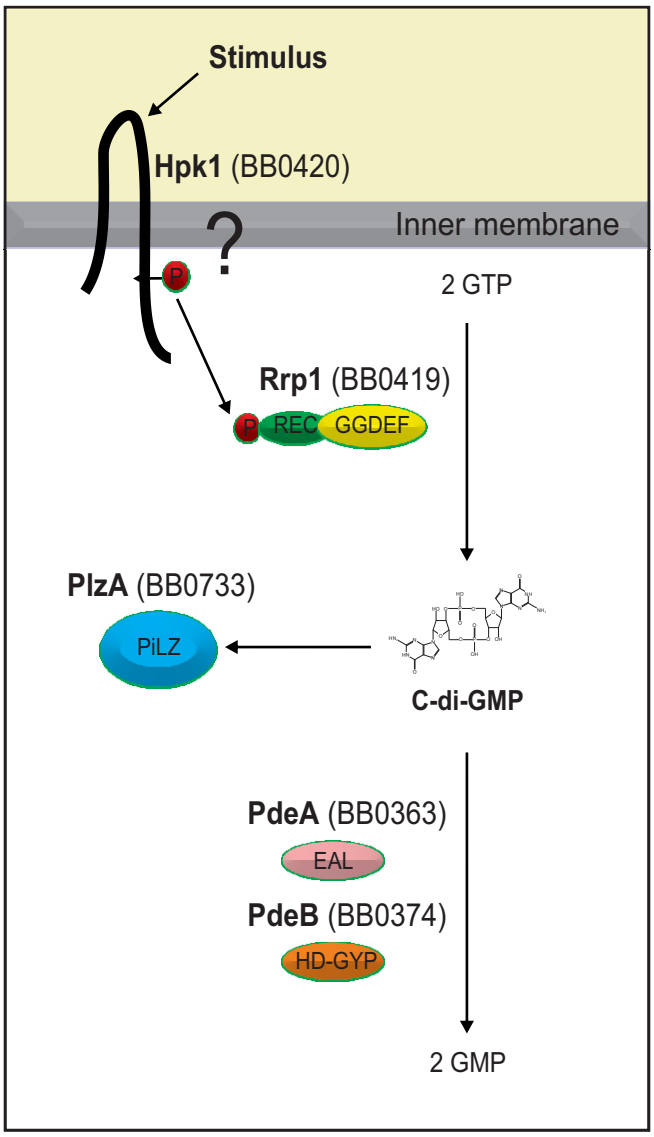

Figure 1-6. *Borrelia burgdorferi* c-di-GMP signaling network. C-di-GMP is controlled and balance by the opposing biosynthesis and hydrolysis activities of the diguanylate cyclase (Rrp1) and phosphodiesterases (PdeA and PdeB), respectively. Functional output of the system occurs by direct or indirect regulation by these proteins and by c-di-GMP effectors. To date, PlzA is the only identified effector in *Borrelia*.

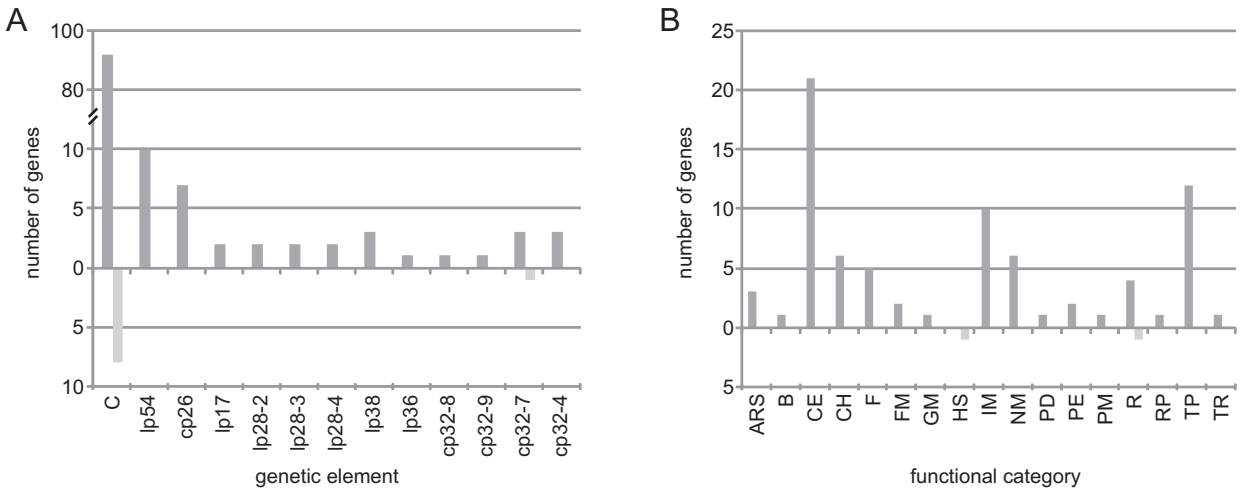

Figure 1-7. Rrp1 is a central regulator of the core *Borrelia* genome. Microarray analysis of B31-5A13 wild type and *rrp1* deletion strains revealed nearly 150 genes are significantly regulated by Rrp1 ($p<0.05$) of which 84% are located on 3 genetic elements that make up the core *Borrelia* genome (chromosome, lp54, cp26). The genes regulated by Rrp1 have been organized by their genetic location (panel A) and by functional category (panel B). Abbreviations: C, chromosome; ARS, amino acid biosynthesis; B, biosynthesis; CE, cell envelope; CH, chemotaxis; F, flagellar biosynthesis; FM, fatty acid metabolism; GM, general metabolism; HS, heat shock; IM, intracellular metabolism; NM, nucleotide metabolism; PD, protein degradation; PE, protein export; PM, protein metabolism; R, replication; RP, ribosomal proteins; TP, transport; TR, transcription. Number of genes which are expressed at a higher or lower level in the *Bb*5A13-Δ*rrp1* strain relative to *Bb*5A13-wt are indicated by the light or dark grey bars, respectively.

enzootic cycle progression. Inactivation of PdeA abolishes murine infection by both needle inoculation and natural tick feeding, but tick colonization capabilities are retained (97). However, PdeB is only required for tick to mouse spirochete transfer (96). This further supports c-di-GMP signaling as an important regulator of Lyme pathogenesis and verifies the specific role of the network in spirochete host transitions. Successful quantitation of spirochete intracellular c-di-GMP levels has yet to be completed to link PDE virulence phenotypes directly to fluctuations in c-di-GMP cellular pools; however this data identifies the need to investigate the direct or indirect mechanisms by which these proteins are applying their effects.

Little is known regarding the effector mechanisms of c-di-GMP in the Lyme disease spirochetes and arthropod-borne pathogens in general. In other bacterial systems, c-di-GMP has been shown to exert its regulatory effects by interacting with several different effector molecules including GEMM riboswitches (87,95), PilZ domain-containing proteins (1,76), ribonucleoprotein complexes (103), and cyclic monophosphate domains (35). Two PilZ domain-containing proteins (PlzA and PlzB) have been identified in *Borrelia* strains, each possessing the RxxxR and DzSxxG motifs associated with c-di-GMP binding (27). All strains produce the chromosomally encoded PlzA protein, while a subset of strains carry the second gene encoding PlzB on a variably sized linear plasmid. To date, only PlzA has been demonstrated to bind c-di-GMP in a highly specific manner (Figure 1-8) (27) and shown to be essential for mammalian disease and proper swarming (63). PlzB remains completely uncharacterized and the effector functions of both PilZ domain-containing proteins have not been defined.

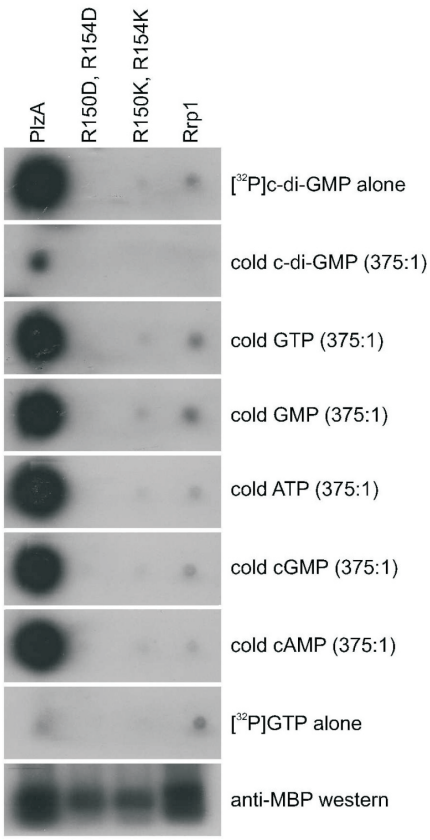

Figure 1-8. C-di-GMP binds PlzA. Recombinant PlzA with a N-terminal maltose-binding protein fusion was generated. In addition, point mutants possessing either a arginine to aspartic acid or lysine change of both arginine residues within the RxxxR c-di-GMP binding motif were created to evaluate PlzA binding to [α-^{32}P] c-di-GMP. Proteins were spotted on nitrocellulose and incubated with the competing nucleotide and respective ratio listed on the right (competing nucleotide to radiolabelled c-di-GMP). r-Rrp was included as a negative control and a anti-MBP immunoblot was performed to assess loading. PlzA bound c-di-GMP with high specificity and disruption of the RxxxR motif abrogated this interaction.

Spirochete motility.

Spirochete migration through tissues is caused by the corkscrew-like motion driven by the flagellar motors (80). Each spirochete harbors two periplasmic flagellar bundles (consisting of 7-11 individual flagella structures) which anchor in the cytoplasmic membrane and wrap around the protoplasmic cylinder (Figure 1-9A) (72). A motor is located at each pole to coordinate flagellar rotation in opposite directions to produce translational motion (runs and reverses) or rotation in the same direction to cause cellular flexing (Figure 1-9B) (50). However, this translational motion pattern is quite different from other pathogens which can only run and tumble, such as *E. coli* and *Salmonella.* Runs are generated in these bacterial systems by flagellar counter-clockwise rotation, while tumbles are produced by a direction reversal to clockwise flagellar rotation (50).

Regulation of the motor rotation is controlled through the C-ring (flagellar motor switch) which is composed of FliG, FliM, and FliN (50). This complex interacts with the stator to energize rotation of the flagellar rotor (31). *Borrelia* possess two FliG proteins (FliG1 and FliG2) instead of a singular FliG (26). FliG2 is believed to be equivalent to the FliG protein of other bacterial systems, while FliG1 only localizes to one pole and its function remains unknown (47).

Motility is a cellular process often affected by c-di-GMP signalling and c-di-GMP has been identified to modulate flagellar motor control in *E. coli* and *Salmonella* (62). The PilZ domain-containing protein, YcgR, has been shown to bind c-di-GMP and to the flagellar motor switch (31). Inactivation of the protein suppresses a motility defect (constant flagellar counter-clockwise rotation) initiated by the deletion of the EAL

A.

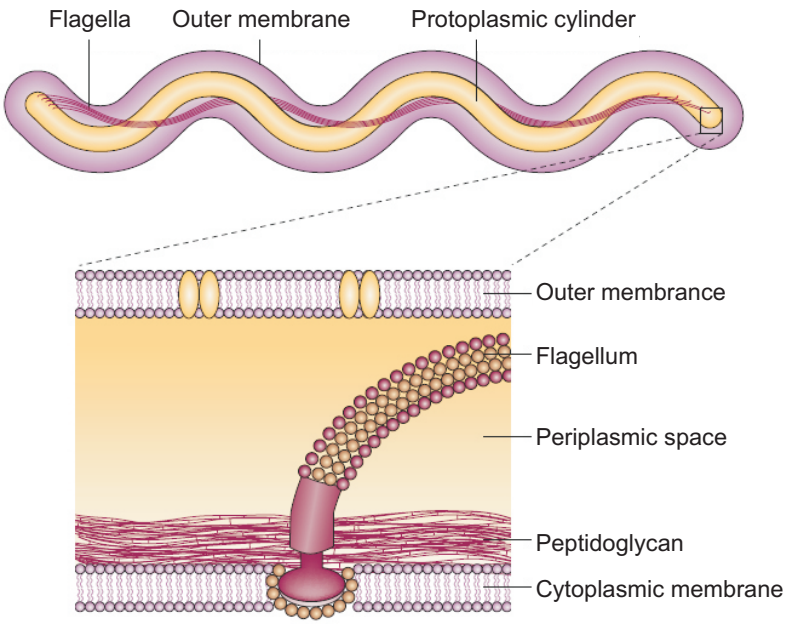

B.

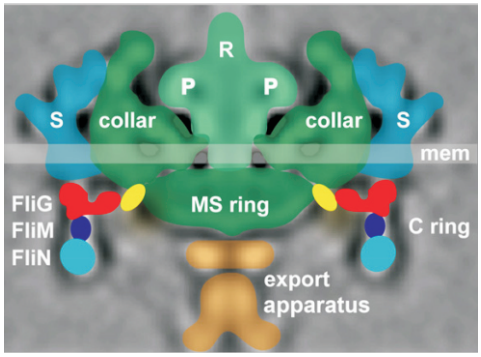

Figure 1-9. ***Borrelia burgdorferi*** **flagellar structure.** Lyme spirochetes possess two flagellar bundles which wrap around the protoplasmic cylinder, anchoring at the poles within the cytoplasmic membrane (Panel A). The motors are polarly located and consist of the MS ring (FliF, base of the flagellar motor), C ring (FliG, FliM, and FliN; switch complex regulation flagellar rotation), export apparatus, rod (connects MS ring and hook), L and P rings (bushings at the membrane), and stator (motor force generator), as displayed in Panel B.

phosphodiesterase (YhjH) and elevated intracellular c-di-GMP levels (31). YcgR controls this function by binding to the flagellar motor switch strongly in the presence of c-di-GMP to reduce motor torque generation and cause a counter-clockwise motor bias. This implicates the involvement of YcgR in a "backstop brake" mechanism (62).

This type of model has never been investigated in *Borrelia*, but Lyme spirochetes possess the c-di-GMP network and the majority of flagellar and chemotaxis genes present in other gram negative bacteria necessary for this type of flagellar motor control (26). Deletion of the *B. burgdorferi* EAL phosphodiesterase or PilZ domain-containing protein (PdeA and PlzA, respectively) decreases spirochete swarming and abrogates murine infection supporting the hypothesis that c-di-GMP has a role in *Borrelial* motility as well as virulence (27). Together, this suggests c-di-GMP likely has a role in spirochete motility but it could have an altered involvement in flagellar motor regulation or be spatially localized due to the unique flagellar structure of spirochetes.

Study objectives

It is evident that c-di-GMP signaling is significant to bacterial pathogenesis in many bacterial systems, yet there is a major lack of understanding of c-di-GMP signaling on *Borrelia* cellular processes. The work presented here seeks to test the hypothesis that the c-di-GMP network, and by extension c-di-GMP, regulates critical steps in the enzootic cycle of the Lyme disease spirochetes. Our investigation is further divided into three research goals; to first focus on the diguanylate cyclase, then evaluate the PdeB phosphodiesterase, and lastly the PilZ domain-containing putative c-di-GMP effector proteins PlzA and PlzB. These analyses will aim to assess the impact

of each protein on intracellular c-di-GMP concentrations, infection, and enzootic cycle progression by generating strains with targeted gene deletions utilizing allelic exchange mutagenesis, followed by HPLC analysis, and infectivity testing using an *Ixodes* tick-C3H-HeJ mouse model. Genetic alteration could drastically alter c-di-GMP pools and respectively modify spirochete flagellar movement and chemotaxis. Therefore, we additionally aim to identify if each protein is a critical regulator of spirochete motility and chemotaxis by examining the ability of each deletion mutant to generate translation motion, swarm, and respond to N-acetyl-D-glucosamine chemotaxis signals. These analyses will provide unique insight into a relatively unexplored area of the role of c-di-GMP signaling in the genetic regulation in *B. burgdorferi* and arthropod borne pathogens.

CHAPTER 2: MATERIALS & METHODS

Bacterial isolates and cultivation.

All *Borrelia burgdorferi* strains generated in this study were constructed using the low passage, B31-5A4 isolate (67) and maintained in BSK-H complete media with 5% CO_2 at 25, 33, or 37ºC. BSK-H media was prepared using bovine serum albumin from Gemini Bio-Products, Inc (lot #C54) as previously described (79) and supplemented with rabbit serum to 6% (Gemini). Spirochetes were harvested by centrifugation (4ºC, 5,000 X g, 20 min) and washed with phosphate buffered saline (PBS).

Production of *rrp1* allelic exchange constructs.

Allelic exchange replacement of *rrp1* with an antibiotic resistance cassette was performed as previously described using plasmid pΔBB0419 (Figure 2-1A) (70) to generate the *B. burgdorferi* strain B31-Δ*rrp1*. Prior to introduction of DNA into *B. burgdorferi* by electroporation, 20 µg of the suicide plasmid was linearized with *Nco*I and *Sca*I (NEB) according to the manufacturer's protocol. This was done to increase transformation efficiency and to inactivate the kanamycin and ampicillin resistance cassettes. Electroporation was performed using the previously described conditions of 2.5 V, 200

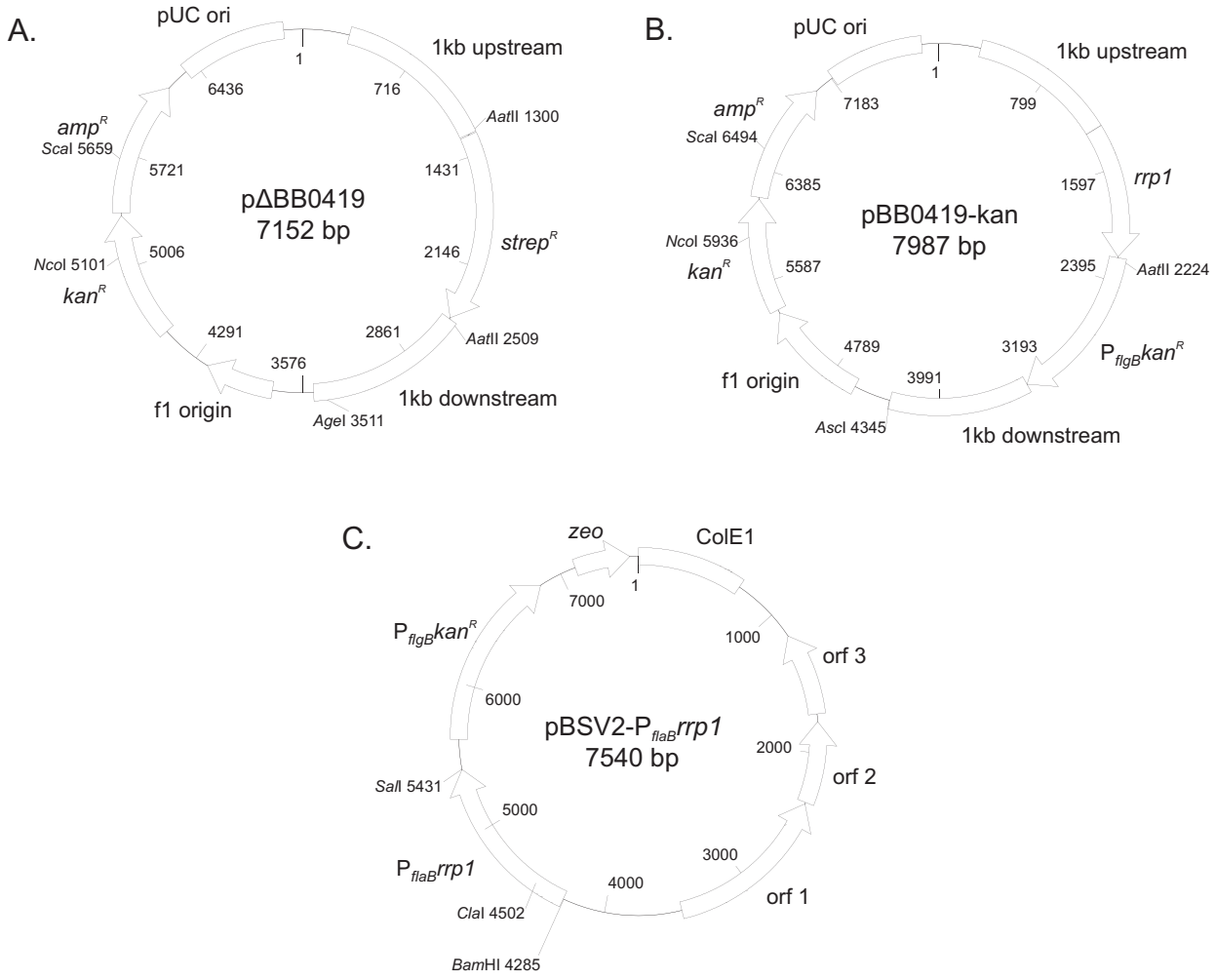

Figure 2-1. Schematics of plasmids for *rrp1* allelic exchange and plasmid-based constitutive expression. Plasmids in Panel A and B were generated using a pCR2.1 backbone that possessed the upstream flanking 1000 bp of the *rrp1* with or without the ORF. Additional features were added via restriction with the enzymes shown above. The allelic exchange constructs in Panel A and B were used to create the B31-Δ*rrp1* and B31-*rrp1* KI strains, respectively. The pBSV2-based vector was produced by directionally cloning the constitutive *flaB* promoter and *rrp1* ORF into the plasmid multiple cloning site, then electroporating the final plasmid into *B. burgdorferi* strain B31-5A4 to produce the B31-*rrp1* OV mutant.

streptomycin and clonal populations obtained by sub-surface plating (as described below).

To complement the *rrp1* deletion, *rrp1* was reintroduced back into the chromosome of B31-Δ*rrp1* using allelic exchange. To generate the construct for complementation, a polymerase chain reaction (PCR) product extending from 1 kb upstream of *rrp1* to the 3' end of *rrp1* (with 3' flanking *Aat*II and *Asc*I sites) was cloned into pCR2.1 using TOPO-TA approaches (Invitrogen) to generate pBB0419-UP. A kanamycin resistance cassette, derived from pBSV2 (93), with a 5' *Aat*II site, was fused by overlap extension to the downstream 1kb sequence flanking *rrp1* (3' *Asc*I site). The kanamycin-downstream fusion was cloned into pCR2.1, digested with *Aat*II and *Asc*I restriction enzymes (NEB), and then inserted into the pBB0419-UP to create pBB0419-kan (Figure 2-1B). The resulting plasmid was purified, linearized with *Sca*I and *Nco*I (NEB), and electroporated into B31-Δ*rrp1* to produce the complemented strain, B31-*rrp1* KI. Selection was achieved with 75 μg ml^{-1} kanamycin and clonal populations were obtained by sub-surface plating.

Modification of the pBSV2 plasmid to constitutively produce *rrp1*.

Overexpression of *rrp1* was accomplished by using a pBSV2 based plasmid (93) with *rrp1* expression under the control of the *flaB* promoter. The *flaB* promoter and complete *rrp1* gene were PCR amplified from B31-5A4 genomic DNA in separate PCR reactions and cloned into pCR2.1-TOPO to yield pCR2.1-P_{flaB} and pCR2.1-*rrp1*. The plasmids were digested with *Cla*I and *Sal*I (NEB). The *rrp1* containing fragment was excised from a gel and ligated into the pCR2.1-P_{flaB} to yield pCR2.1-P_{flaB}-*rrp1*. pBSV2

and pCR2.1-P_{flaB}-*rrp1* were linearized with *Bam*HI and *Sal*I (NEB). The P_{flaB}-*rrp1* fragment was ligated into the pBSV2 vector to generate pBSV2-P_{flaB}-*rrp1* (Figure 2-1C). The final plasmid was propagated and electroporated into B31-5A4 cells. Selection of the overexpression strain (B31-OV) was achieved using kanamycin (200 µg ml^{-1}). Clones were selected by sub-surface plating and plasmid content determined by PCR.

Generation of the *plzA* and *pdeB* deletion mutants and complementing strains.

Gene inactivation of *plzA* and *pdeB* was performed as described by (79). The 1 kb upstream and downstream of each open reading frame (ORF) was PCR amplified in two separate reactions and cloned into the pCR2.1-TOPO vector to produce the pBB0733-UP or pBB0374-UP and pBB0733-DN or pBB0374, respectively. The upstream PCR fragment contained 3' flanking *Aat*II and *Age*I restriction sites, while the downstream fragment possessed a 5' *Aat*II and 3' *Age*I site. The downstream 1 kb amplicon was excised from the DN vectors with *Aat*II and and *Age*I restriction enzymes (NEB), then ligated into the pBB0733-UP or pBB0374-UP vector to generate pBB0733-UPDN and pBB0374-UPDN. A spectinomycin/streptomycin resistance cassette, derived from pKFSS1-*Aat*II (25), was inserted with flanking *Aat*II sites between the 1 kb up and downstream PCR fragments to produce pΔBB0733 and pΔBB0374 (Figure 2-2A & Figure 2-3A, respectively). The plasmids were linearized with *Nco*I and *Sca*I, then electroporated into infectious *Borrelia burgdorferi* 5A4 to generate the B31-Δ*plzA* and B31-Δ*pdeB*, respectively. Selection for the deletion strains was achieved by supplementing BSK-H media with 75 µg ml^{-1} streptomycin. Sub-surface plating was utilized to isolate clonal populations.

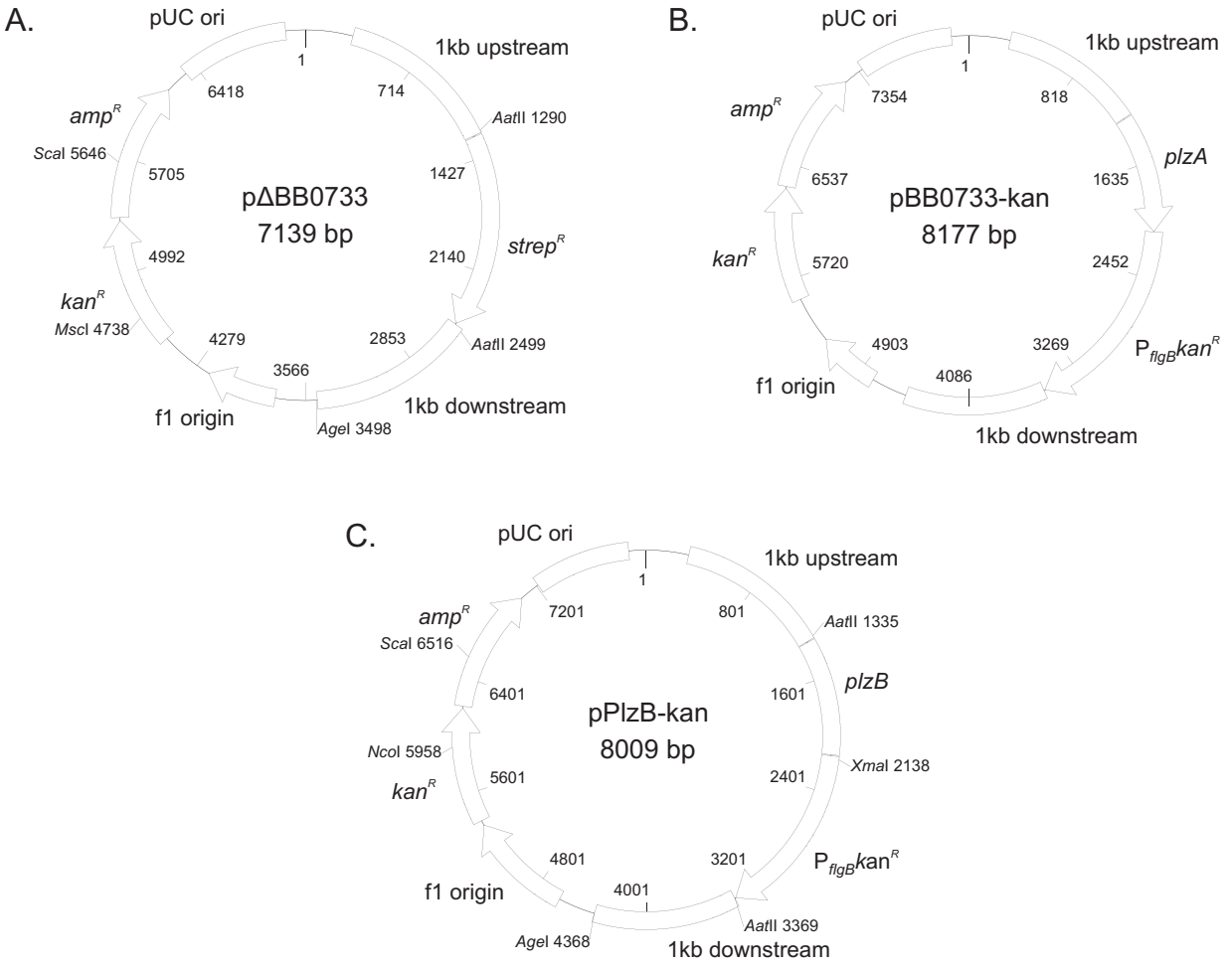

Figure 2-2. *plzA* allelic exchange constructs. Each plasmid was created using a pCR2.1 backbone containing the upstream 1000 bp of *plzA.* The *strep*^{R} cassette, *plzA* or *plzB* phusion with P$_{flgB}$*kan*^{R}, and downstream 1000 bp flanking region of *plzA* were inserted using respective restriction enzymes displayed above. The vectors in Panel A, B, and C were used to produce the B31-Δ*plzA*, B31-*plzA* KI, and B31-Δ*plzA::plzB* strains, respectively.

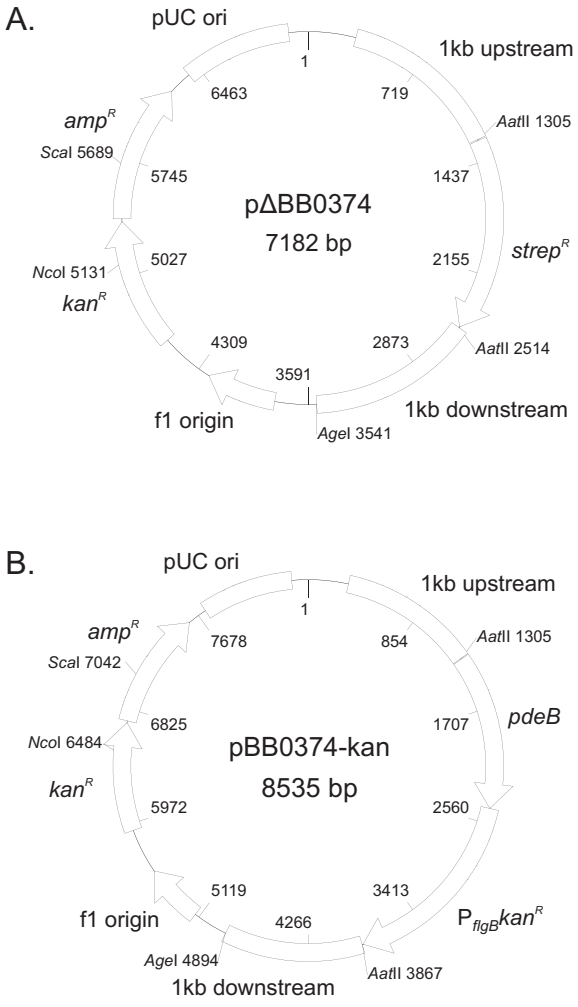

Figure 2-3. HD-GYP phosphodiesterase, *pdeB,* allelic exchange plasmids. The *strep*^{R} cassette, *pdeB* phusion with P$_{flgB}$*kan*^{R}, and downstream 1000 bp flanking *pdeB* were inserted using restriction sites (shown above) into pCR2.1 containing the 1000 bp upstream of *pdeB* to complete the plasmids in Panel A and B. These constructs were electroporated into *B. burgdorferi* B31-5A4 cultures to create strains B31-Δ*pdeB* and B31-*pdeB* KI, respectively.

Complementation was obtained by allelic exchange mutagenesis of B31-Δ*plzA* and B31-Δ*pdeB* to replace the spectinomycin/streptomycin cassette with the original open reading frame harboring a 3' flanking kanamycin resistance cassette. A PCR product containing 1 kb upstream of the select gene, the ORF, and 3' flanking *Aat*II and *Asc*I sites, was TOPO cloned into pCR2.1 to generate pBB0733-UP+BB0733 and pBB0374-UP+BB0374. A kanamycin resistance cassette was PCR amplified from pBSV2 (93) with a 5' *Aat*II site. Overlap extension PCR fused the kanamycin PCR product to the 1000bp located immediately downstream of the targeted gene, and added a 3' *Asc*I site. The kanamycin-downstream fusions were TOPO cloned into pCR2.1, then digested and ligated into the pBB0733-UP+BB0733 and pBB0374-UP+BB0374 plasmids to create pBB0733-kan and pBB0374-kan (Figure 2-2B & Figure 2-3B). The plasmids were linearized with *Sca*I and *Nco*I then subsequently electroporated into B31-Δ*plzA* or B31-Δ*pdeB* to produce the complemented strains, B31-*plzA* KI and B31-*pdeB* KI. Selection was achieved with 75 μg ml^{-1} kanamycin and clonal populations were isolated.

***plzB* allelic replacement of *plzA*.**

Replacement of *plzA* with *plzB* was achieved by allelic exchange mutagenesis. The upstream 1 kb region of *plzA* was PCR amplified to include the *plzA* ribosome binding site (RBS) and cloned into pCR2.1-TOPO to generate plasmid pBB0733-UP-2. The downstream 1 kb was excised from pBB0733-DN with *Aat*II and *Age*I and ligated into pBB0733-UP-2 to create pBB0733-UPDN-2. Next, *plzB* (BBUZS7F20) was PCR amplified from *B. burgdorferi* strain CA12 to include a 5' *Aat*II site and a 3' overlap with

the $P_{flgB}kan^R$ cassette. The $P_{flgB}kan^R$ cassette was amplified from pBSV2 (93) to possess a 5' overlap with the 3' *plzB* ORF and a 3' *Age*I restriction site. A *plzB*-$P_{flgB}kan^R$ fusion was created by overlap extension PCR, then digested with *Aat*II and *Age*I, and ligated into pBB0733-UPDN-2 to produce pPlzB-kan (Figure 2-2C). pPlzB-*kan* was linearized with *Sca*I and *Nco*I, electroporated into *B. burgdorferi* clone B31-Δ*plzA*, and B31-Δ*plzA::plzB* transformants selected by cultivation in media containing 75 μg ml^{-1} kanamycin.

Isolation of clonal spirochete populations by subsurface plating.

One week post-electroporation, clonal isolates were obtained from transformed cultures by subsurface plating. Plating was performed using 2% GTG agarose (Seakem) and BSK-H complete media. The agarose was first autoclaved then incubated in a 55º water bath to cool. The media was simultaneously heated in a 45º water bath. Each plate possessed a bottom 25 ml layer containing a 2:1 BSK to agarose ratio. This layer was allowed to solidify before the pouring of the final top layer which contained 1ml of a diluted transformed culture, 4 ml BSK-H, and 6.5 ml agarose. The completed plates were allowed to cool and solidify at room temperature, and then incubated at 33º for ~2 weeks till colonies became visible. Clones were punched with a sterile 1 ml pipet tip and ejected into a 2 ml microcentrifuge tube containing BSK-H and appropriate antibiotic selection. Clonal cultures were incubated at 33º and cultivated for further verification and experimentation.

Polymerase chain reaction verification of plasmid content and proper construct integration.

To verify integration of the allelic exchange mutant constructs into their respective chromosomal locations, PCR was performed with primers designed to amplify inwards from locations outside the 1 kb upstream and downstream of the genes replaced and outwards from the 5' or 3' locations of the gene and/or resistance cassette. Primers used for each strain are listed in Appendix A. Upon PCR confirmation of successful allelic exchange, plasmid content was assessed by PCR utilizing primers specific for all 21 linear and circular plasmids as described by Rogers et al (69). Evaluation of plasmid content was necessary to ensure a consistent genetic background between strains and to maintain spirochete infection capabilities. Only strains possessing all plasmids were used for further experimentation.

Growth curve analysis.

To determine growth rates for the mutant strains generated, an equal number of actively growing spirochetes (33ºC) were transferred into fresh BSK-H complete media without antibiotics and incubated at 25º, 33º, and 37º. Cells were counted every 24 hr for 20 days using dark field microscopy. The average number of spirochetes per field was determined by averaging the counts from 10 fields for each time point.

SDS-PAGE and immunoblotting.

Lysates were fractionated using 12.5% Criterion Precast Gels (BioRad) by sodium dodecyl sulfate- polyacrylamide gel electrophoresis (SDS-PAGE) at 200 V for 1

hr and transferred to polyvinylidene difluoride membrane (Millipore) as previously described (Rogers *et al.*, 2009a). The membranes were blocked (1 x PBS, 0.2% tween, 5% non-fat dry milk) and screened with a variety of antisera including mouse anti-Rrp1 (1:1000), rat anti-FliG2 (1:500, gifted by Dr. Chunhao Li), rat anti-CheY3 (1:500, gifted by Dr. Nyles Charon), mouse anti-*Borrelia* infection sera (1:1,000), and mouse anti-FlaB (1:400,000). Antibody binding was detected using horseradish peroxidase-conjugated goat anti-mouse IgG secondary antibody (Pierce -1:40,000) and SuperSignal West Pico chemiluminescence substrate (Pierce).

RNA isolation and real time reverse transcriptase polymerase chain reaction (qRT-PCR).

RNA was isolated from *Borrelia* cultures using the RNeasy Midi kit as described by the manufacturer (Qiagen) and treated with DNase I (Invitrogen). cDNA was generated using the Superscript III First Strand cDNA Synthesis kit (Invitrogen), 50 ng random hexamer primers, and 1 µg total RNA. qRT-PCR was performed with SYBR green PCR Master Mix (Applied Biosystems) and the CFX96 Real Time System (BioRad) with primers listed in Appendix A. The following cycle parameters were used: 1 cycle of 10 min at 95º followed by 40 cycles of 10 sec at 94º, 30 sec at 50º, and 30 sec at 72º. Melting curves were generated over the temperature range 45-95º to assess amplification specificity. All reactions were run in triplicate with three biological replicates and the data were normalized against enolase (*eno*; BB0377). Statistical analyses were performed using a paired, two-tailed t-test. Alterations of gene expression were considered significant if $p<0.05$.

Infectivity in mice: seroconversion and cultivation analyses.

The potential ability of each strain to infect C3H-HeJ mice (Jackson) was assessed by subcutaneous needle inoculation of 10^4 spirochetes between the shoulder blades (in 100 µl BSK-H complete media). Four weeks post-inoculation, the mice were sacrificed and blood, organs, and tissues were harvested. Seroconversion was assessed by ELISA. The ELISA plates were first coated with 0.1 OD B31-5A4 spirochetes/ml in 100 µl of carbonate buffer (pH 9.6) overnight, then incubated for 2 hr at RT with shaking, and blocked with 1% bovine serum albumin in PBS-T. Antiserum from each mouse was applied in serial 3-fold dilutions (1:50-1:109,350) for 1 hr with shaking at RT. The plates were then washed three times and bound IgG detected with peroxidase conjugated goat-anti-mouse IgG antiserum (1:20,000) and ABTS chromagen. Plate readings were taken at OD_{405} for each plate. Statistical analysis was performed using a one-way ANOVA. In addition to the ELISA, seroconversion was assessed through immunoblotting (1:1000 mouse anti-*Borrelia* sera) for confirmation. Lastly, a third measure of infection was by cultivation. Tissues and organ biopsies were immediately inserted into complete BSK-H media containing *Borrelia* antibiotic cocktail (phosphomycin, rifampicin, and amphotericin B) and incubated at 33º for 2-3 weeks followed by dark-field microscopy.

Tick studies.

Naïve larval stage *Ixodes scapularis* ticks (Oklahoma State University Tick Rearing Facility) were brushed onto mice 4 weeks post-inoculation with each of the strains described above. The ticks were fed to repletion, collected, and DNA isolated

using the DNeasy Blood and Tissue kit (Qiagen). qPCR was performed using a *B. burgdorferi flaB* primer set and the data were normalized against tick rDNA using the RIB-3 and RIB-4 primers (109). Ticks were also infected using immersion methods (64). Larval ticks were submerged in *B. burgdorferi* cultures (10^8 cells/ml; 33°C; 2 hr, with shaking), washed, dried, and then fed on naive mice. One week after drop off, DNA was isolated and analyzed by qPCR. Four weeks post-tick bite, the mice were sacrificed and evaluated for infection by ELISA, immunoblot, and cultivation as described above.

Motility analyses.

Motility in BSK-H complete media with and without 1% methylcellulose (Sigma) was assessed using dark-field and differential interference contrast (DIC) microscopy. Time lapse movies were recorded and analyzed using Slidebook 5 (Intelligent Imaging Inovations) motion-tracking software. Each motion track was created by manually marking individual spirochetes in consecutive frames. Velocity measurements were calculated from twenty tracks per strain. Spirochete flexing was determined by manual flex counts of twenty individual cells over the course of a track divided by total motion track time. Statistics were performed using one-way ANOVA analysis. Microscopy was performed at the VCU Department of Anatomy and Neurobiology Microscopy Facility.

Swarm plate and capillary tube chemotaxis assays.

Swarm assays were adapted from Li et al (46) and Motaleb et al (55). Plates containing 0.35% (wt/vol) Seakem GTG agarose in BSK-H were punched 3 times with a

1 ml pipette tip. $5x10^5$ spirochetes were resuspended in 5 µl of a 1:10 BSK-H dilution in dPBS, and then placed in the punched holes. Plates were incubated at 33ºC and colony diameters assessed at 2, 4, and 6 days using a caliper. Statistics were generated using a one-way ANOVA on the means from 3 independent experiments.

The capillary assay was performed using a 96 well format as previously described (56) with some modifications. All experiments were conducted in triplicate. In brief, cells were harvested from liquid cultures by centrifugation and suspended at 10^7 cells ml^{-1} in motility buffer containing 1% (wt/vol) BSA and 1% (wt/vol) methylcellulose (84). The cells were placed in the wells of a 96 well plate in triplicate for each condition with 150 µl cell suspension per well. Capillary tubes, filled with motility buffer plus or minus chemoattractant were inserted into the wells and the open end was sealed with Critoseal (Leica). The plates were incubated at 33º for 2 hr and then the contents of the capillary tubes were expelled into microcentrifuge tubes. The average number of spirochetes per field using dark-field microscopy was determined by averaging 10 fields of view. One-way ANOVA statistical analysis was performed on the means from 3 separate experiments. Chemoattractants utilized include 0.1 M N-acetyl-D-glucosamine (Sigma), macerated whole-tick debris, 10 mM chitin (MP Biomedicals, LLC), and 10 mM chitobiose (Sigma). For the assays utilizing chitin and tick debris, the entire assembly was tilted on its side for the incubation period to prevent the insoluble chemoattractant particles from settling out of the capillary tubes and into the wells.

Intracellular c-di-GMP quantitation.

C-di-GMP determination in *B. burgdorferi* acid soluble extracts was performed as previously described (2) with minor modifications. *Borrelia* cultures (50 ml) were grown to and OD_{600} >2.0. Bacterial cells were collected by centrifugation (5,000 x g; 20 min; 4ºC), washed with PBS, then centrifuged again to recollect cells. The pellet was resuspended in 350 µl 0.4 M ice-cold $HClO_4$ and lysed by sonication. After centrifugation (16,000 x g; 3 min; 4ºC) to remove cell debris, supernatants were neutralized with 62 µl 0.8 M K_2CO_3, kept on ice for 10 min, and centrifuged (16,000 × g; 3 min; 4ºC). Neutralized samples were injected into an HPLC system equipped with a diode-array detector. Nucleotides separation was performed on a Sinergi 4.0 µ Fusion-RP 250 x 4.6 mm column (18ºC; Phenomenex, Inc). Elution conditions were 12 min at 100% buffer A (100 mM potassium phosphate, pH 6.0), 8 min up to 12% buffer B (buffer A containing 20% methanol), 3 min up to 45% buffer B, and 4 min up to 100% buffer B, holding at 100% buffer B for 7 min, and returning to 100% buffer A in 6 min. Flow rate was maintained at 1 ml min^{-1}.

Generation and expression of recombinant proteins, PlzA and PlzB.

Primers were designed to amplify *plzA, plzB,* and *rrp1* with 5' *Bam*HI and 3' *Sal*I restriction sites. Products were digested and cloned into pCR2.1-TOPO, transformed into TOP10 *E. coli* (Invitrogen), and positive colonies were selected by PCR. The resulting plasmids were propagated and subcloned into pMAL-c4x (New England Biolabs) via the *Bam*HI and *Sal*I restriction sites to produce the vectors pMAL-c4x PlzA, pMAL-c4x PlzB, and pMAL-c4x Rrp1 (Figure 2-4). The resulting plasmids were

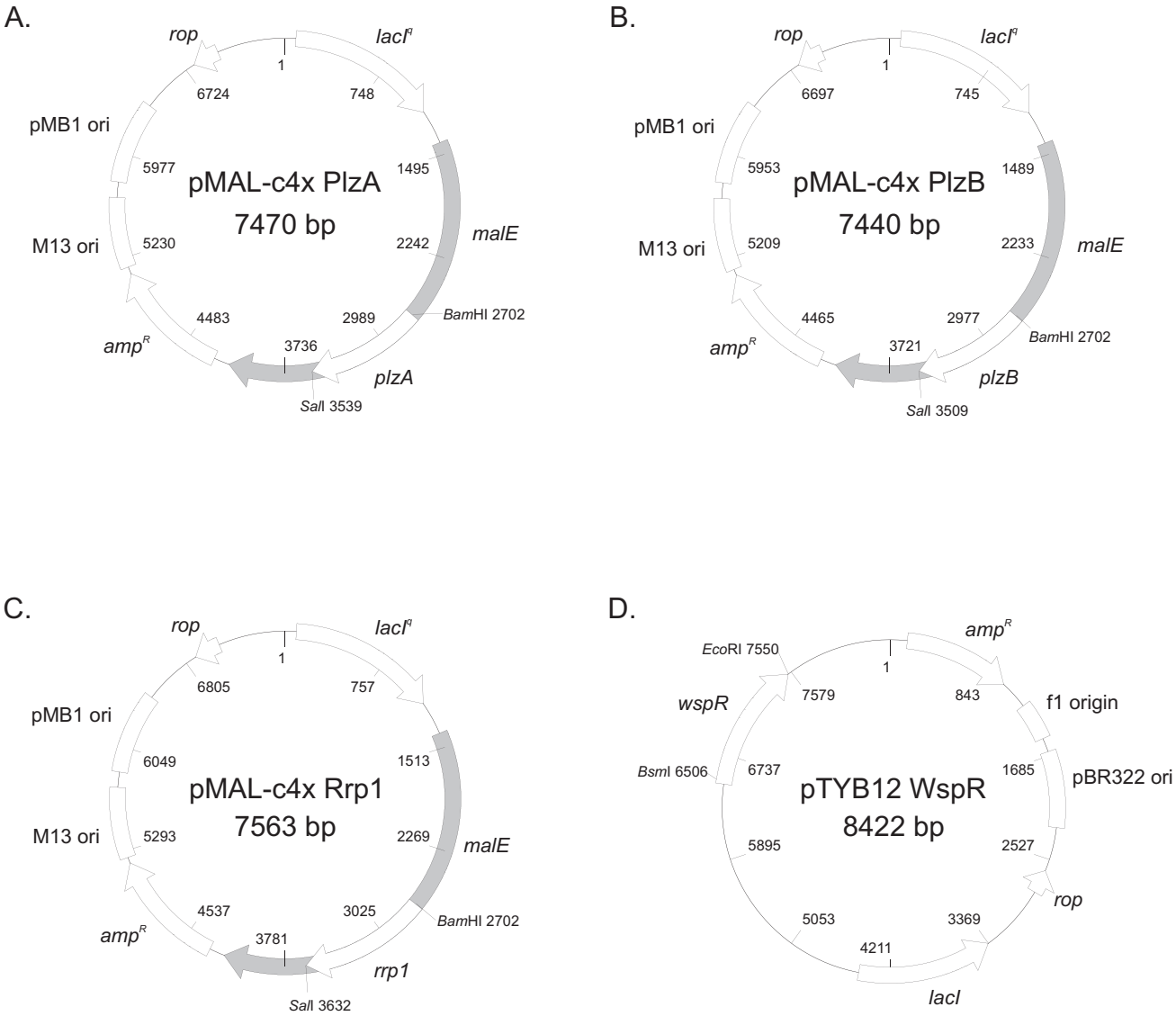

Figure 2-4. Recombinant protein expression plasmids. The open reading frames of *plzA, plzB, rrp1,* and *wspR* were PCR amplifed to contain flanking restriction sites (shown above) for insertion into pMAL-c4x or pTYB12. Upon verification, r-proteins were induced, purified, and utilized to synthesize c-di-GMP or assess r-protein c-di-GMP binding capabilities.

transformed into BL21 (DE3) *E. coli* cells for protein expression. Cells were grown at 37º to an OD_{600} of 0.6, shifted to 23º, and induced with isopropyl-beta-D-1-thiogalactopyranoside (IPTG; 1 mM; 3 h). After induction, cells were lysed via sonication, and soluble protein was purified by amylose affinity chromatography as instructed by New England Biolabs.

Synthesis of radiolabelled c-di-GMP.

Cyclic di-GMP binding assays were carried out as previously described (27). C-di-GMP was enzymatically synthesized using recombinant WspR, cloned from *Pseudomonas aeruginosa* FRG-1 into pTYB12 (New England Biolabs) using 5' *Bsm*I and 3' *Eco*RI sites to generate the pTYB12 WspR plasmid (Figure 2-4). To activate the r-WspR, 5 µM of the protein was incubated with 25 µM acetyl phosphate for 30 min at 37º. Then, the acetyl phosphate treated r-WspR (5 µM) was incubated with radiolabeled GTP [α-^{32}P] (0.33 µM, Perkin Elmer) or non-radiolabeled GTP (200 µM, Sigma-Aldrich) to generate both radiolabeled and cold c-di-GMP. Reactions were incubated for 1 hr at 37ºC. C-di-GMP concentrations and purity were assessed using HPLC as described by Ryjenkov et al (77). GTP and unlabeled c-di-GMP served as standards. Briefly, the samples were boiled, filtered (Ultrafree centrifugal filters; Millipore), applied to a 15 x 4.6 cm Supelcosil LC-18-T column (Supelco), and separated on an AKTApurifier (GE Health Sciences) by reverse phase HPLC. The gradient system utilized buffers A (100 mM KH_2PO_4, 4 mM tetrabutyl ammonium hydrogen sulfate, pH 5.9) and B (75% buffer A, 25% methanol). Nucleotides were detected at a wavelength of 254 nm.

PlzA & B c-di-GMP binding assays.

Cyclic di-GMP binding assays were carried out as previously described (27,65). The recombinant proteins (0.25 µg r-PlzA, PlzB, and Rrp1 (negative control)) were spotted onto nitrocellulose and allowed to air dry. The membranes were incubated with [α-^{32}P] c-di-GMP (2 nM) alone, or in combination with 750 nM of GTP, GMP, ATP, cGMP, or cAMP (PBS with 1% milk; 2 h; RT). Membranes were washed twice with PBS for 10 min and exposed to film overnight.

CHAPTER 3: RESULTS

ANALYSIS OF THE DIGUANYLATE CYCLASE, RRP1.

Generation and analysis of an *rrp1* deletion mutant, *rrp1* over-expressing strain, and cis-complemented strain.

To determine if Rrp1 regulates cellular processes required for completion of the enzootic cycle, *rrp1* of *B. burgdorferi* strain B31 clone 5A4 (an infectious clone) was replaced by a spectinomycin/streptomycin resistance cassette (*strep*^{R}) to yield strain B31-Δ*rrp1* (Figure 3-1A). A functional *cis*-complemented strain, B31-KI ("knock-in"), was generated by replacing the *strep*^{R} cassette of B31-Δ*rrp1* with wild-type *rrp1* and a downstream kanamycin resistance cassette (Figure 3-1B). To generate a strain that constitutively produces elevated levels of Rrp1, B31-wt was transformed with pBSV2-P$_{flaB}$*rrp1* (Figure 3-1C) to yield a strain carrying a plasmid and chromosomal copy of *rrp1*. Clonal populations of each strain were assessed for insertion of the cassette or for the presence of the pBSV2-P$_{flaB}$*rrp1* plasmid using PCR (Figure 3-1D). The *Borrelia* genome is segmented and consists of a linear chromosome and twenty or more linear and circular plasmids (7). Genetic manipulation can result in the loss of plasmids required for survival in mammals (44,66). To assess plasmid content, PCR was performed with specific primer sets for each of the twenty one circular and linear plasmids (data not shown) (54). Only clones harboring the full set of plasmids were

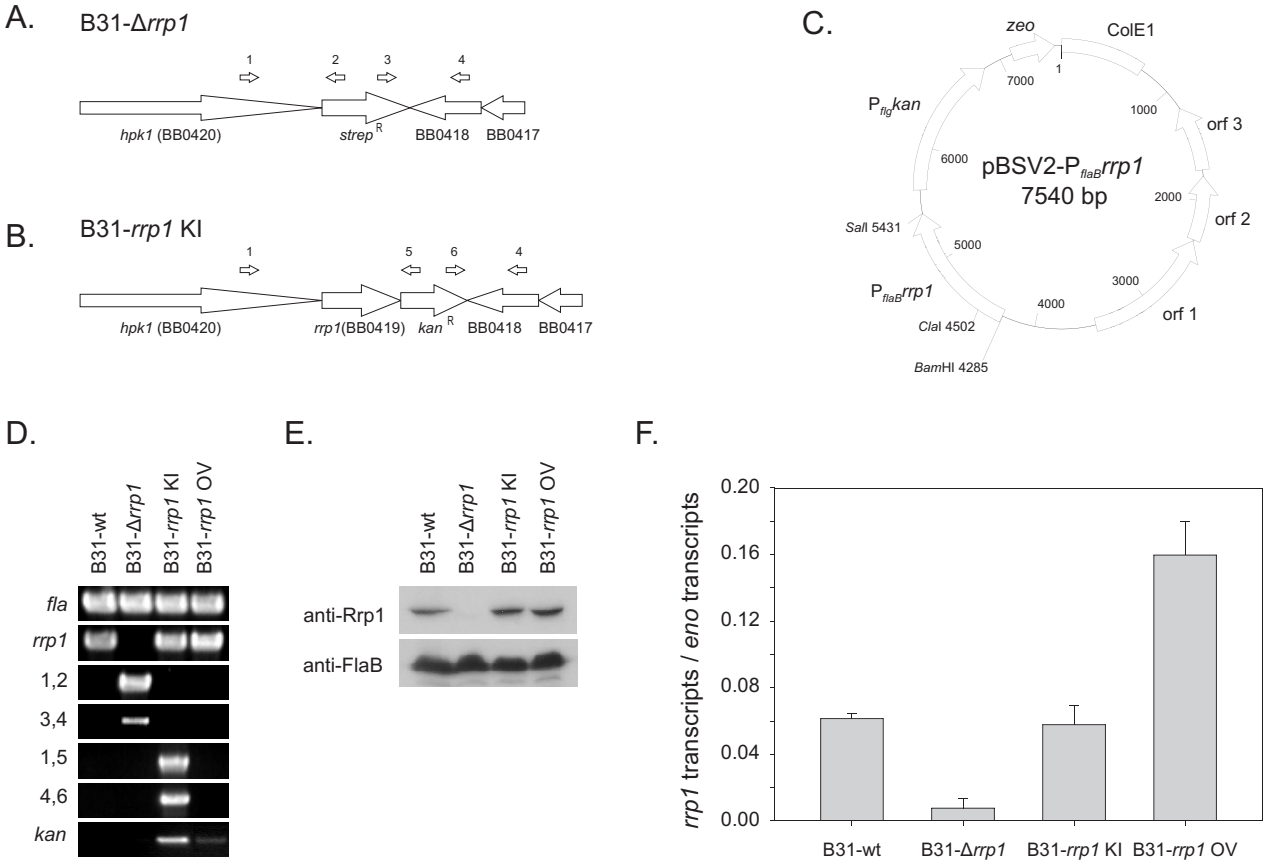

Figure 3-1. Generation and verification of *rrp1* deletion, complementation, and overexpression. Schematics in panel A and B represent the chromosome of the B31-Δ*rrp1* and B31-*rrp1* KI complement mutants after allelic replacement, respectively. Schematic C depicts the pBSV2-P_{flaB}*rrp1* plasmid construct utilized in this study for the B31-OV mutant. Successful allelic exchange mutagenesis deleting and reinserting *rrp1* was confirmed by PCR (Panel D), western blot (Panel E), and qRT-PCR analysis (Panel F). Verification of pBSV2-based overexpression of Rrp1 was likewise performed by PCR (Panel D), western blot (Panel E), and qRT-PCR (Panel F). Primers used for validation of proper integration are indicated by numbers above the schematic arrows and are listed to the left of the respective PCR panels. All primers used are listed in Appendix A.

selected for further analyses. To evaluate Rrp1 protein and transcript levels, immunoblot, and qRT-PCR analyses were conducted (Figure 3-1E &F, respectively). *rrp1* transcript and protein was detected in the B31-wt, B31-*rrp1* KI, and B31-*rrp1* OV strains, but not in B31-Δ*rrp1*. In vitro, B31-*rrp1* OV produced 2-fold more *rrp1* mRNA than B31-wt or B31-*rrp1* KI (Figure 3-1F).

In nature, *B. burgdorferi* encounters radically different environmental conditions as it cycles between ticks and mammals. One environmental variable the pathogen must adapt to during this enzootic cycle is temperature. Cultivation in the laboratory at 25º to 27ºC is thought to mimic at least in part the tick environment. Hence, we determined growth rates at 27º, 33º, and 37ºC (Figure 3-2). B31-Δ*rrp1* displayed an extended lag phase at 27ºC (7 days) and did not enter stationary phase for 13 days. All remaining strains entered log phase within 2 days and stationary phase by day 7. It can be concluded that Rrp1 is not required for growth in vitro, but its absence influences growth at lower temperatures. This suggests that Rrp1 may play an important role in the tick environment. Consistent with a potential role for Rrp1 and c-di-GMP in the tick, *rrp1* transcription has been demonstrated to be dramatically upregulated in ticks after ingestion of a bloodmeal (70).

Analysis of c-di-GMP levels.

C-di-GMP production by each strain was assessed through HPLC analysis of nucleotides extracted from in vitro cultivated bacteria in collaboration with Lee Szkotnicki, PhD (former Marconi laboratory postdoctoral fellow), as well as Paola Bocci and Nadia Raffaelli (Università Politecnica della Marche). This approach has been

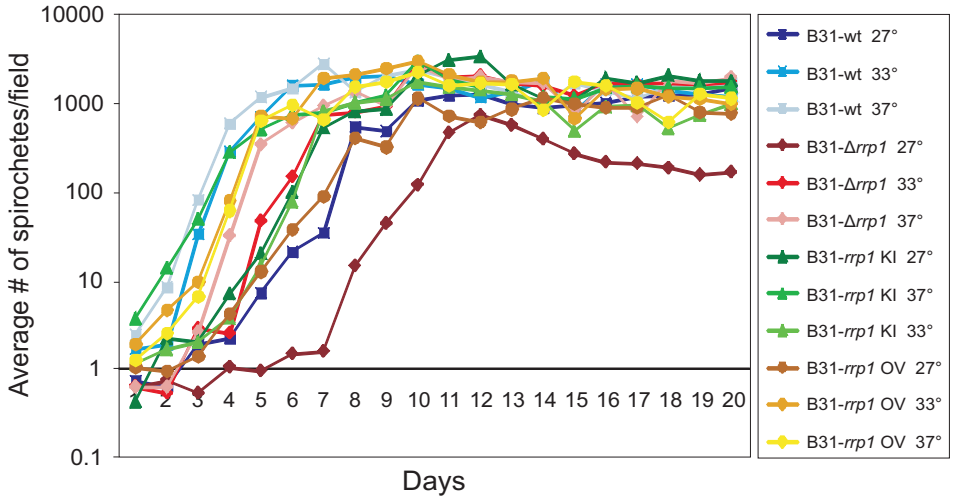

Figure 3-2. Rrp1 mutant growth curves. Growth of each strain was assessed at 27°, 33° and 37° over twenty days in BSK-H complete media. Cultures were seeded at one cell per 400X field of magnification and average number of spirochetes per ten 400X fields was determined every twenty four hours.

successfully applied to measure c-di-GMP in *E. coli* (2) and it has a sensitivity of 0.3 pmol nucleotide/mg cells (data not shown). *Borrelia hermsii* DAH (tick-borne relapsing fever) and *Treponema denticola* (periodontal disease) were included as controls. *B. hermsii* harbors orthologs of each of the proteins which have been demonstrated to participate in the synthesis and breakdown of c-di-GMP in *B. burgdorferi*, hence we reasoned that it would behave similarly to the Lyme pathogen. *T. denticola* was included because it actively produces several diguanylate cyclases during in vitro cultivation (R.T. Marconi, unpublished data), thereby making it a good positive control for c-di-GMP detection. In addition, because *B. hermsii* and *T. denticola* have a similar membrane composition to *B. burgdorferi* (no lipopolysaccharide with a lipoprotein rich outer membrane), we reasoned that they could serve as controls for the nucleotide extraction process. C-di-GMP was readily detected in *T. denticola* but not in *B. hermsii* (data not shown), *B. burgdorferi* B31-wt, B31-Δ*rrp1,* B31-*rrp1* KI, or B31-*rrp1* OV (Figure 3-3) demonstrating that c-di-GMP concentrations are inherently low in cultivated *Borrelia*. This is consistent with the low level expression of *rrp1* during in vitro cultivation (70).

Demonstration that Rrp1 directly or indirectly influences infectivity and dissemination and or secondary colonization of *B. burgdorferi* in mice.

Mice were subcutaneously needle inoculated with each strain and infection assessed by seroconversion (ELISA and immunoblotting) 4 weeks post-inoculation (Figure 3-4A). All mice inoculated with B31-wt, B31-Δ*rrp1,* and B31-*rrp1* KI were seropositive with equivalent IgG titers. The B31-*rrp1* OV strain had a significantly lower

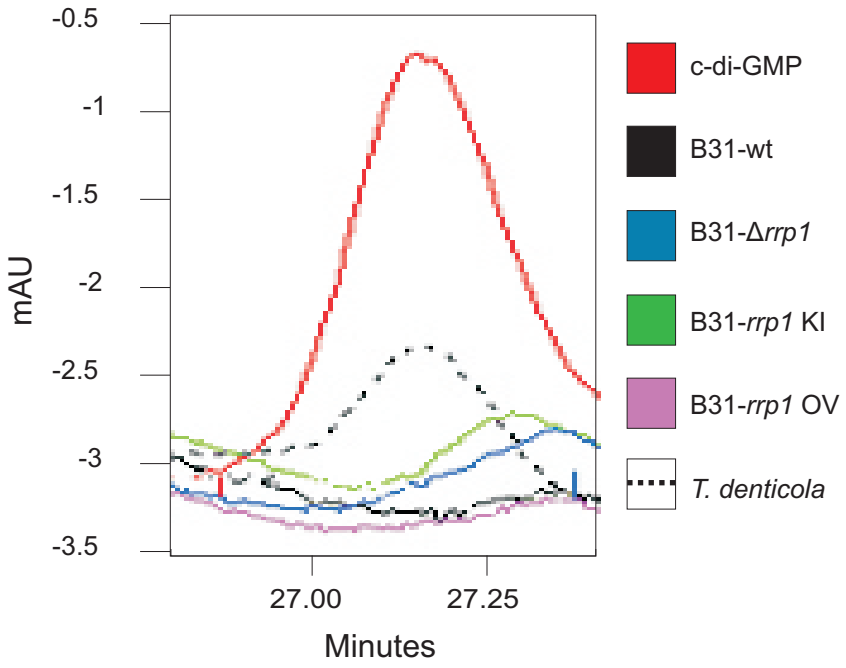

Figure 3-3. Analysis of *Borrelia burgdorferi* intracellular c-di-GMP levels. Nucleotides were extracted from in vitro cultivated *rrp1* strains and c-di-GMP concentrations quantitated by HPLC. Chromatograms of nucleotide extracts from each strain are presented. The elution time of purified c-di-GMP is shown for reference. *Treponema denticola* nucleotide extracts were assessed as a positive control.

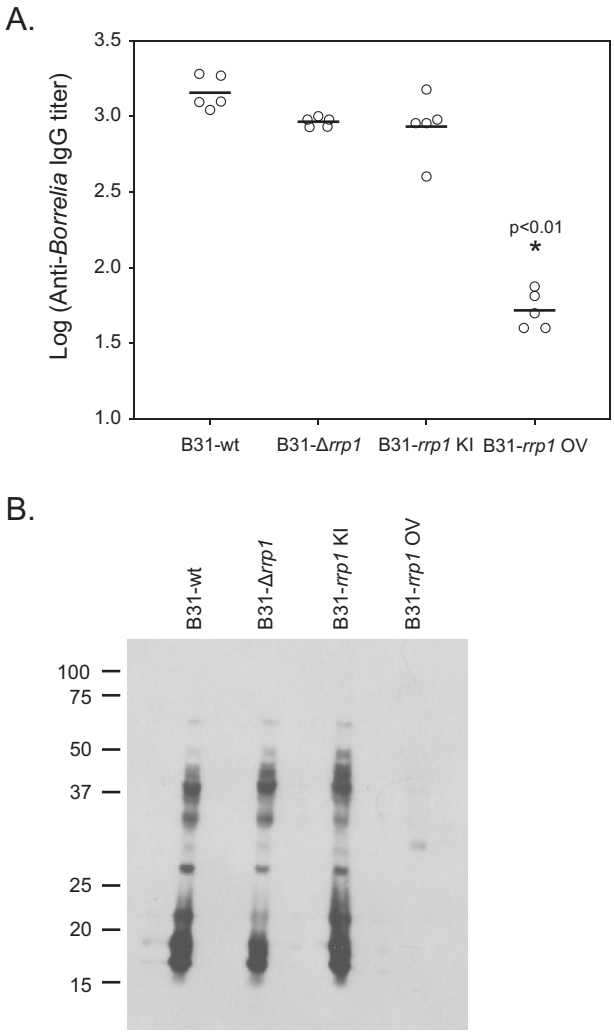

Figure 3-4. Rrp1 is not essential to mammalian infection, but overproduction inhibits disease establishment. C3H-HeJ mice were needle inoculated subcutaneously with 10^4 spirochetes (five mice per strain). Four weeks post-infection, mice were bled and sera collected. Seroconversion was evaluated using whole-cell ELISA (Panel A) and immunoblot (Panel B). Deletion of *rrp1* did not alter the murine anti-*Borrelial* immunological response in comparison to the wild type strain, however B31-*rrp1* OV exhibited a significantly lower anti-*Borrelial* IgG titer.

IgG titer that all other strains ($p<0.01$). The low level IgG titer elicited by the B31-*rrp1* OV strain is similar to that observed for other non-infectious isolates and it presumably results from an antibody response to the inoculum itself (22). To compare antibody responses evoked by each strain, the overall pattern of immunoreactive proteins detected was determined by immunoblotting (Figure 3-4B). Consistent with the ELISA data, serum from mice inoculated with B31-*rrp1* OV did not recognize any proteins in the immunoblot analyses. No significant differences in immunoreactive profiles were observed with the serum collected from mice infected with B31-wt, B31-Δ*rrp1,* and B31-*rrp1* KI.

To further assess infectivity, dissemination, and or secondary colonization, biopsies from each mouse were collected from organs and tissues distal to the inoculation site and placed in BSK-H media for spirochete cultivation. Cultures were obtained from all clinical specimens recovered from B31-wt and B31-*rrp1* KI inoculated mice (Table 3-1). None of the heart biopsies and only a subset of the bladder and skin samples harvested from B31-Δ*rrp1* inoculated mice yielded positive cultures. Positive cultures were not obtained from mice inoculated with B31-*rrp1* OV. This observation is consistent with the immunological data described above. It can be concluded that Rrp1 is not required for infectivity but is required for maximal dissemination and or secondary colonization.

Rrp1 is essential for spirochete acquisition by *Ixodes scapularis.*

To assess the ability of each strain to transit from infected mammals to feeding ticks, larval stage *Ixodes scapularis* ticks were fed to repletion on mice (four weeks

Table 3-1. Murine infection study of *rrp1* strains.

Strain	# spirochete positive cultures from each tissue or organ biopsy			
	bladder	heart	skin	# of culture positive / # tested
B31-wt	5/5	5/5	5/5	5/5
B31-Δ*rrp1*	3/5 (mice 1 and 3 were negative)	0/5	3/5 (mice 2 and 5 were negative)	5/5
B31-*rrp1* KI	5/5	5/5	5/5	5/5
B31-*rrp1* OV	0/5	0/5	0/5	0/5

post-inoculation), collected, DNA extracted, and qPCR was performed (Figure 3-5A & B). Ticks fed on B31-wt and B31-*rrp1* KI infected mice had an average of ~2.0 and ~2.4 *flaB* copies per 1000 tick genome equivalents indicating establishment of a productive population in ticks. Spirochetes were not detected in ticks fed on mice inoculated with B31-*rrp1* OV or B31-Δ*rrp1*. The results with the B31-*rrp1* OV strain are as expected since this strain did not establish a detectable infection in mice. To determine if the B31-*rrp1* OV and B31-Δ*rrp1* strains can survive in ticks, a mouse-independent route of infecting ticks was employed. Larval ticks were submerged in cultures of each strain and then fed on mice to provide bloodmeal derived nutrients (Figure 3-5B). The efficiency of infecting ticks by this approach was 20 to 40% with each strain except B31-Δ*rrp1* (0%). These data suggest that Rrp1 directly or indirectly regulates processes which are required for survival in ticks.

Aberrant motility and chemotaxis patterns of the B31-Δ*rrp1* and B31-OV strains.

Several approaches were employed to determine if *rrp1* deletion or elevated production of Rrp1 regulates *B. burgdorferi* motility and or chemotaxis. General motility patterns were assessed for spirochetes in BSK-H media with and without 1% methylcellulose using dark-field and differential interference contrast (DIC) microscopy in collaboration with Dr. Lee Szkotnicki. These studies utilized methylcellulose to increase media viscosity in a matrix-dependent manner (74). All strains displayed wave propagation but their translational motion patterns (directional forward movement) and flex frequency differed (Figure 3-6). Note that all figures of motility depict cells that are representative of the population as a whole. Consistent with earlier analyses of *B.*

A.

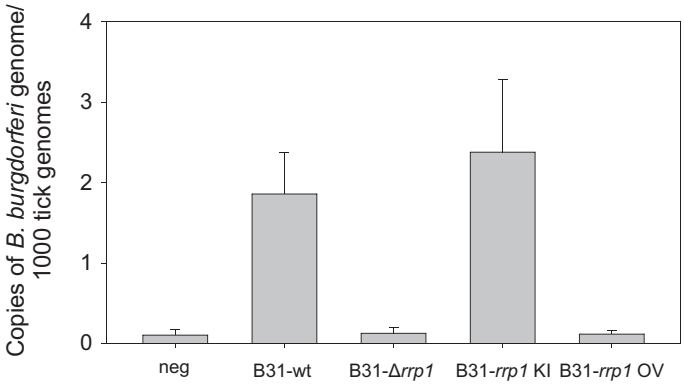

B.

Infection method	B31-wt	B31-Δ*rrp1*	B31-*rrp1* KI	B31-*rrp1* OV
Natural infection	10/10	0/10	10/10	0/10
Immersion	4/10	0/10	2/10	4/10

Figure 3-5. The diguanylate cyclase, Rrp1, is necessary for *Ixodes* infection. Evaluation of spirochete acquisition by *Ixodes* ticks was assessed by qPCR. DNA was isolated from naive ticks fed on infected mice till repletion (Panel A & B). Larval ticks were also immersed into spirochete culture, washed, fed, and assessed for spirochete uptake (Panel B).

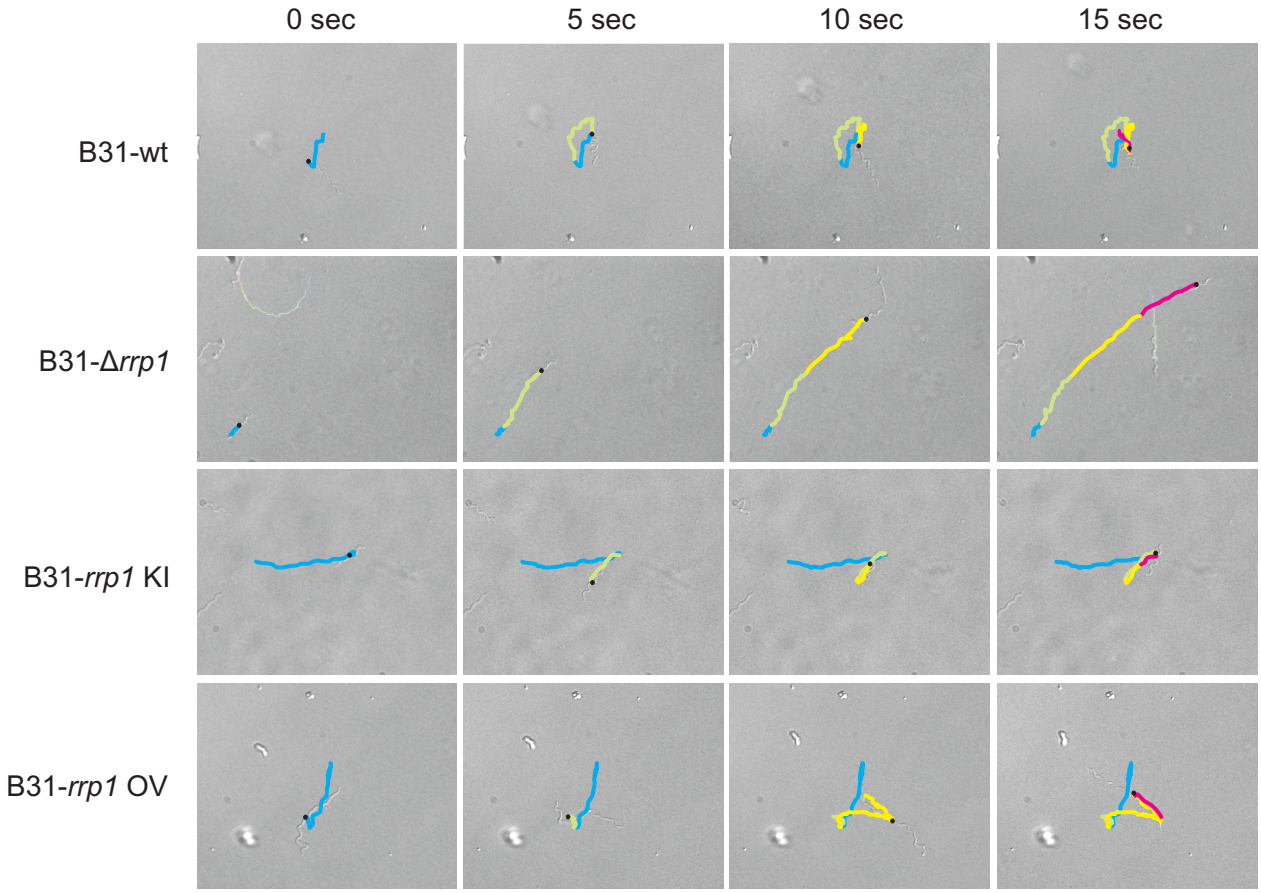

Figure 3-6. Translational motion patterns require Rrp1. Movement patterns of the B31-wt, B31-Δ*rrp1*, B31-*rrp1* KI, and B31-*rrp1* OV strains were visualized using DIC microscopy. Images captured at five sec intervals are shown. Motion tracks were manually recorded and overlayed on the images using motion tracking software. The tracks are colored according to motion achieved during each time lapse (blue - 0 sec, green - 5 sec, yellow - 10 sec, pink - 15 sec).

burgdorferi motility, B31-wt moves short distances, flexes, and reverses direction (Table 3-2) (46,97). Motion-tracking revealed that B31-Δ*rrp1* had a faster run speed and a significantly decreased flex frequency ($p<0.01$). Hence, it was locked in a constant straight run (Table 3-2). In contrast, elevated production of Rrp1 as in the B31-*rrp1* OV strain had no effect on motility patterns. As expected, the B31-*rrp1* KI strain displayed motility patterns consistent with B31-wt. Motility was also assessed in semi-solid media using swarm assays. The B31-Δ*rrp1* swarm diameter was found to be reduced by 47% relative to B31-wt ($p<0.01$). The swarm diameters of B31-*rrp1* KI and B31-*rrp1* OV were similar to B31-wt (Figure 3-7A and B). The results demonstrate that Rrp1, presumably through its production of c-di-GMP, plays an important role in regulating flagellar motor function.

C-di-GMP has been indicated to play a role in regulating chemotaxis in several gram negative enteric bacteria (62). To determine if the presence or absence of Rrp1 directly or indirectly influences chemotaxis, capillary assays were performed using NAG (Figure 3-7C). NAG is a known chemoattractant of *B. burgdorferi* (4,84). The B31-Δ*rrp1* strain was highly attenuated in its NAG driven chemotactic response ($p<0.05$) while the response of B31-*rrp1* OV was not statistically different from that of the B31-wt strain. Complementation of *rrp1* (B31-*rrp1* KI) restored wild type chemotactic responses to B31-Δ*rrp1*. Collectively, the data indicate Rrp1 is required for regulation of flagella motor activity and NAG driven chemotactic responses.

Table 3-2. *rrp1* strain swimming patterns and observations.

Strain	BSK-H	1% methylcellulose
B31-wt	Motile	Translational motion: runs, stops/flexes, reverses Avg run velocity: 4.1426 ± 0.9442 μm/sec Flexes/sec: 0.1738 ± 0.0319
B31-Δ*rrp1*	Motile	Translational motion: runs with very infrequent stops/flexes Avg run velocity: 5.5815 ± 1.3920 μm/sec Flexes/sec: 0.0150 ± 0.0430
B31-*rrp1* KI	Motile	Translational motion; runs, stops stops/flexes, reverses Avg run velocity: 3.9116 ± 0.7613 μm/sec Flexes/sec: 0.1429 ± 0.0679
B31-*rrp1* OV	Motile	Translational motion; runs, stops stops/flexes, reverses Avg run velocity: 4.0359 ± 0.7859 μm/sec Flexes/sec: 0.1593 ± 0.0340

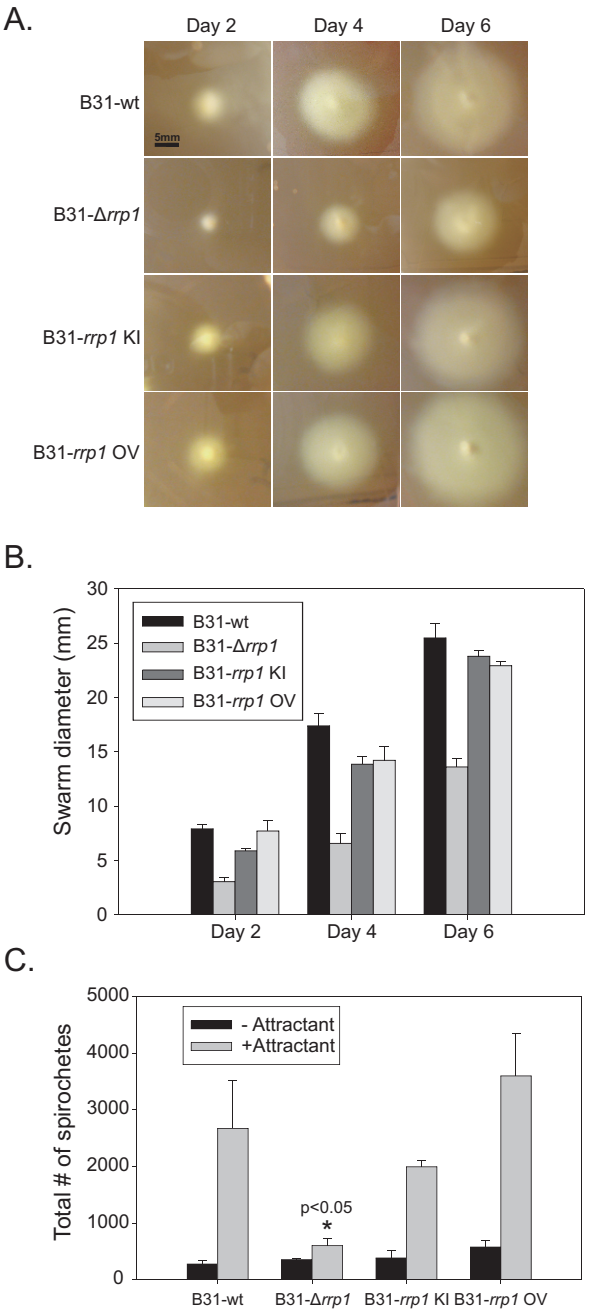

Figure 3-7. Rrp1 positively regulates motility and chemotaxis. The B31-wt, B31-Δ*rrp1*, B31-*rrp1* KI, and B31-*rrp1* OV strain motility and chemotaxis abilities were assessed by swarming assay and capillary chemotaxis assay. *Borrelia* were spotted into punched wells and diameters were measured at day 2, 4 and 6 (Panel B) from the respective swarms (Panel A). Mutant movement toward N-acetyl-D-glucosamine was analyzed by capillary assay. Spirochetes in capillary tubes with and without chemoattractant were counted after a 2 hr incubation at 33º (Panel C). Mutants were compared to B31-wt for statistical analysis.

Transcriptional analysis of genes involved in NAG metabolism.

NAG, which is abundant in ticks and in glycosaminoglycans of mammalian tissue, is required for in vitro growth of *Borrelia* (6). To determine if Rrp1 regulates the transcription of genes involved in NAG metabolism, qRT-PCR analyses were performed. The expression levels of *nagA* (NAG-6-phosphate deaminase), *nagB* (glucosamine-6-phosphate-isomerase), *ptsG* (PTS system, glucose-specific IIBC component), and ORF BB0002 (β-N-acetylhexosaminidase; a putative chitobiase) were examined (Table 3-3). Deletion of *rrp1* resulted in a significant decrease in the amount of *nagA* and *nagB* mRNA but had no effect on BB0002 and *ptsG* (BB0645) transcription. B31-*rrp1* OV also had decreased *nagB* expression but transcription of the other three genes was not significantly affected. These results indicate that Rrp1 directly or indirectly regulates the transcription of important genes involved in the utilization of NAG. The decreased transcription of these genes could influence the ability of *B. burgdorferi* to survive in tissues rich in NAG and in the tick.

Flagellar and chemotaxis gene regulation by Rrp1

Borrelia burgdorferi have complicated and redundant chemotaxis signaling cascades to regulate flagellar motor directional bias, which remain poorly understood. It is generally believed that CheY3 is the main chemotaxis response regulator that is modified in various ways, including phosphorylation and possibly acetylation, to cause adherence to the flagellar motor and ultimately favor rotation in a given direction (58). The Rrp1-mediated modulation of flagellar and chemotaxis gene expression has been demonstrated by microarray studies utilizing a *rrp1* deletion mutant in a non-virulent

Table 3-3. Glucosamine metabolism pathway qRT-PCR analysis of the *rrp1* strains.

Description	Functional Category[a]	Δ*rrp1*/WT	p-value	OV/WT	p-value
BB0002 glycosyl hydrolase family 3 N domain protein (β-–acetylhexosaminidase)	EM	0.2941	0.0536	0.4964	0.0996
BB0151 N-acetylglucosamine-6-phosphate deaminase (*nagA*)	IM	0.4611	0.0029	0.8787	0.2872
BB0152 glucosamine-6-phosphate isomerase (*nagB*)	IM	0.3320	0.0176	0.4331	0.0319
BB0645 PTS system, glucose-specific IIBC component (*ptsG*)	TP	0.4444	0.0921	0.5196	0.1137

a- As published in TIGR *B. burgdorferi* B31MI genome database.

Borrelia burgdorferi strain 5A13 background. qRT-PCR was performed to determine if specific flagellar and chemotaxis genes have altered gene transcription patterns as a response *rrp1* to inactivation or constitutive expression in a pathogenic clone 5A4 background. Primers were designed to evaluate the 54 known flagellar and chemotaxis open reading frames (Appendix A). To date, tests have been completed for 21 of these genes (Table 3-4), but the study remains ongoing. The constitutive strain did not exhibit any significant transcript upregulation or downregulation in the selected motility and chemotaxis panel, however this is expected since B31-*rrp1* OV was not defective in swarming or NAG chemotaxis. Surprisingly, 3 of 21 genes displayed significant variations in transcription including a 3-4 fold induction of the flagellar-specific ATP synthase (*fliI*), flagellar motor switch protein (*fliG2),* and chemotaxis response regulator (*cheY3*) in the *rrp1* deletion mutant. The upregulation of CheY3 was further verified by immunoblot (Figure 3-8). Thus, Rrp1 and by extension c-di-GMP may control chemotaxis by modulating CheY3 directly or indirectly via c-di-GMP effectors.

THE ROLE OF PLZA AND PLZB IN LYME ENZOOTIC CYCLE PROGRESSION

PlzB binds to cyclic-di-GMP with high specificity.

PilZ domain-containing proteins are key c-di-GMP effectors in a variety of bacterial systems. Since this is the only type of effector identified in *Borrelia burgdorferi*, we hypothesized that both *Borrelial* PilZ domain-containing proteins (PlzA and PlzB) could affect enzootic cycle progression, motility, and NAG metabolism in a similar manner as Rrp1. PlzA has been demonstrated to bind specifically to c-di-GMP

Table 3-4. Flagellar and chemotaxis gene qRT-PCR analysis.

Description	Functional Category[a]	KO/WT	p-value	OV/WT	p-value
BB0147 flagellin (*flaB*)	F	1.9131	0.1377	1.1505	0.4166
BB0149 flagellar hook-associated protein 2 (*fliD*)	F	0.8358	0.3620	0.8990	0.4055
BB0180 flagellar protein, putative	F	1.9063	0.1359	1.2763	0.3141
BB0182 flagellar hook-associated protein 3 (*flgL*)	F	1.1670	0.3981	1.2469	0.3343
BB0221 flagellar motor switch protein (*fliG1*)	F	2.6940	0.0999	2.0852	0.1223
BB0279 flagellar basal body-associated protein (*fliL*)	F	2.6364	0.0672	1.1231	0.4129
BB0284 flagellar basal body rod modification protein (*flgD*)	F	1.8132	0.1470	1.7409	0.1918
BB0288 flagellum-specific ATP synthase (*fliI*)	F	4.2110	0.0351	1.6447	0.1780
BB0290 flagellar motor switch protein (*fliG2*)	F	3.9017	0.0443	2.0922	0.1159
BB0291 flagellar MS-ring protein (*fliF*)	F	1.8215	0.1413	1.1362	0.3981
BB0292 flagellar hook-basal body protein (*fliE*)	F	1.9752	0.1256	1.0747	0.4885
BB0294 flagellar basal-body rod protein (*flgB*)	F	2.0803	0.1114	0.8695	0.3944
BB0565 purine-binding chemotaxis protein (*cheW2*)	CH	3.1515	0.0627	1.1502	0.3944
BB0567 chemotaxis histidine kinase (*cheA1*)	CH	2.4525	0.0782	0.6776	0.2380
BB0570 chemotaxis response regulator (*cheY2*)	CH	1.6968	0.1871	0.9292	0.4428
BB0596 methyl-accepting chemotaxis protein (*mcp2*)	CH	0.8193	0.3515	0.8645	0.3871
BB0597 methyl-accepting chemotaxis protein (*mcp3*)	CH	2.2321	0.1175	0.7847	0.3208
BB0671 chemotaxis operon protein (*cheX*)	CH	1.6406	0.1871	0.8420	0.3656
BB0672 chemotaxis response regulator (*cheY3*)	CH	3.3504	0.0482	1.1859	0.3691
BB0680 methyl-accepting chemotaxis protein (*mcp4*)	CH	2.1710	0.0973	0.4550	0.1838
BB0681 methyl-accepting chemotaxis protein (*mcp5*)	CH	1.0431	0.4732	0.4814	0.1377

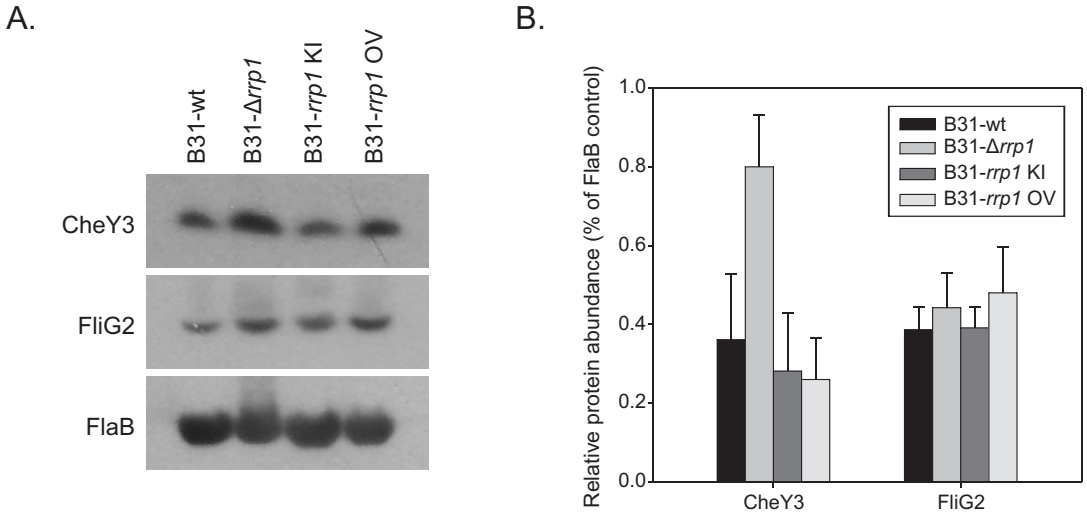

Figure 3-8. Chemotaxis response regulator, CheY3, is upregulated upon *rrp1* deletion. Whole-cell lysates were probed with antisera directed against CheY3 and FliG2 to verify motility and chemotaxis qRT-PCR results. FlaB was included for loading control and normalization purposes. Panel A depicts a representative immunoblot for each antisera tested. Immunoblots from three separate experiments were scanned and evaluated by spot densitometry analysis to determine protein abundance relative to FlaB (Panel B).

through the RxxxR binding motif located within the protein interior (27). Since PlzB possesses the same conserved binding motif, the ability of PlzB to bind c-di-GMP was assessed using ligand binding assays (study performed by John Courtland Freedman, Marconi laboratory graduate student). As previously demonstrated with PlzA, PlzB binds to c-di-GMP with high specificity as compared to PlzB incubated with the cold competitor nucleotides GTP, ATP, cAMP, or cGMP. Coincubation of PlzB with radiolabeled c-di-GMP and its cold c-di-GMP competitor displayed decreased signal as compared to PlzB incubated with the radiolabeled dinucleotide alone, demonstrating that the binding abilities of PlzB are specific for c-di-GMP (Figure 3-9).

Generation and characterization of a *plzA* deletion mutant and a *plzB* cis-complemented strain.

The gene encoding PlzA is chromosomally located in all *B. burgdorferi* strains, while *plzB* is only found on a plasmid in a few isolates. Hence, PlzB may not be critical to strain virulence but could functionally complement PlzA for specific cellular processes. To understand the role of both PlzA and PlzB in the pathogenesis of *Borrelia burgdorferi,* allelic exchange mutagenesis was employed. The constructs for allelic exchange mutagenesis were generated by Elizabeth Abdunnur, PhD (a former postdoctoral research of the Marconi laboratory) and John Courtland Freedman. *plzA* was first deleted from *B. burgdorferi* strain B31-5A4 by replacement of the ORF with a spectinomycin/streptomycin resistance cassette (*strep*^{R}) to yield the strain B31-Δ*plzA* (Figure 3-10A). A *cis*-complemented *plzA* strain was generated by replacing the *strep*^{R} cassette of B31-Δ*plzA* with the *plzA* ORF and a downstream kanamycin resistance

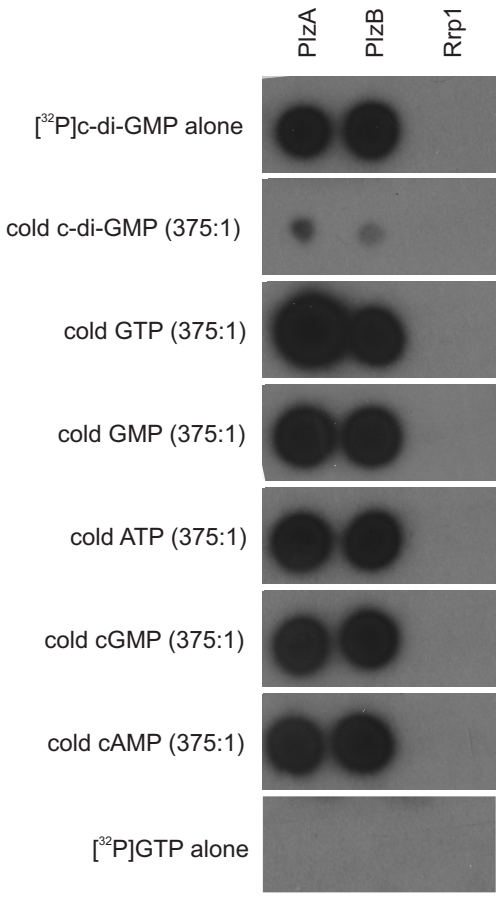

Figure 3-9. *Borrelia burgdorferi* PlzB binds to c-di-GMP with high specificity. r-PlzA, r-PlzB, and r-Rrp1 were expressed with N-terminally located maltose binding protein (MBP) fusions and evaluated for their [^{32}P]c-di-GMP binding capabilities. Competitive inhibitors tested are listed to the left of each panel with the respective inhibitor to [^{32}P]c-di-GMP ratio. The panels located at the top and second from the bottom were only screened with the indicated nucleotide.

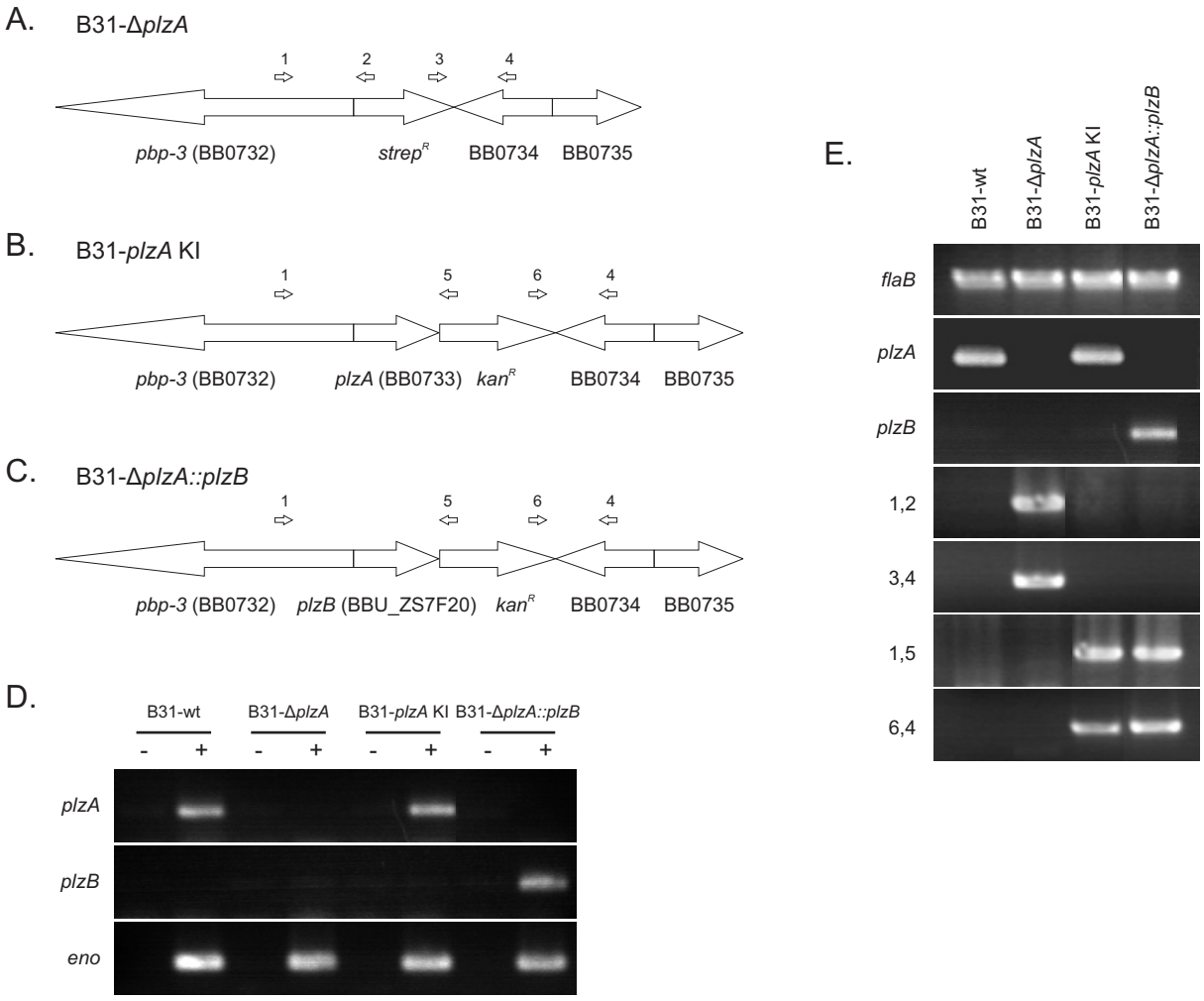

Figure 3-10. Generation and confirmation of *plzA* deletion and complementation. The chromosome of the B31-Δ*plzA,* B31-*plzA* KI, and B31-Δ*plzA::plzB* mutants after allelic replacement are depicted in Panel A, B, and C, respectively. Successful mutagenesis was verified by RT-PCR (Panel D) and PCR analysis (Panel E). RT-PCR was performed with and without reverse transcriptase. Primers used for validation of proper integration are indicated by numbers above the schematic arrows and are listed to the left of the respective PCR panels. All primers used are listed in Appendix A.

cassette (*kan*^{R}) (Figure 3-10B). This strain was designated B31-*plzA* KI (KI indicating "knock-in"). Lastly, *plzA* was replaced by *plzB* and a downstream kanamycin resistance cassette to produce the B31-Δ*plzA::plzB* strain (Figure 3-10C). The B31-Δ*plzA::plzB* strain was produced by John Courtland Freedman. Clonal populations of each strain were evaluated for proper insertion of the cassette using PCR and multiple primer sets (Figure 3-10E). Multiple clones of each strain harboring the expected insertions were identified. The plasmid content of each clone was determined using plasmid specific primer sets in PCR analyses (data not shown). Only clones possessing the 21 circular and linear plasmids carried by the parental strain (B31-wt) were selected for further analyses. Using RT-PCR analyses we confirmed that *plzA* transcription was eliminated in the B31-Δ*plzA* strain only and *plzB* was only transcribed in the B31-Δ*plzA::plzB* mutant (Figure 3-10D).

Spirochete growth rate was evaluated to identify potential growth defects (in collaboration in John Courtland Freedman). Each strain was cultivated in BSK-H media at 27º, 33º, and 37º (Figure 3-11). The average number of spirochetes per ten fields (400X magnification) was recorded for 20 days at 24 h intervals. All strains tested had similar growth patterns.

PlzA is essential for establishing murine infection.

To evaluate if PlzA or PlzB is important for mammalian infection, C3H-HeJ mice were subcutaneously injected with each strain. Four weeks post-inoculation, spirochete infectivity was assessed by multiple approaches. Whole-cell ELISA (Figure 3-12A) and immunoblot (Figure 3-12B) were employed to analyze seroconversion of each mouse.

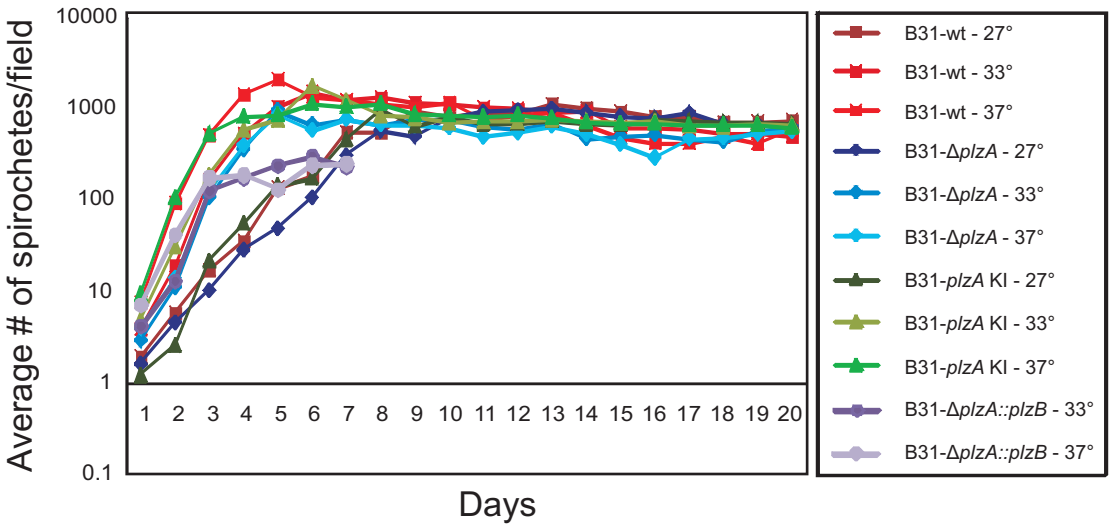

Figure 3-11. Growth curve analysis of *plzA* and *plzB* strains. Spirochetes were grown for twenty days at 27°, 33°, and 37°. Average number of cells per ten 400X fields of magnification was calculated every 24 h for 20 days.

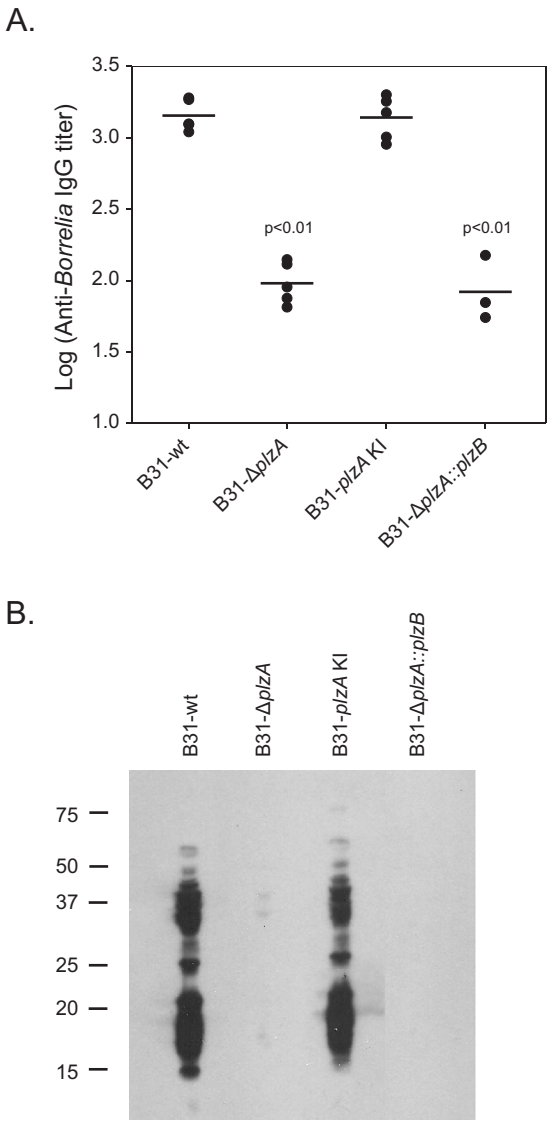

Figure 3-12. PlzA is essential to mammalian infection. C3H-HeJ mice were inoculated by a subcutaneous needle injection with 10^4 spirochetes per strain. Four weeks post-infection, mice were bled by tail-nick and sera was isolated. Seroconversion was assessed using whole-cell ELISA (Panel A) and immunoblot (Panel B).

Both the B31-wt and B31-*plzA* KI elicited an immunological response with equivalent IgG titers, while the B31-Δ*plzA* and B31-Δ*plzA::plzB* strains were not positive for seroconversion ($p<0.01$). Immunoblots with B31-wt whole cell lysates and pooled sera samples were used to verify the ELISA results and visually compare the antibody responses of each strain. The protein banding pattern of the B31-wt and B31-*plzA* KI strain was similar, indicating antigenic profiles were unaltered by the genetic manipulation. As previously indicated by ELISA, the deletion mutant nor *plzB* complement did not produce immunological responses.

Upon sacrifice, biopsies and organs were collected and immediately placed in BSK-H media for cultivation to analyze spirochete survival within the isolated tissues. All cultures were positive, except the B31-Δ*plzA* and B31-Δ*plzA::plzB* strains did not yield any outgrowth (Table 3-5) (B31-Δ*plzA::plzB* strain cultivation was performed by John Courtland Freedman). This data is consistent with the immunological studies, showing the deletion mutant was unable to establish a productive infection within mice and the B31-Δ*plzA::plzB* strain was not able to replace the function of PlzA in a mammalian disease model.

Infection and survival in *Ixodes scapularis* ticks does not require PlzA or PlzB.

To test the ability of the *plz* strains to persist within ticks, immersion feeding was investigated. Laboratory reared, pathogen free, naive *Ixodes scapularis* larval ticks were immersed in actively growing cultures of each strain and then fed on naive mice until repletion. qPCR of DNA extracted from the ticks revealed that all strains tested were able to establish productive populations (Table 3-6). Additionally, the naive mice

Table 3-5. Plz mutant murine infection study.

Strain	# spirochete positive cultures from each tissue or organ biopsy			
	bladder	heart	skin	# of culture positive / # tested
B31-wt	5/5	5/5	5/5	5/5
B31-Δ*plzA*	0/5	0/5	0/5	0/5
B31-*plzA* KI	5/5	5/5	5/5	5/5
B31-Δ*plzA::plzB*	0/3	0/3	0/3	0/3

Table 3-6. Plz strain tick to mouse spirochete transmission.

Strain	# of ticks positive / # tested	# of mice positive / # tested
B31-wt	10/10	3/3
B31-Δ*plzA*	8/10	0/3
B31-*plzA* KI	8/10	1/3
B31-Δ*plzA::plzB*	10/10	0/3

used for the feeding were assayed for seroconversion by whole-cell ELISA and immunoblot (Figure 3-13) to evaluate spirochete natural transmission. Confirming infection results via subcutaneous inoculation, the B31-Δ*plzA* and B31-Δ*plzA::plzB* strains were incapable of establishing an infection by tick transmission. Therefore, it can be concluded that PlzA and PlzB are not required for *B. burgdorferi* to infect ticks.

Aberrant motility and chemotaxis patterns of the B31-Δ*plzA* and B31- Δ*plzA::plzB* strains.

The potential effects of *plzA* deletion and replacement with *plzB* on spirochete motility and chemotaxis were investigated. The motility of each strain was analyzed by DIC microscopy (study conducted by Lee Szkotnicki, PhD). Still images from 0, 10, and 20 sec time points of a representative movie for each strain are presented in Figure 3-14. All strains were capable of translational motion. B31-wt exhibited normal motility patterns with a short run, followed by turns, flexes, and direction reversal (Table 3-7). B31-Δ*plzA* had significantly slower run speeds than wild-type and a reduced flexing frequency, resulting in a slow constant run with infrequent stops ($p<0.01$). The B31-*plzA* KI strain displayed motion patterns consistent with B31-wt, while the B31-Δ*plzA::plzB* mutant exhibited a phenotype similar to the *plzA* deletion mutant with a reduced average run velocity and flexing frequency ($p<0.01$). To further assess the motion patterns defects associated with PlzA deletion, swarm assays were performed in BSK-H semi-solid media (Figure 3-15). Both B31-Δ*plzA* and B31-Δ*plzA::plzB* had significantly reduced swarms relative to B31-wt by approximately 43% ($p<0.05$). The B31-*plzA* KI swarm diameter was comparable to B31-wt. N-acetyl-D-glucosamine

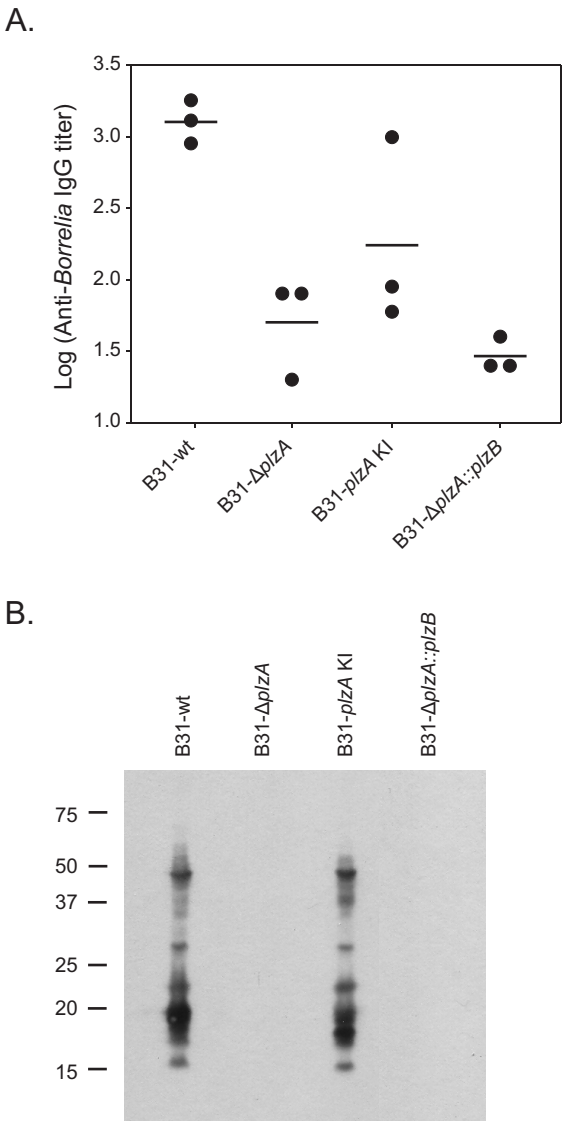

Figure 3-13. Tick to mouse transmission requires PlzA. Ticks infected by immersion methods were fed on C3H-HeJ mice. Four weeks post-infection, mice were bled by tail-nick and sera was isolated. Seroconversion was assessed using whole-cell ELISA (Panel A) and immunoblot (Panel B). The circles in Panel A represent individual mice.

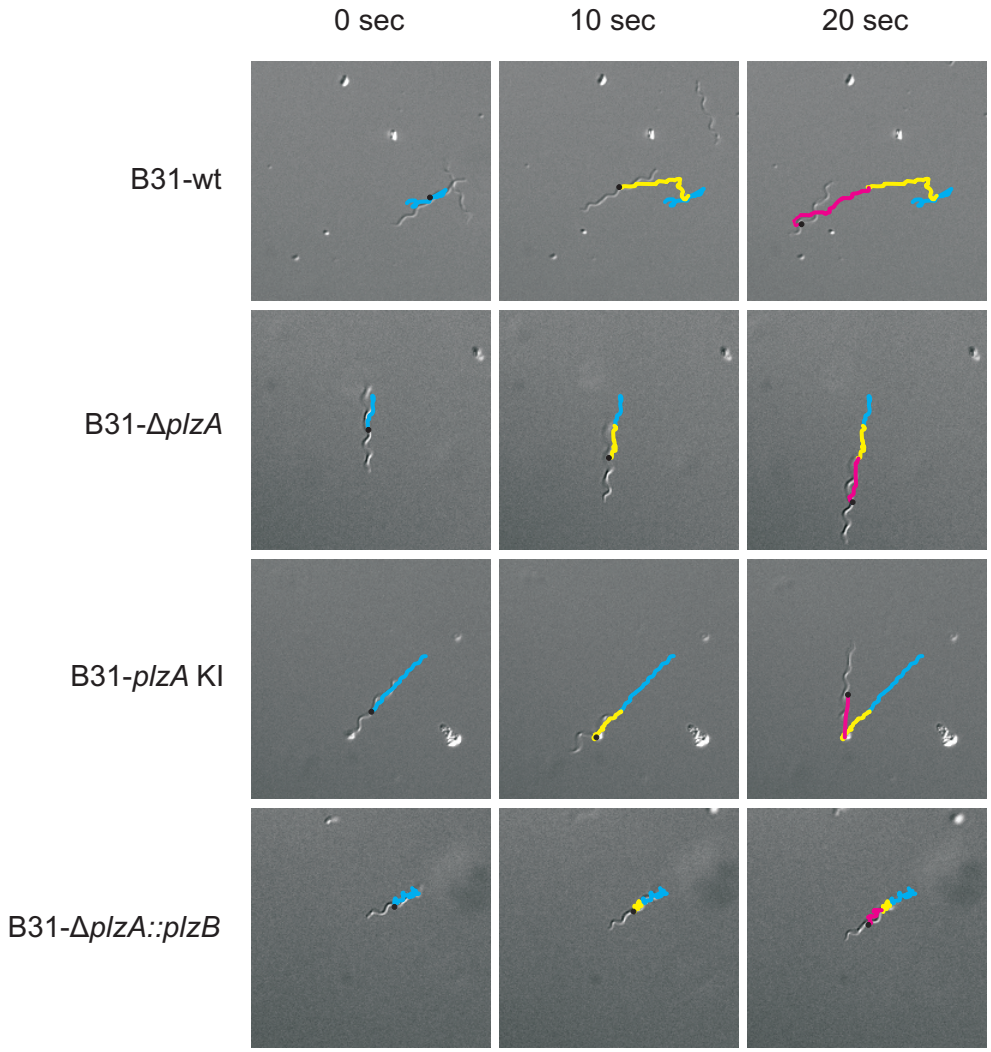

Figure 3-14. Deletion of *plzA* prevents translational motion. DIC microscopy was utilized to track the movement patterns of the strains. Images were captured at five sec intervals. Spirochete tracks were manually recorded and overlayed on the images using motion tracking software. Motion acheived during each time lapse is color coded according to the respective 10 sec period (blue - 0 sec, yellow - 10 sec, pink - 20 sec).

Table 3-7. Motility analysis of *plzA* and *plzB* strains.

Strain	BSK-H	1% methylcellulose
B31-wt	Motile	Translational motion: runs, stops/flexes, reverses Avg run velocity: 4.1578 ± 0.7788 μm/sec Flexes/sec: 0.0783 ± 0.0313
B31-Δ*plzA*	Motile	Translational motion: runs with very infrequent stops/flexes and low speed Avg run velocity: 1.6500 ± 0.7339 μm/sec Flexes/sec: 0.0043 ± 0.0115
B31-*plzA* KI	Motile	Translational motion; runs, stops stops/flexes, reverses Avg run velocity: 4.1706 ± 0.8714 μm/sec Flexes/sec: 0.1024 ± 0.0541
B31-Δ*plzA::plzB*	Motile	Translational motion; runs, stops stops/flexes, reverses Avg run velocity: 1.5793 ± 0.7369 μm/sec Flexes/sec: 0.0078 ± 0.0109

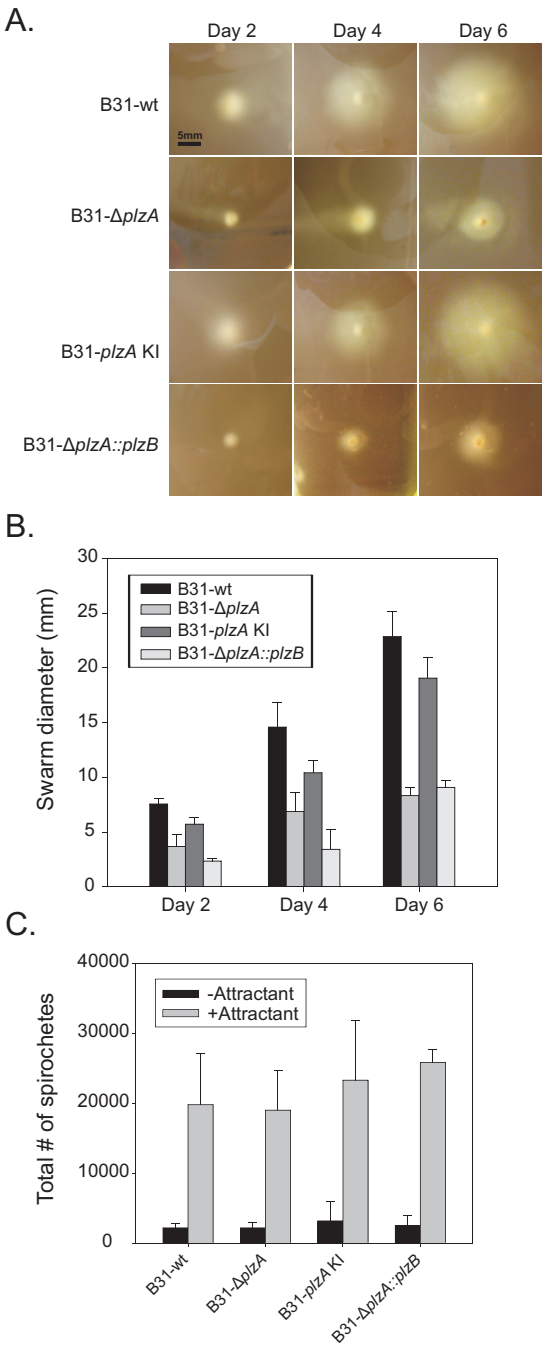

Figure 3-15. PlzA positively regulates motility. The B31-wt, B31-Δ*plzA,* B31-*plzA* KI, B31-Δ*plzA::plzB* were evaluated for motility and chemotaxis abilities by swarming and capillary chemotaxis assay. Spirochetes were spotted into punched wells of agarose plates. Diameters were measured 2, 4, and 6 days post-plating (Panel B). Representative swarms are shown in Panel A. Strain migration towards N-acetyl-D-glucosamine was tested by capillary assay (Panel C). Spirochetes contained within capillary tubes were enumerated after a 2 h incubation at 33° with or without chemoattractant.

(NAG) capillary chemotaxis assays were utilized to determine if the deficiency is due to reduced migration towards defined chemoattractants (Figure 3-15C). All strains exhibited a NAG chemotactic response. Altogether, this data suggests that PlzA is necessary for proper flagellar motor regulation but not NAG chemotaxis, second that its role in *Borrelial* motility cannot be complemented by PlzB.

Transcriptional analysis of the genes involved in the NAG metabolic pathway.

Intracellular c-di-GMP levels are suggested to impact NAG chemotaxis and genes involved in NAG metabolism (41). Since PlzA is a c-di-GMP effector and shown by capillary assay to not regulate NAG chemotaxis, qRT-PCR analysis was conducted to confirm PlzA does not elicit a change in NAG metabolism, as was seen by the diguanylate cyclase. The expression levels of *nagA* (NAG-6-phosphate deaminase), *nagB* (glucosamine-6-phosphate-isomerase), *ptsG* (PTS system, glucose-specific IIBC component), and ORF BB0002 (β-N-acetylhexosaminidase; a putative chitobiase) were analyzed (Table 3-8). Gene expression was not significantly affected by the deletion of *plzA*, verifying the capillary chemotaxis assay results.

THE PHOSPHODIESTERASE, PDEB, REGULATES TRANSMISSION FROM *IXODES* TICKS

Production of a *pdeB* deletion mutant and its cis-complemented strain.

C-di-GMP levels are balanced and controlled by the opposing activities of the diguanylate cyclases and phosphodiesterases. *B. burgdorferi* possess both an EAL and

Table 3-8. Glucosamine metabolism pathway qRT-PCR analysis of the *plzA* strains.

Description		Functional Category[a]	Δ*plzA*/WT	p-value
BB0002	glycosyl hydrolase family 3 N domain protein (β-acetylhexosaminidase)	EM	0.9925	0.6647
BB0151	N-acetylglucosamine-6-phosphate deaminase (*nagA*)	IM	1.2394	0.9541
BB0152	glucosamine-6-phosphate isomerase (*nagB*)	IM	0.6016	0.3299
BB0645	PTS system, glucose-specific IIBC component (*ptsG*)	TP	0.3721	0.3721

HD-GYP phosphodiesterase (PdeA and PdeB, respectively) for c-di-GMP degradation. Since disruption of *pdeA* prevented mammalian infection (97) similarly to the constitutive diguanylate cyclase strains (B31-*rrp1* OV), we hypothesized that mutagenesis of *pdeB* would also impact pathogen virulence. The study detailed below was performed in collaboration with Dr. Lee Szkotnicki.

To understand the role of PdeB in *B. burgdorferi* pathogenesis, allelic exchange mutagenesis was utilized to delete and complement *pdeB* in the infectious B31-5A4 clone (performed by Lee Szkotnicki, PhD). Generation of the deletion mutant (B31-Δ*pdeB*) involved the replacement of the gene ORF with a spectinomycin/streptomycin resistance cassette (*strep*^{R}) (Figure 3-16A). Complementation was achieved by reinserting *pdeB* in its original chromosomal location with a 3' flanking kanamycin resistance cassette (*kan*^{R}) (Figure 3-16B). This strain was designated B31-*pdeB* KI. Successful transformants were screened for proper construct integration by PCR (Figure 3-16D) using multiple primer sets shown in Appendix A. Clones of each strain containing the desired insertions were subsequently screened for plasmid content (data not shown). All selected clones possessed the complete set of 21 circular and linear plasmids present within the parental B31-5A4 strain. The disruption of *pdeB* transcription and reestablishment of expression by the selected B31-Δ*pdeB* and B31-*pdeB* KI clones, respectively, was confirmed by qRT-PCR analyses (Figure 3-16C).

Growth rate of each strain was assessed to determine if growth defects arose from genetic manipulation of *pdeB*. Spirochetes were cultivated in BSK-H media at 27º, 33º, and 37º (Figure 3-17) (assay conducted by Lee Szkotnicki, PhD). The average number of spirochetes per ten fields (400X magnification) was recorded for 13 days at

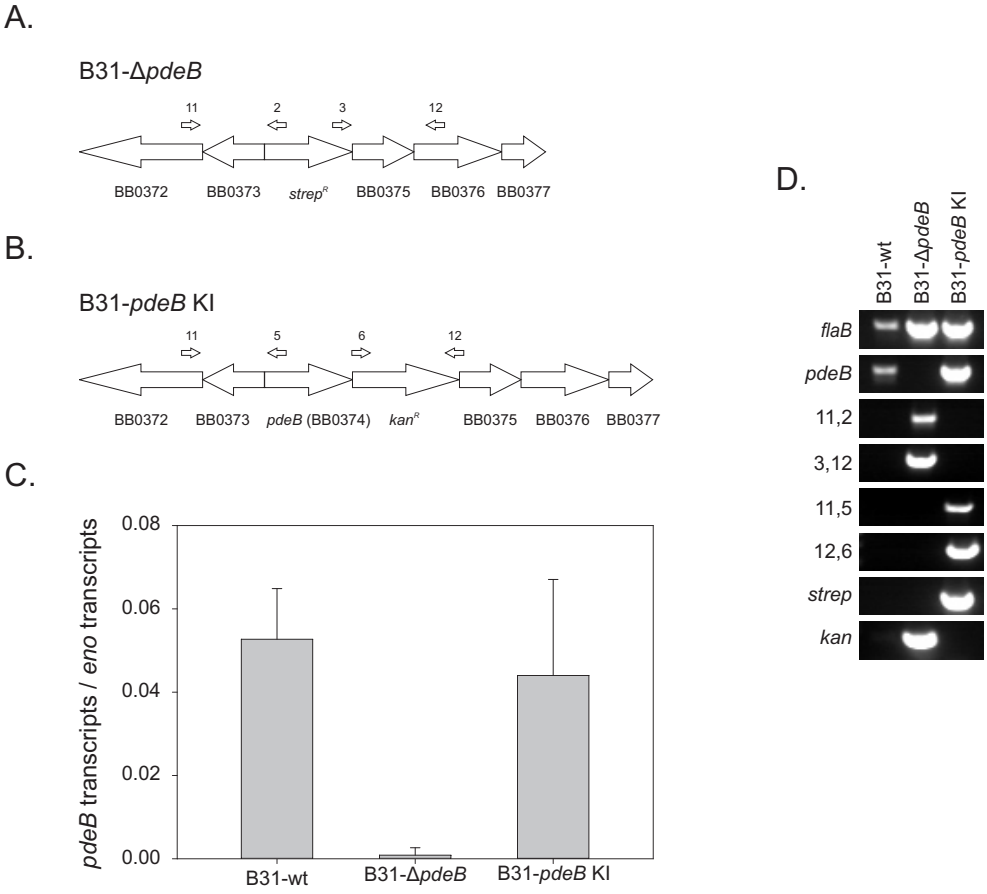

Figure 3-16. Construction and verification of *pdeB* deletion and complementation mutants. Panel A and B display schematics representing the chromosome of the B31-Δ*pdeB* and B31-*pdeB* KI mutants after allelic exchange mutagenesis. Successful recombination was verified by qRT-PCR (Panel C) and PCR analysis (Panel D). Primers used for validation of proper integration are indicated by numbers above the schematic arrows and are listed to the left of the respective PCR panels. All primers used are listed in Appendix A.

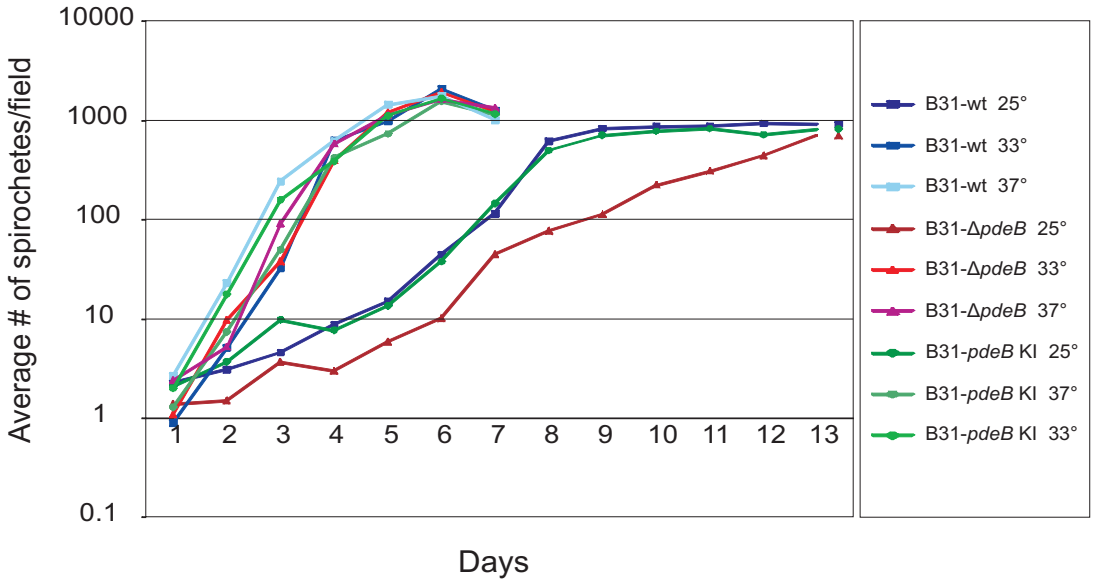

Figure 3-17. PdeB strains exhibit normal growth patterns. Strain growth curves were assessed for thirteen days at 25°, 33°, and 37°. Spirochetes were enumerated every twenty four hours and average number of cells per ten 400X magnification field was calculated.

24 h intervals. No significant growth differences were discovered between the mutants and the wild type strain at the various temperatures.

Murine infection via needle inoculation does not require PdeB.

To identify if PdeB is essential for mammalian infection, C3H-HeJ mice were subcutaneously inoculated with 10^4 spirochetes of each strain (study performed in collaboration with Lee Szkotnicki and assistance from Katie Mallory). Four weeks post-inoculation, the spirochete infection capabilities were evaluated using cultivation and seroconversion methods. Bladder, heart, and skin tissue biopsies were harvested from each mouse after sacrifice and inserted immediately into BSK-H growth media for *Borrelia* cultivation (Table 3-9). The B31-wt, B31-Δ*pdeB*, and B31-*pdeB* KI strains all yielded outgrowth from every tissue, demonstrating PdeB is not necessary for disease establishment of *B. burgdorferi*. To confirm biopsy cultivation results, whole-cell ELISA (Figure 3-18A) and immunoblot (Figure 3-18B) were employed to assess murine immunological responses. As shown by the tissue outgrowth, all strains retained the infection abilities of the B31-wt strain as indicated by the production of equivalent IgG titers. Immunoblots, with B31-wt whole cell lysates and pooled sera, also displayed identical banding patterns which verify antigenic similarity between the tested strains.

PdeB is critical for natural transmission via infected *Ixodes* ticks.

Despite lacking significance in murine infection by needle inoculation, the PdeB still could serve as a key factor in tick colonization and *Borrelial* enzootic cycle progression. To first identify if deletion of *pdeB* inhibits spirochete transfer to ticks,

Table 3-9. Murine study of *pdeB* mutant infection capabilities.

Strain	# spirochete positive cultures from each tissue or organ biopsy			
	bladder	joint	skin	# of culture positive / # tested
B31-wt	3/3	3/3	3/3	3/3
B31-Δ*pdeB*	3/3	3/3	3/3	3/3
B31-*pdeB* KI	3/3	3/3	3/3	3/3

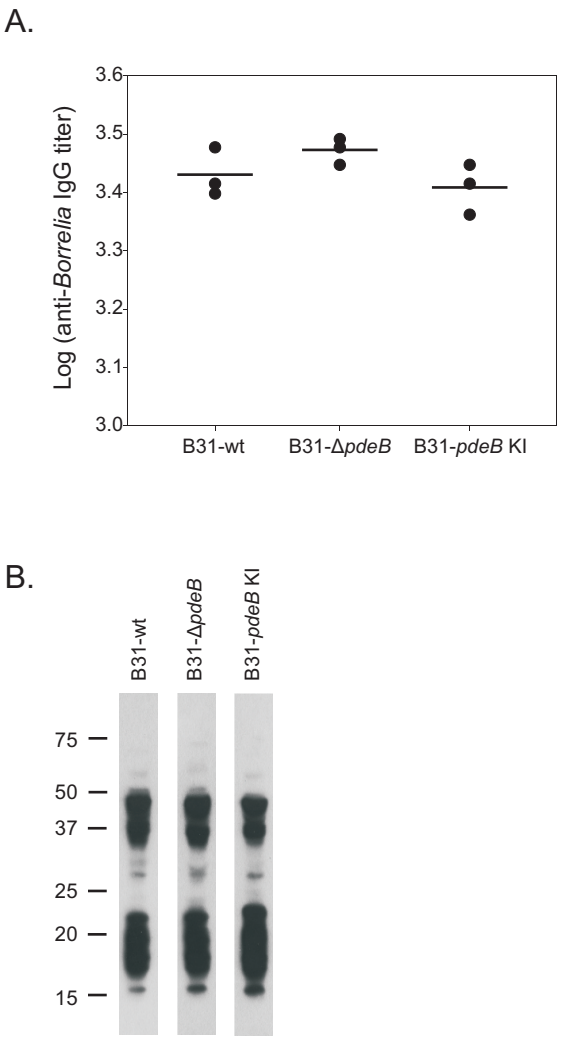

Figure 3-18. PdeB is not essential for murine infection via subcutaneous needle inoculation. Immersion-infected ticks were fed on C3H-HeJ mice. Four weeks post-infection, mice were bled by tail-nick and sera was isolated. Seroconversion was assessed using whole-cell ELISA (Panel A) and immunoblot (Panel B). The circles in Panel A represent individual mice.

three mice per strain were needle inoculated subcutaneously. Four weeks post-inoculation, infection was confirmed (as described above) and naive larval *Ixodes* ticks were allowed to feed on the mice until repletion. qPCR was performed on DNA isolated from the collected ticks one week post-feeding. All strains were capable of infection; however the B31-Δ*pdeB* strain infected at a lower frequency (20%) than B31-wt (80%) and B31-*pdeB* KI (100%) (Table 3-10). To assess whether this decreased tick colonization efficiency affects natural transmission to uninfected mice, naïve larval ticks were infected by each strain via immersion methods and then fed on naïve mice. Tick colonization frequency was assessed by qPCR. All strains were efficient in tick infection ability by both methods. B31-Δ*pdeB* was more readily acquired by ticks using immersion techniques compared to natural tick infection.

Spirochete transmission to the naïve mice was evaluated by biopsy cultivation (Table 3-10) and seroconversion analysis (Figure 3-19). Surprisingly, B31-Δ*pdeB* was not able to persist in mice via tick bite as was done by B31-wt and B31-*pdeB* KI, despite its ability to establish murine infection by needle inoculation. This suggests that *pdeB* has a functional role in spirochete transmission and migration between hosts or that *pdeB* could interfere with tick colonization processes, as implicated by decreased tick colonization efficiency. In addition, the deletion mutant presents a unique infection phenotype which is not presented by any of the c-di-GMP network *Borrelia* mutants constructed and tested thus far, including the *pdeA* deletion strain of Sultan et al (97). Thus, this indicates that *pdeB* may have an additional function in vivo which is not shared by the EAL phosphodiesterase, PdeA.

Table 3-10. Acquisition and transmission of the *pdeB* mutants.

Strain	Natural	Immersion	
	# of ticks positive / # tested	# of ticks positive / # tested	# of mice cultivation positive / # tested
B31-wt	8/10	8/10	3/3
B31- Δ*pdeB*	2/10	5/10	0/3
B31-*pdeB* KI	10/10	6/6	2/3

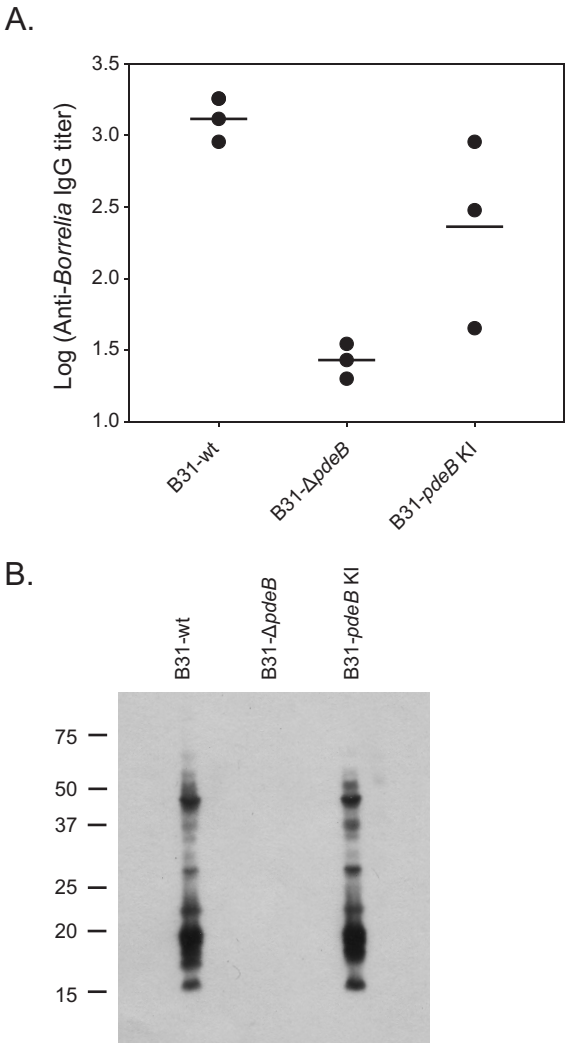

Figure 3-19. Natural spirochete transmission requires *pdeB*. C3H-HeJ mice were inoculated with 10^4 spirochetes per strain by a subcutaneous injection. Four weeks post-infection, mice were bled by tail-nick and sera was isolated. Whole-cell ELISA (Panel A) and immunoblot (Panel B) were used to evaluate seroconversion. The circles in Panel A represent individual mice.

Induction of abnormal spirochete morphology and motility upon *pdeB* deletion.

To investigate the impact of *pdeB* on spirochete motility, DIC microscopy was coupled with motion tracking software to evaluate the motion patterns of each strain (analysis performed by Lee Szkotnicki, PhD). Movies were recorded and overlaid with tracks of cellular motion. Still images from 0-7 sec time points of a representative movie for each strain are presented in Figure 3-20. Both the B31-wt and B31-*pdeB* KI strains retained normal flat wave morphology, as well as translational motion patterns. However, B31-Δ*pdeB* possessed an abnormal morphology and loss of cellular waves. The strain also exhibited a constant flexing phenotype and was incapable of translational motion when visualized in BSK-H containing 1% methylcellulose. This may be due to disruption of normal flagellar structure and bundles, which could prevent cellular translational movement. As well, regulation of the flagellar motor direction could be altered to lock both flagellar bundles rotating in the same direction, causing a flex.

Further analyses were conducted to determine if this motility defect correlates with swarming and chemotaxis capabilities utilizing swarming (Figure 3-21A &B) and NAG capillary chemotaxis assays (Figure 3-21C) (study performed in collaboration with Lee Szkotnicki, PhD). Interestingly, B31-Δ*pdeB* was able to swarm (with only a 30% reduction) and chemotax despite the lack of translational motion in BSK-H containing 1% methylcellulose and the obvious defect in flat wavelength morphology. Thus, the reduced swarming is not due to changes in NAG chemotaxis and may be a result of the disruption of cellular flat wave morphology and state of flexing.

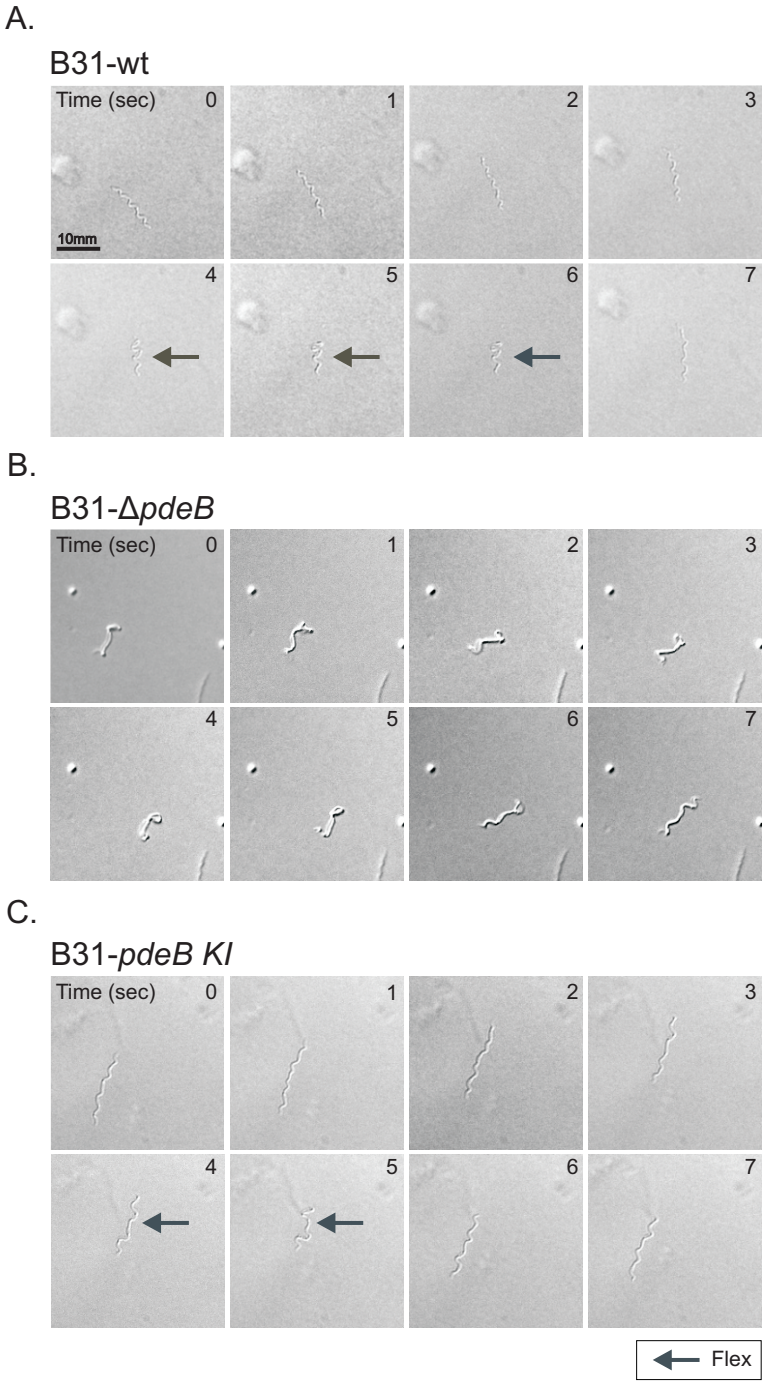

Figure 3-20. *pdeB* deletion alters spirochete morphology and motility. To assess the motility patterns, cells were assessed by DIC microscopy and time lapse imaging. Still images captured at one sec intervals are presented above. Flexes are indicated in Panel A & C, while B31-Δ*pdeB* (Panel B) remains in a state of constant flexing.

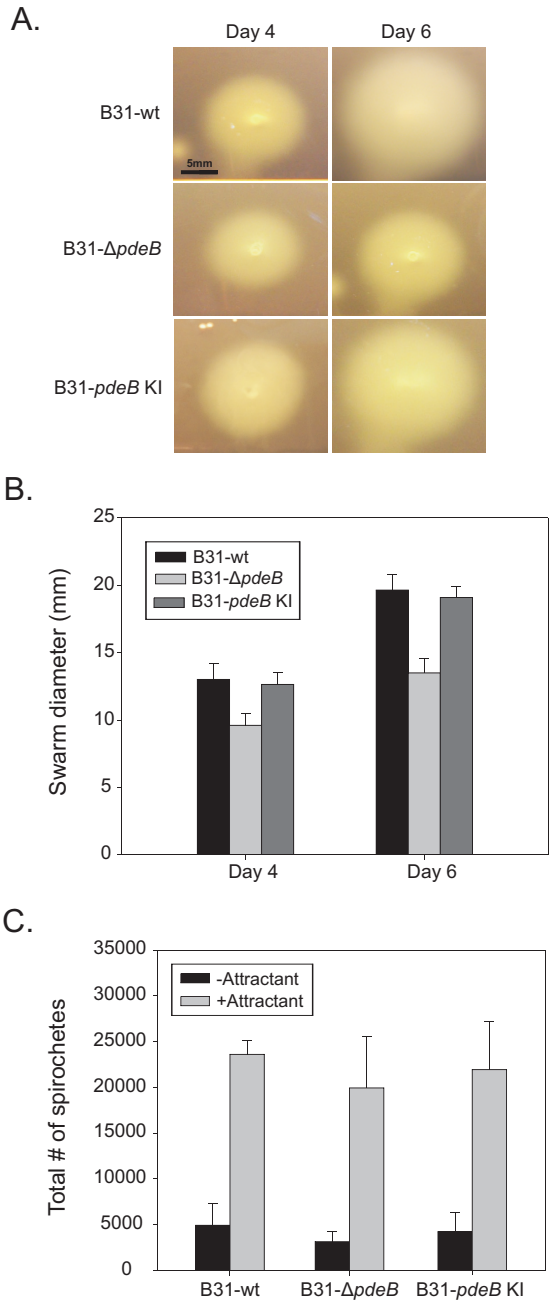

Figure 3-21. Deletion of *pdeB* results in decreased spirochete swarming. Spirochetes were spotted into punched wells of agarose plates to measure strain swarming. Diameters were measured 2, 4, and 6 days post-plating (Panel B). Representative swarms are shown in Panel A. Spirochete chemotaxis towards N-acetyl-D-glucosamine was evaluated by enumerating cells expelled from capillary tubes after a 2 h incubation at 33° with or without chemoattractant (Panel C).

CHAPTER 4: DISCUSSION

In the Lyme disease spirochete, *B. burgdorferi,* c-di-GMP has been postulated to regulate cellular processes required for completion of the enzootic cycle (27,63,70,97). Until the completion of this study and recent work by Motaleb and colleagues, the *Borrelial* c-di-GMP signaling network remained uncharacterized and its role in Lyme pathogenesis completely unknown. Since 2009, this area of study has rapidly expanded and provided significant new insight into the genetic regulatory mechanisms of the *B. burgdorferi* enzootic cycle and c-di-GMP signaling in arthropod-borne pathogens.

Rrp1 regulation of virulence and chemotaxis.

The synthesis of c-di-GMP was the initial research target to understand how production of Rrp1, the sole diguanylate cyclase, affected intracellular c-di-GMP concentrations, as well as regulation of the *Borrelial* genome. Previous studies demonstrated that the deletion of *rrp1* results in pronounced changes within the *B. burgdorferi* transcriptome and identified key groups of genes which are regulated by the diguanylate cyclase including flagellar biosynthesis, chemotaxis, transport, and nucleotide/amino acid metabolism (70). Since Rrp1 lacks a DNA binding domain or other known functional domains, its regulatory capability is thought to be linked specifically to its diguanylate cyclase activity. Until this study, the potential requirement

for c-di-GMP over the course of the enzootic cycle of a tick-borne bacterial pathogen has not been assessed. Recent analyses of *B. burgdorferi pdeA* (EAL domain phosphodiesterase) and *plzA* (PilZ domain c-di-GMP binding protein) mutants, which display attenuated virulence, have provided indirect evidence that c-di-GMP is an important regulatory molecule in vivo (63,97). The Lyme disease spirochetes offer an excellent model system for studying diguanylate cyclase mediated regulation over the course of the enzootic cycle because *B. burgdorferi* can be genetically manipulated and there is a well characterized and biologically relevant mouse-tick enzootic model.

In this study, we tested the hypothesis that high c-di-GMP levels interfere with passage of spirochetes from ticks to mammals (transmission stage) while the absence of c-di-GMP attenuates the ability of *B. burgdorferi* to transit from mammals to ticks (acquisition phase). To assess these possibilities, strains that lack *rrp1* (B31-Δ*rrp1*) or produce it at elevated levels (B31-OV) were generated. While B31-Δ*rrp1* retained its ability to infect mice the B31-OV strain was not infectious. B31-Δ*rrp1* was also found be less efficient at dissemination and/or secondary colonization as it was not cultivated from heart biopsies and was inconsistently cultured from biopsies collected from sites distal to the inoculation site. In addition, while B31-Δ*rrp1* readily infected mice, natural tick feeding experiments revealed that this strain is not able to transit into ticks and establish a productive population. Recently, this phenotype was shown to be exhibited by a strain possessing an inactive form of the cognate histidine kinase of Rrp1, Hpk1, providing further evidence that Rrp1 function and c-di-GMP synthesis is required for spirochete survival within ticks (16). Because B31-OV cannot infect mice, we were not able to assess its potential to transit from mammals to ticks via natural tick feeding. To

allow us to assess the ability of this strain to survive in ticks an immersion feeding approach was employed (64). B31-OV established a productive population in ticks while B31-Δ*rrp1* did not. The data presented here and in earlier studies suggest that c-di-GMP levels regulate processes involved in transmission, acquisition, and survival of *B. burgdorferi* in ticks (70,97).

The inability of the B31-Δ*rrp1* to transit from ticks to mammals and/or survive in ticks could be due to impaired chemotactic responses or the inability to efficiently utilize tick derived nutrients. Earlier transcriptional analyses demonstrated that genes which encode proteins involved in chemotaxis (*che* and *mcp*) and NAG utilization (*nagA* and *nagB*) are positively regulated by Rrp1 (70). Consistent with the transcriptional data, a 75% reduction in the chemotactic response of B31-Δ*rrp1* to NAG was observed. Complementation restored wild type chemotactic responses to NAG. Wild type levels of *nagA* and *nagB* transcription were also restored by complementation. NAG, which is a major constituent of chitin and chitobiose, is highly abundant in the peritrophic membrane of the tick midgut (75,110). The inability of B31-Δ*rrp1* to pass from infected animals into ticks could be due to the reduced ability of this strain to sense tick derived NAG and migrate to the tick bite site. It stands to reason that efficient acquisition would be dependent on such responses and that the ability of *B. burgdorferi* to survive in ticks would require efficient utilization of NAG.

Studies of other bacteria indicate an inverse correlation between c-di-GMP levels and bacterial motility (40,53,62,86,104). The influence of Rrp1 on motility of *B. burgdorferi* was first assessed by evaluating basic flagella motor function with wave propagation as a read out. All strains displayed wild type wave propagation patterns.

To assess translational motion (i.e., directional movement away from the point of origin) methylcellulose was added to the media (74). In standard BSK-H media, which lacks methylcellulose, spirochetes display limited translational motion due to low viscosity and the absence of an inherent matrix. For spirochetes to undergo translational motion, the flagella motors located at each end of the cell must rotate in opposite directions (i.e., clockwise and counterclockwise). When the flagella motors rotate in the same direction, the cells flex, unlike when both flagella motors reverse direction, a change in direction occurs (18). All strains had translation motion but B31-Δ*rrp1* was drastically reduced in flex frequency and was locked in constant one-directional motion. Failure to reverse and translation in one direction is associated with chemotaxis-deficient *Borrelial* cells (46), suggesting a link between the motility defect and lack of NAG chemotaxis associated with *rrp1* deletion.

Specifically, B31-Δ*rrp1* mimics the phenotype of a *B. burgdorferi cheY3* deletion mutant (58). CheY3 is an important chemotaxis response regulator which can alter flagellar rotation in a phosphorylation dependent manner. To balance and control the actions of CheY3, *Borrelia* possess the phosphatase, CheX (56). Upon inactivation of CheX, spirochetes elicit a constant flex phenotype which is indicative of high levels of the CheY3 in its phosphorylated state, CheY3-P. This may suggest that disruption of Rrp1 prevents accumulation of CheY3-P. To understand the impact of Rrp1 on cheY3 and other genes involved in flagellar and chemotaxis processes, qRT-PCR was performed on key genes in each of these functional categories. No significant modifications in transcript levels were seen for the majority of genes tested, except for the flagellum-specific ATP synthase (*fliI*), flagellar motor switch protein (*fliG2*), and

cheY3. All exhibited a 3-4 fold increase in transcription. Upregulation of CheY3 was confirmed by immunoblots. These results indicate an accumulation of CheY3 is occurring upon *rrp1* deletion, but the constant run phenotype suggests the majority of the CheY3 protein molecules remain in the dephosphorylated state, causing a decreased affinity for the flagellar motor and reduced cellular ability to change flagellar motor directional bias.

In *E. coli*, c-di-GMP has been demonstrated to influence protein-protein interactions that control flagella motor rotation (23,62). The motility phenotype of B31-Δ*rrp1* suggests that c-di-GMP may contribute to flagella motor activity in *B. burgdorferi* as well. However, the wild type motility phenotype of the B31-OV strain, which would be predicted to have elevated levels of c-di-GMP, seems at odds with the paradigm that high levels of c-di-GMP inhibit motility and promote a sessile life style (34). Because the diguanylate cyclase activity of Rrp1 is strictly dependent on its phosphorylation state (27,77), elevated production of Rrp1 may not necessarily lead to an increase in c-di-GMP. Rrp1 is cotranscribed with the histidine kinase, Hpk1, which is thought to serve as its phosphate donor (70). Increased production of c-di-GMP may require elevated production and autophosphorylation of Hpk1. The series of events required for this to occur may be dependent on environmental stimuli which are unique to the tick-mammal interface (70) and these stimuli may not be encountered during in vitro cultivation.

To determine if Rrp1 production levels correlate with c-di-GMP concentration, we sought to measure the relative intracellular c-di-GMP concentration for each strain. Nucleotide extracts were assayed using reverse phase-high performance liquid chromatography. Precedent for the application of this highly sensitive approach comes

from studies of c-di-GMP levels in *E. coli* (2). However, c-di-GMP levels in in vitro cultivated *B. burgdorferi* proved to be below the detection threshold. This raises the question: if the concentration of c-di-GMP is so low that it can't be detected during in vitro cultivation, is it even produced in vitro and is it plausible that the unique properties of the B31-Δ*rrp1* strain are in fact due to the loss of diguanylate cyclase activity? The recent demonstration that c-di-GMP pools are asymmetrical and localized within a cell offers a possible explanation (20). It is possible that *B. burgdorferi* flagellar motor function is controlled by a concentrated local pool of c-di-GMP that represents a small fraction of the total cellular nucleotide pool. The deletion of *rrp1* would eliminate this pool and thus result in aberrant motility and chemotactic responses. Additional evidence for c-di-GMP production by the *Borrelia* during in vitro growth has come from the study of a *B. hermsii pdeA* deletion mutant. Deletion of *pdeA*, the primary phosphodiesterase involved in c-di-GMP breakdown in the *Borrelia*, leads to the accumulation of c-di-GMP thus allowing it to be detected by HPLC (R.T. Marconi, unpublished results). While it would be informative to measure c-di-GMP levels in spirochetes in vivo, such analyses are technically challenging due to the low numbers of spirochetes in mammals and ticks. It may be possible in future analyses to employ FRET based c-di-GMP biosensor approaches to assess changes in c-di-GMP levels in response to environmental stimuli (20).

The role of PlzA and PlzB as c-di-GMP effectors and regulators of motility.

C-di-GMP signaling mediates a variety of processes necessary for altering bacterial cellular lifestyles, as demonstrated by the Rrp1 data presented here along with

a multitude of other studies (21,28,34,71). The regulatory effects of the c-di-GMP system are instituted through c-di-GMP interaction with a variety of effector molecules including GEMM riboswitches (87,95), PilZ domain-containing proteins (1,76), ribonucleoprotein complexes (103), and cyclic monophosphate domains (35). To date, only two proteins have been identified as effectors within *B. burgdorferi*, both of which possess PilZ domains. The type strain of *B. burgdorferi*, strain B31, produces a single chromosomally encoded c-di-GMP binding protein designated as PlzA (27). This protein is necessary for murine infection and proper spirochete swarming, as shown by this study and Pitzer et al (63). Interestingly, a second PilZ domain containing protein, encoded by a variable linear plasmid, has been identified in some isolates. This protein has been designated as PlzB. No functional analysis has ever been conducted to understand the role of PlzB in *B. burgdorferi* pathogenesis.

In this study, we investigated if the c-di-GMP binding protein, PlzA, is important to *B. burgdorferi* virulence and enzootic cycle progression of strain B31-5A4. Since this clone does not contain PlzB, we additionally investigated if PlzB can functionally complement PlzA in the infection cycle and particular cellular processes such as motility, swarming, and NAG metabolism/chemotaxis. A strain lacking *plzA* (B31-Δ*plzA*) and its complement (B31-*plzA* KI) were generated, along with a mutant possessing a copy of *plzB* in the chromosomal location of *plzA* (B31-Δ*plzA::plzB*). Each stain was tested for their ability to infect mice by subcutaneous inoculation. B31-wt and B31-*plzA* KI were able to persist and disseminate, while B31-Δ*plzA* and B31-Δ*plzA::plzB* were non-infectious. This result is typical of high c-di-GMP concentrations, indicating PlzA is

necessary for proper c-di-GMP signaling for mammalian disease establishment but that PlzB cannot be substituted for PlzA.

The lack of a murine infection would inhibit spirochete acquisition by natural tick feeding; therefore, we tested if the strains were capable of tick colonization in a mouse-independent manner by immersion. All strains developed productive tick infections, including B31-Δ*plzA*, demonstrating PlzA is only crucial for spirochete transmission to murine hosts. Also this data suggests that PlzB, despite possessing the ability to bind c-di-GMP in vitro, is not necessary for *Borrelial* enzootic cycle progression. Thus, PlzB may be utilized for some other purpose besides virulence regulation or contribute to the pathogenesis of specific *B. burgdorferi* strains.

Studies in other bacterial systems, as well as in *B. burgdorferi*, show motility is correlated to c-di-GMP (37,96). The PilZ-containing c-di-GMP binding protein, YcgR, of *E. coli* and *Salmonella* binds directly to the flagellar motor-switch complex proteins, FliG and FliM, while in the presence of c-di-GMP to alter flagellar motor direction and speed (62). Within *B. burgdorferi*, deletion of the diguanylate cyclase inhibits spirochete flexes and locks the flagellar motors into a constant run, thus showing a role of c-di-GMP in regulation of motor direction (41). To assess motility and basic motor function, the strains were first evaluated in BSK-H media only. All strains retained proper wave propagation and twitching, showing overall flagellar structure and function was not altered. Next, translational motion was recorded by motion-tracking software in BSK-H containing 1% methylcellulose for increased viscosity. Similar to the *rrp1* deletion mutant, B31-Δ*plzA* had a severe reduction in flexes and appeared locked in a constant run. The most evident motility defect, however, was the dampening of average

spirochete run speed. The B31-Δ*plzA* strain functioned at an average run speed equivalent to 40% of the wild type. The B31-Δ*plzA::plzB* also exhibited these motility defects, which further confirms the importance of PlzA in flagellar motor regulation and demonstrates the inability of PlzB to functionally complement PlzA in these processes.

In contrast to YcgR of *E. coli* and *Salmonella* which is involved in a flagellar backstop brake mechanism (62), this data indicates proper flagellar motor regulation and speed is dependent upon PlzA, perhaps for torque generation and directional motor changes. *Borrelia* possess a significantly more complicated flagellar and chemotaxis signaling cascade than other bacterial systems. In particular, the motor switch contains two FliG proteins (FliG1 and FliG2) instead of a singular FliG (26). FliG2 resembles a component of the typical bacterial motor switch and is required for flagellation and motility (47). FliG1 is only located at one of the flagellar motors and deletion mutants remain motile, fail to translate in highly viscous media, and are quickly cleared during murine infection. This strain phenotype resembles the B31-Δ*plzA* strain and implicates a direct or indirect interaction between PlzA and FliG1, in addition to the possible localization of PlzA to one pole to facilitate c-di-GMP control of flagellar motor bias.

It is likely that the influence of c-di-GMP on flagellar directional rotation could be correlated with chemotaxis processes. Both PilZ domain-containing proteins and the chemotaxis response regulator, CheY, have been shown to bind to the *E. coli* motor switch to promote rotation bias (62,78), but it is unknown if cooperation exists between the control mechanisms of these proteins. Microarray analysis, previously reported by our lab, demonstrated Rrp1 and c-di-GMP positively regulate numerous motility and chemotaxis genes (70). Therefore, we tested if PlzA and PlzB, as downstream c-di-

GMP effectors, could influence spirochete chemotaxis using swarming and capillary chemotaxis assays. PlzA, not PlzB, was necessary for proper swarming; however, B31-Δ*plzA* and B31-Δ*plzA::plzB* were not significantly defective in NAG chemotaxis. This data indicates the reduced run speed could be directly impacting spirochete swarm capabilities and mammalian infection ability. Although, a chemotaxis defect independent of the NAG pathway could also be occurring. Transcription of the genes involved in chitobiose and NAG metabolism was likewise unaffected by the various genetic manipulations of PlzA, as shown by qRT-PCR. This confirms PlzA is not important for the key NAG metabolic process required for survival within ticks and correlates with the host infection and NAG chemotaxis pattern of the constitutive *rrp1* mutant.

Overall, this PlzA study supports the existence of other c-di-GMP effectors in *B. burgdorferi*. The swarming abilities of both the *rrp1* and *plzA* deletion mutants are comparable, yet the distinct motility phenotype and NAG chemotaxis response of each strain highlights the obvious differences in the regulatory abilities of each gene. If PlzA was the sole downstream c-di-GMP effector, the B31-Δ*plzA* strain would be expected to exhibit characteristics like the *rrp1* deletion or constitutive strain, thus being utilized for the functional output associated with high or low intracellular c-di-GMP levels. However, this is clearly not seen by all experiments in this study. The data demonstrates that the c-di-GMP signaling cascade in *Borrelia* is much more complex than just these two proteins. PlzA does appear to be a downstream effector in virulence and swarming mechanisms. Although, it is likely that other effectors are utilized as well, specifically for NAG chemotaxis and metabolism. Rrp1 could also be functioning

independently to regulate NAG, since PlzA status does not impact these processes. Studies of Rrp1 and PlzA are both critical to understanding Lyme spirochete pathogenesis, but identification of other molecules involved in this signaling network is necessary to solve the puzzle of this complicated signaling scheme.

PdeB, c-di-GMP, and the Lyme enzootic cycle.

The balancing of *Borrelial* intracellular c-di-GMP levels is maintained by hydrolysis activities of phosphodiesterases (96,97) These proteins typically contain either an EAL or HD-GYP domain to degrade the dinucleotide to pGpG or GMP (34,81,98). The *B. burgdorferi* genome encodes two chromosomally encoded phosphodiesterases, each protein harboring an EAL (PdeA) or HD-GYP domain (PdeB) (70,96,97). PdeA is necessary for pathogen virulence in mammals (97) and deletion mimics the constitutive *rrp1* conditions, and by extension high c-di-GMP, demonstrating that Rrp1 and PdeA must operate in a cooperative manner to balance c-di-GMP for retention of strain pathogenicity. However, little is known about HD-GYP proteins within bacterial systems in general. Since *B. burgdorferi* PdeA was critical for murine infection, we hypothesized that inactivation of *pdeB* would provide a similar phenotype. In addition, we believed the phosphodiesterases may act in a cooperative manner to accomplish c-di-GMP degradation, perhaps by causing localized hydrolysis within specific cellular compartments or by sequentially breaking the phosphodiester bonds of the dinucleotide.

To determine if the role of PdeB in the enzootic cycle progression of *B. burgdorferi*, *pdeB* was replaced with a spectinomycin/streptomycin resistance cassette

within the chromosome by allelic exchange mutagenesis to produce the deletion strain B31-Δ*pdeB*. Expression of the phosphodiesterase was restored by cis-complementation at the chromosomal location of *pdeB* to generate B31-*pdeB* KI. Both strains were evaluated for mammalian infection capabilities by subcutaneous inoculation of C3H-HeJ mice. Unlike PdeA, PdeB was not required for mammalian disease and all strains established a productive infection.

Spirochete passage to *Ixodes* ticks was analyzed to determine if loss of *pdeB* expression resulted in defective pathogen uptake. Naïve ticks were fed until repletion on needle inoculated mice four weeks post-infection. qPCR revealed all mutants were acquired by the *Ixodes* ticks, yet the B31-Δ*pdeB* strain displayed a decreased efficiency in colonization. To validate the natural feeding results and assess if PdeB functions mainly in the tick to mouse transmission, ticks were infected via immersion methods and fed on naïve mice. The decreased tick colonization of the *pdeB* deletion strain in comparison to the wild type and complemented strains was also shown using this technique. This deficiency could make the spirochetes less suitable for survival within the tick environment and there is evidence that loss of *pdeB* results in spirochete killing post-tick engorgement (96) rather than during the blood meal, as occurs with cells lacking *rrp1*/*hpk1* (33). Additionally, the B31-Δ*pdeB* strain was not transmitted to uninfected murine hosts by tick bite, demonstrating PdeB is essential for proper regulation of tick factors critical for transmission. PdeB could be necessary for modification of gene expression of genes differentially expressed between tick and murine environments, thus preventing transfer to and/or survival within the mammalian host. Together, this data supports the idea of tightly controlled regulation of intracellular

c-di-GMP levels in *Borrelia burgdorferi* for all phases of the pathogen's enzootic cycle and that each gene of the c-di-GMP signaling network is required for full virulence in both the mammalian host and tick vector.

Uniquely, PdeA and PdeB both abrogate murine infection; however these defects are distinctive from one another. PdeA is a critical factor within the mammal since it is able to effectively colonize ticks and both tick feeding as well as needle inoculation are unable to initiate mammalian disease. PdeB is only necessary for pathogen transmission by tick bite, identifying the gene as a key factor only within the tick. This distinguishing difference in virulence patterns between the PdeA and PdeB suggests each phosphodiesterase possesses a unique niche in *Borrelial* pathogenesis rather than working in concert to accomplish the same task.

Deletion of *pdeB* also results in a distinct motility and morphological phenotype. Cells were locked in constant state of flexing which prevented translational motion in highly viscous media (BSK-H + 1% methylcellulose), disrupted flagellar wave propagation, and reduced swarming. The constant flex state has also been described in a mutant possessing a *cheX* deletion (CheY phosphatase) (56), which suggests PdeB could be involved in chemotaxis processes like Rrp1. Although, PdeB was not found to be necessary for NAG chemotaxis in this work, the phosphodiesterase may be involved in chemotaxis towards other molecules. A recent study by Sultan et al, demonstrated a mutant containing deletions of *pdeB* and *plzA* also resulted in the same constant flexing phenotype (96), while inactivation of *plzA* alone caused constant running, reduced flexing, and slower run speeds. This indicates PdeB may alter c-di-GMP intracellular concentrations to cause PlzA-independent modification of CheX or CheY3 to change

flagellar rotational bias. However, PlzA may still be involved in motor directional change through the control of PdeA since inactivation of *plzA* resulted in a constant run phenotype equivalent to that of the *pdeA* deletion mutant.

In summary, this study demonstrates that Rrp1, PlzA, and PdeB regulate stage specific steps in the enzootic cycle of Lyme disease spirochetes. Deletion of *rrp1* prevented the establishment of a productive population in ticks, while elevated production blocked infectivity in mice. Disruption of *plzA* inhibited murine infection but did not alter tick colonization. Lastly, PdeB was identified as a tick-specific factor which is necessary for tick to mouse transmission via natural infection methods. Each component was found to be intricately linked to flagellar motor regulation and perhaps through chemotactic responses, processes which are likely to be critical for completion of the enzootic cycle. Since diguanylate cyclase and phosphodiesterase activity is the only known function of Rrp1 and PdeB, respectively, it is highly probable that c-di-GMP levels are responsible for the phenotypes observed for the strains generated in this report. In constructing future models for *Borrelia* pathogenesis, genetic regulation and motility, it will be important to consider the far reaching regulatory potential of c-di-GMP.

CHAPTER 5: PERSPECTIVES

In bacterial pathogenesis, c-di-GMP has emerged as an important modulator of virulence and pathogen lifestyle by regulation of motility state, biofilm formation, etc (98). The molecule maintains its versatility and ability to rapidly influence many processes through the integration of various classes of effectors (34). Until recently, the multiplicity of diguanylate cyclase, phosphodiesterase, and c-di-GMP effector domains has greatly impeded understanding the full biological implication of this signaling mechanism. The field of c-di-GMP regulation is now in a time of great expansion. Cutting edge studies have demonstrated the spatial localization of c-di-GMP during cellular division of various gram negative bacteria and allowed for imaging of c-di-GMP binding within live cells using advanced intracellular fluorescent resonance energy transfer techniques (FRET) (20). Additionally, a unique and simplified model has been identified within Lyme disease spirochetes, in particular *Borrelia burgdorferi,* which is ideal to investigate the specific functions of each component of the c-di-GMP network and characterize this type of signaling in arthropod-borne pathogens (27,41,63,70,96,97).

Throughout the course of this dissertation, the *Borrelia burgdorferi* c-di-GMP network components have been shown to be major regulators of Lyme pathogenesis. This work specifically highlights the coordination of motility and chemotaxis processes with cellular virulence and enzootic cycle completion, signifying the integration of c-di-

GMP control into the global regulatory networks of *Borrelia*. It is not yet known if intracellular c-di-GMP levels produce the virulence, motility, and chemotaxis phenotypes or if the changes are independent of c-di-GMP. However, since similar phenotypes are exhibited between select mutants, it is likely that the recorded changes and enzootic cycle disruption are directly correlated with cellular c-di-GMP fluctuations.

Collectively, these analyses also present a distinct paradigm shift in the overall association of c-di-GMP levels with specific phenotypes. High c-di-GMP concentrations are generally thought to inhibit virulence and motility by promoting sessility and biofilm formation, while low levels would enhance cell mobility and infection capability within gram negative pathogens. However, *Borrelia burgdorferi* spirochetes are quite divergent from these bacterial systems, do not produce biofilms, and possess an enzootic cycle requiring both passage and colonization of various hosts. The data presented here suggests c-di-GMP signaling in *Borrelia* is employed for environmental adaption to the vector and mammalian host rather than for an individual host or host-independent conditions, as displayed with *Vibrio* and *Bordetella* (71). In theoretically high intracellular c-di-GMP conditions (constitutive Rrp1 or inactivated PdeA), spirochetes are unable to establish a productive mammalian infection (41,97), while low c-di-GMP levels (deletion of *rrp1*) block spirochete acquisition by ticks, thus implicating enzootic cycle completion requires fine-tuned regulation and maintenance of a specific intracellular c-di-GMP concentration (Figure 5-1).

Overall, the use of c-di-GMP as a secondary messenger is a rapid and efficient signal transduction method which is vital to bacterial pathogenesis. The identification and characterization of c-di-GMP regulation in *Borrelia* represents an important step

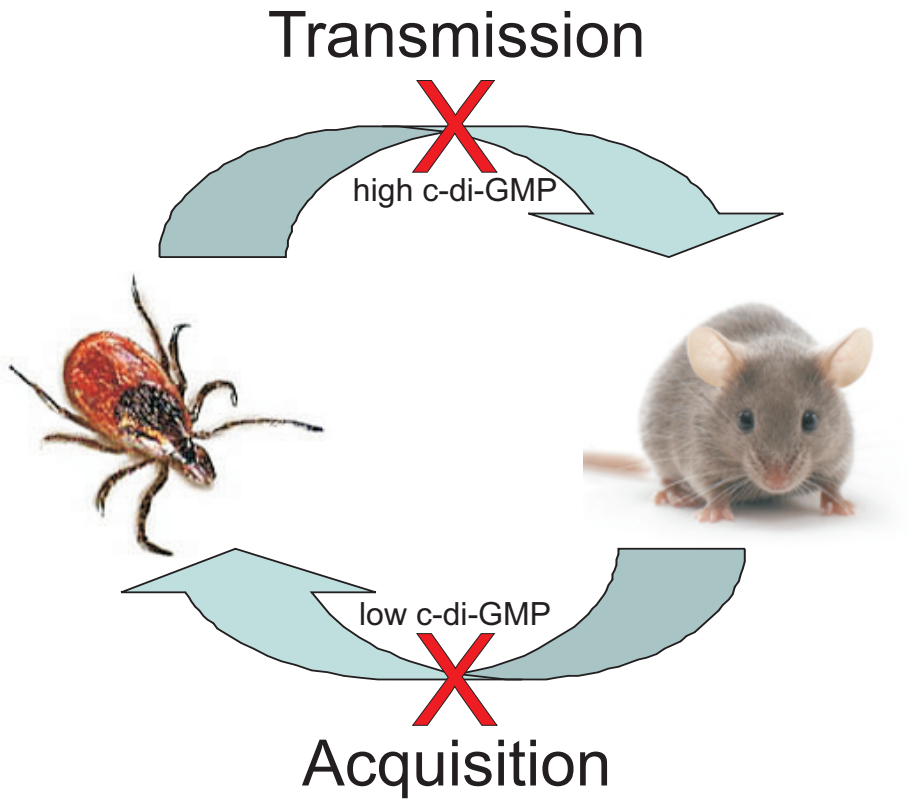

Figure 5-1. Putative c-di-GMP regulatory concepts of the *Borrelia burgdorferi* enzootic cycle. Successful spirochete transmission and acquisition requires maintenance of a specific intracellular c-di-GMP concentration. Deletion of *rrp1,* the sole diguanylate cyclase, inhibits pathogen transfer from infected mammals to feeding *Ixodes* ticks by theoretically abrogating c-di-GMP synthesis. Conversely, inactivation of the PdeB phosphodiesterase and/or constitutive expression of the diguanylate cyclase abolishes Lyme disease establishment within murine hosts by promoting c-di-GMP accumulation.

forward in the comprehension of pathogenic mechanisms of bacteria in general, as well as Lyme spirochetes and other arthropod-borne pathogens. C-di-GMP signaling additionally represents a new target for the development of Lyme disease therapeutics. Enhanced knowledge of *Borrelia burgdorferi* c-di-GMP processes is necessary to further understand specific molecular interactions and the complex functional output of this system for innovative drug design and advanced preventative strategies.

Future analyses

Despite the progress in *Borrelial* c-di-GMP research, many important questions remain unanswered. The intracellular concentrations are not yet known and measurement is limited by the sensitivity of current quantitation methods, preventing assessment of c-di-GMP concentrations upon diguanylate cyclase and phosphodiesterase genetic manipulation. It is also unknown if this measurement limitation is due to the instrumentation, if the dinucleotide merely exists in low levels in *Borrelia*, and/or if c-di-GMP is only present in specific cellular compartments. Recently, studies have revealed that c-di-GMP is asymmetrically distributed between mother and daughter cells during cell division of *Caulobacter* and *Pseudomonas* (20). It is also generally believed that the functional redundancy of c-di-GMP networks suggest localized subcellular pools of the dinucleotide exist within cells (34). Since c-di-GMP signaling in *Borrelia* impacts flagellar motor regulation, it is possible that c-di-GMP concentrations are tightly regulated at the poles in order to control motor directional bias. Current efforts are underway to characterize intracellular levels and the spatial localization of c-di-GMP within *B. burgdorferi* via an alternative method to HPLC. FRET

analysis will be employed to determine cellular concentrations and identify where c-di-GMP is located within the organism using a verified *E. coli* and *Salmonella* biosensor, YcgR (kindly shared by Dr. Samuel I. Miller) (20). Likewise, this method will be used to distinguish if c-di-GMP binds PlzA and to detect if these protein-dinucleotide interactions are targeted to the cellular poles and flagellar motors. These analyses will provide direct evidence that c-di-GMP signaling does occur within the pathogen and pinpoint the spatial orientation of PilZ domain interactions with c-di-GMP.

The molecular mechanisms by which c-di-GMP exerts its effects is still unknown. PilZ domain-containing proteins are currently the only effector molecule type known to exist within *Borrelia,* however it is highly probable that other c-di-GMP effectors are present. The lack of identification may be due to the use of improper parameters for bioinformatic detection of other effectors in *B. burgdorferi,* the dissimilarity between *Borrelial* effectors and those of gram negative pathogens, etc. Furthermore, there also is a possibility that the identified c-di-GMP effectors, PlzA and PlzB, could possess functions independent of c-di-GMP signaling. Until clarity is achieved with the state of other effectors, we will aim to focus our studies to the PilZ domain-containing proteins to identify targets for c-di-GMP regulation, specifically. Pulldown assays will be performed and coupled with mass spectrometry to detect key protein-protein interactions with PlzA and PlzB in the presence of c-di-GMP. This data would aim to provide the first example of specific molecular interactions which are dependent upon c-di-GMP.

PilZ-containing proteins have been shown to bind the flagellar motor switch (62), therefore PlzA green fluorescent protein (GFP) and FliG1 red fluorescent protein (mRFP) fusions will be constructed and then co-transformed to characterize the spatial

orientation of each protein in relation to one another within *B. burgdorferi* pathogenic strain B31-5A4. Deletion mutants of *plzA* and *fliG1* both exhibited similar motility, swarming, and virulence phenotypes, thus it is hypothesized that PlzA and FliG1 may work in cooperation or interact to control these processes and motor rotational control. Data demonstrating co-localization would provide evidence of the unique ability of PlzA to localize to the specific location of FliG1, thus suggesting PlzA may possess the ability to regulate FliG1 function and thereby alter spirochete motility.

C-di-GMP has been also linked to *Borrelial* chemotaxis processes, yet this mechanism is still uncharacterized and the degree of crosstalk between the Rrp1-Hpk1 and chemotaxis TCS is unknown. To further understand the method of chemotaxis control by c-di-GMP, multiple approaches will be utilized. First, the role of Rrp1 and PlzA in CheY3 regulation and phosphorylation state will be investigated. A CheY3 site-directed mutant deficient in phosphorylation will be generated to assess the motility and chemotaxis patterns associated with CheY3 in its dephosphorylated state and compare phenotypes with the *rrp1* and *plzA* deletion strains. If phenotypes exhibited by deletion of *rrp1* and the site-directed *cheY3* mutants are comparable, studies will be performed to determine if these proteins interact and bind the flagellar motor to cause these motor bias phenotypes. The results could potentially represent the first identified c-di-GMP signaling cascade in *Borrelia* which impacts the chemotaxis TCS, further demonstrating the far-reaching global regulatory ability of c-di-GMP.

In summary, it is evident that c-di-GMP is a major regulator of the Lyme enzootic cycle, yet characterization has truly just begun and c-di-GMP signaling in *Borrelia* still remains in its infancy. These analyses represent the next generation in spirochete c-di-

GMP research by focusing on the identification of specific molecular interactions and understanding the expansive scope c-di-GMP regulation. Targeting c-di-GMP signaling mechanisms holds great promise for the development of countermeasures to combat the increasingly persistent and emerging infection, Lyme disease.

REFERENCES

REFERENCES

1. **Amikam, D. and M. Y. Galperin.** 2006. PilZ domain is part of the bacterial c-di-GMP binding protein. Bioinformatics **22**(1): 3-6.

2. **Antoniani, D., P. Bocci, A. Maciag, N. Raffaelli and P. Landini.** 2010. Monitoring of diguanylate cyclase activity and of cyclic-di-GMP biosynthesis by whole-cell assays suitable for high-throughput screening of biofilm inhibitors. Appl Microbiol Biotechnol **85**(4): 1095-104.

3. **Ausmees, N., R. Mayer, H. Weinhouse, G. Volman, D. Amikam, M. Benziman and M. Lindberg.** 2001. Genetic data indicate that proteins containing the GGDEF domain possess diguanylate cyclase activity. FEMS Microbiol Lett **204**(1): 163-7.

4. **Bakker, R. G., C. Li, M. R. Miller, C. Cunningham and N. W. Charon.** 2007. Identification of specific chemoattractants and genetic complementation of a *Borrelia burgdorferi* chemotaxis mutant: flow cytometry-based capillary tube chemotaxis assay. Appl Environ Microbiol **73**(4): 1180-8.

5. **Baranton, G., D. Postic, I. Saint Girons, P. Boerlin, J.-C. Piffaretti, M. Assous and P. A. D. Grimont.** 1992. Delineation of *Borrelia burgdorferi* sensu stricto, *Borrelia garinii* sp. nov., and group VS461 associated with Lyme borreliosis. Int J Syst Bacteriol **42**: 378-383.

6. **Barbour, A. G.** 1984. Isolation and cultivation of Lyme disease spirochetes. Yale J Biol Med **57**: 521-525.

7. **Barbour, A. G. and C. F. Garon.** 1987. Linear plasmids of the bacterium *Borrelia burgdorferi* have covalently closed ends. Science **237**: 409-411.

8. **Barbour, A. G. and S. F. Hayes.** 1986. Biology of *Borrelia* species. Microbiol Rev **50**: 381-400.

9. **Benach, J., S. S. Swaminathan, R. Tamayo, S. K. Handelman, E. Folta-Stogniew, J. E. Ramos, F. Forouhar, H. Neely, J. Seetharaman, A. Camilli and J. F. Hunt.** 2007. The structural basis of cyclic diguanylate signal transduction by PilZ domains. EMBO J **26**(24): 5153-66.

10. **Benach, J. L., E. M. Bosler, J. P. Hanrahan, J. L. Coleman, G. S. Habicht, T. F. Bast, D. J. Cameron, J. L. Ziegler, A. G. Barbour, W. Burgdorfer, R.**

Edelman and R. A. Kaslow. 1983. Spirochetes isolated from the blood of two patients with Lyme disease. N Engl J Med **308**(13): 740-2.

11. **Boardman, B. K., M. He, Z. Ouyang, H. Xu, X. Pang and X. F. Yang.** 2008. Essential role of the response regulator Rrp2 in the infectious cycle of *Borrelia burgdorferi*. Infect Immun **76**: 3844-53.

12. **Brown, R. N. and R. S. Lane.** 1992. Lyme disease in California: A novel enzootic transmission cycle of *Borrelia burgdorferi.* Science **256**: 1439-1442.

13. **Burgdorfer, W., A. G. Barbour, S. F. Hayes, J. L. Benach, E. Grunwaldt and J. P. Davis.** 1982. Lyme disease--a tick-borne spirochetosis? Science **216**: 1317-1319.

14. **Burtnick, M. N., J. S. Downey, P. J. Brett, J. A. Boylan, J. G. Frye, T. R. Hoover and F. C. Gherardini.** 2007. Insights into the complex regulation of *rpoS* in Borrelia burgdorferi. Mol Microbiol **65**(2): 277-93.

15. **Caimano, M. J., R. Iyer, C. H. Eggers, C. Gonzalez, E. A. Morton, M. A. Gilbert, I. Schwartz and J. D. Radolf.** 2007. Analysis of the RpoS regulon in *Borrelia burgdorferi* in response to mammalian host signals provides insight into RpoS function during the enzootic cycle. Mol Microbiol **65**(5): 1193-217.

16. **Caimano, M. J., M. R. Kenedy, T. Kairu, D. C. Desrosiers, M. Harman, S. Dunham-Ems, D. R. Akins, U. Pal and J. D. Radolf.** 2011. The hybrid histidine kinase Hk1 is part of a two-component system that is essential for survival of *Borrelia burgdorferi* in feeding Ixodes scapularis ticks. Infect Immun **79**(8): 3117-3130.

17. **Chan, C., R. Paul, D. Samoray, N. C. Amiot, B. Giese, U. Jenal and T. Schirmer.** 2004. Structural basis of activity and allosteric control of diguanylate cyclase. Proc Natl Acad Sci USA **101**(49): 17084-9.

18. **Charon, N. W., S. F. Goldstein, M. Marko, C. Hsieh, L. L. Gebhardt, M. A. Motaleb, C. W. Wolgemuth, R. J. Limberger and N. Rowe.** 2009. The flat-ribbon configuration of the periplasmic flagella of *Borrelia burgdorferi* and its relationship to motility and morphology. J Bacteriol **191**(2): 600-7.

19. **Christen, M., B. Christen, M. Folcher, A. Schauerte and U. Jenal.** 2005. Identification and characterization of a cyclic di-GMP-specific phosphodiesterase and its allosteric control by GTP. J Biol Chem **280**(35): 30829-37.

20. **Christen, M., H. D. Kulasekara, B. Christen, B. R. Kulasekara, L. R. Hoffman and S. I. Miller.** 2010. Asymmetrical distribution of the second messenger c-di-GMP upon bacterial cell division. Science **328**(5983): 1295-7.

21. **Cotter, P. A. and S. Stibitz.** 2007. c-di-GMP-mediated regulation of virulence and biofilm formation. Curr Opin Microbiol **10**(1): 17-23.

22. **Earnhart, C. G., D. V. Leblanc, K. E. Alix, D. C. Desrosiers, J. D. Radolf and R. T. Marconi.** 2010. Identification of residues within ligand-binding domain 1 (LBD1) of the *Borrelia burgdorferi* OspC protein required for function in the mammalian environment. Mol Microbiol **76**(2): 393-408.

23. **Fang, X. and M. Gomelsky.** 2010. A post-translational, c-di-GMP-dependent mechanism regulating flagellar motility. Mol Microbiol **76**(5): 1295-305.

24. **Fisher, M. A., D. Grimm, A. K. Henion, A. F. Elias, P. E. Stewart, P. A. Rosa and F. C. Gherardini.** 2005. From the Cover: *Borrelia burgdorferi* σ54 is required for mammalian infection and vector transmission but not for tick colonization. Proc Natl Acad Sci **102**(14): 5162-5167.

25. **Frank, K. L., S. F. Bundle, M. E. Kresge, C. H. Eggers and D. S. Samuels.** 2003. *aadA* confers streptomycin resistance in *Borrelia burgdorferi*. J Bacteriol **185**(22): 6723-7.

26. **Fraser, C. M., S. Casjens, W. M. Huang, G. G. Sutton, R. Clayton, R. Lathigra, O. White, K. A. Ketchum, R. Dodson, E. K. Hickey, M. Gwinn, B. Dougherty, J. F. Tomb, R. D. Fleischmann, D. Richardson, J. Peterson, A. R. Kerlavage, J. Quackenbush, S. Salzberg, M. Hanson, R. van Vugt, N. Palmer, M. D. Adams, J. Gocayne, J. Weidman, T. Utterback, L. Watthey, L. McDonald, P. Artiach, C. Bowman, S. Garland, C. Fuji, M. D. Cotton, K. Horst, K. Roberts, B. Hatch, H. O. Smith and J. C. Venter.** 1997. Genomic sequence of a Lyme disease spirochaete, *Borrelia burgdorferi*. Nature **390**(6660): 580-6.

27. **Freedman, J. C., E. A. Rogers, J. L. Kostick, H. Zhang, R. Iyer, I. Schwartz and R. T. Marconi.** 2009. Identification and molecular characterization of a cyclic-di-GMP effector protein, PlzA (BB0733): additional evidence for the existence of a functional cyclic-di-GMP regulatory network in the Lyme disease spirochete, *Borrelia burgdorferi*. FEMS Immunol Med Microbiol **58**(2): 285-294.

28. **Galperin, M. Y.** 2006. Structural classification of bacterial response regulators: diversity of output domains and domain combinations. J Bacteriol **188**(12): 4169-82.

29. **Galperin, M. Y., A. N. Nikolskaya and E. V. Koonin.** 2001. Novel domains of the prokaryotic two-component signal transduction systems. FEMS Microbiol Lett **203**(1): 11-21.

30. **Gern, L. and P. F. Humair.** 1998. Natural history of *Borrelia burgdorferi sensu lato*. Wien Klin Wochenschr **110**(24): 856-8.

31. **Girgis, H. S., Y. Liu, W. S. Ryu and S. Tavazoie.** 2007. A comprehensive genetic characterization of bacterial motility. PLoS Genet **3**(9): 1644-60.

32. **Gray, J.** (2002). Lyme borreliosis : biology, epidemiology, and control. Wallingford, UK ; New York, CABI Pub.

33. **He, M., Z. Ouyang, B. Troxell, H. Xu, A. Moh, J. Piesman, M. V. Norgard, M. Gomelsky and X. F. Yang.** 2011. Cyclic di-GMP is Essential for the Survival of the Lyme Disease Spirochete in Ticks. PLoS Pathog **7**(6): e1002133.

34. **Hengge, R.** 2009. Principles of c-di-GMP signalling in bacteria. Nat Rev Microbiol **7**(4): 263-73.

35. **Hickman, J. W. and C. S. Harwood.** 2008. Identification of FleQ from *Pseudomonas aeruginosa* as a c-di-GMP-responsive transcription factor. Mol Microbiol **69**(2): 376-89.

36. **Hubner, A., X. Yang, D. M. Nolen, T. G. Popova, F. C. Cabello and M. V. Norgard.** 2001. Expression of *Borrelia burgdorferi* OspC and DbpA is controlled by a RpoN-RpoS regulatory pathway. Proc Natl Acad Sci USA **98**: 12724-12729.

37. **Jenal, U. and J. Malone.** 2006. Mechanisms of cyclic-di-GMP signaling in bacteria. Annu Rev Genet **40**: 385-407.

38. **Kader, A., R. Simm, U. Gerstel, M. Morr and U. Romling.** 2006. Hierarchical involvement of various GGDEF domain proteins in rdar morphotype development of *Salmonella enterica serovar Typhimurium*. Mol Microbiol **60**(3): 602-16.

39. **Keirans, J. E., H. J. Hutcheson, L. A. Durden and J. S. Klompen.** 1996. *Ixodes* (*Ixodes*) *scapularis* (*Acari:Ixodidae*): redescription of all active stages, distribution, hosts, geographical variation, and medical and veterinary importance. J Med Entomol **33**(3): 297-318.

40. **Kim, Y. K. and L. L. McCarter.** 2007. ScrG, a GGDEF-EAL protein, participates in regulating swarming and sticking in *Vibrio parahaemolyticus*. J Bacteriol **189**(11): 4094-107.

41. **Kostick, J. L., L. T. Szkotnicki, E. A. Rogers, P. Bocci, N. Raffaelli and R. T. Marconi.** 2011. The diguanylate cyclase, Rrp1, regulates critical steps in the enzootic cycle of the Lyme disease spirochetes. Mol Microbiol **81**(1): 219-231.

42. **Kulasakara, H., V. Lee, A. Brencic, N. Liberati, J. Urbach, S. Miyata, D. G. Lee, A. N. Neely, M. Hyodo, Y. Hayakawa, F. M. Ausubel and S. Lory.** 2006. Analysis of *Pseudomonas aeruginosa* diguanylate cyclases and

phosphodiesterases reveals a role for bis-(3'-5')-cyclic-GMP in virulence. Proc Natl Acad Sci USA **103**(8): 2839-44.

43. **Kuo, M. M., R. S. Lane and P. C. Giclas.** 2000. A comparative study of mammalian and reptilian alternative pathway of complement-mediated killing of the Lyme disease spirochete (*Borrelia burgdorferi*). J Parasitol **86**(6): 1223-1228.

44. **Labandeira-Rey, M. and J. T. Skare.** 2001. Decreased infectivity in *Borrelia burgorferi* strain B31 is associated with the loss of either linear plasmid 25 or 28-1. Infection and Immunity **69**: 446-455.

45. **Lane, R. S., J. Piesman and W. Burgdorfer.** 1991. Lyme borreliosis: relation of its causative agent to its vectors and hosts in North America and Europe. Annu Rev Entomol **36**: 587-609.

46. **Li, C., R. G. Bakker, M. A. Motaleb, M. L. Sartakova, F. C. Cabello and N. W. Charon.** 2002. Asymmetrical flagellar rotation in *Borrelia burgdorferi* nonchemotactic mutants. Proc Natl Acad Sci USA **99**(9): 6169-74.

47. **Li, C., H. Xu, K. Zhang and F. T. Liang.** 2010. Inactivation of a putative flagellar motor switch protein FliG1 prevents *Borrelia burgdorferi* from swimming in highly viscous media and blocks its infectivity. Mol Microbiol **75**(6): 1563-76.

48. **Li, Y., Y. Hu, W. Fu, B. Xia and C. Jin.** 2007. Solution structure of the bacterial chemotaxis adaptor protein CheW from *Escherichia coli*. Biochem Biophys Res Commun **360**(4): 863-7.

49. **Lim, B., S. Beyhan, J. Meir and F. H. Yildiz.** 2006. Cyclic-diGMP signal transduction systems in Vibrio cholerae: modulation of rugosity and biofilm formation. Mol Microbiol **60**(2): 331-48.

50. **Liu, J., T. Lin, D. J. Botkin, E. McCrum, H. Winkler and S. J. Norris.** 2009. Intact flagellar motor of *Borrelia burgdorferi* revealed by cryo-electron tomography: evidence for stator ring curvature and rotor/C-ring assembly flexion. J Bacteriol **191**(16): 5026-36.

51. **LoGiudice, K., R. S. Ostfeld, K. A. Schmidt and F. Keesing.** 2003 The ecology of infectious disease: Effects of host diversity and community composition on Lyme disease risk. Proc Natl Acad Sci **100** (2): 567-571

52. **Margos, G., S. A. Vollmer, N. H. Ogden and D. Fish.** 2011. Population genetics, taxonomy, phylogeny and evolution of B*orrelia burgdorferi sensu lato*. Infection, Genetics and Evolution **In Press, Corrected Proof**.

53. **Martinez-Wilson, H. F., R. Tamayo, A. D. Tischler, D. W. Lazinski and A. Camilli.** 2008. The *Vibrio cholerae* hybrid sensor kinase VieS contributes to motility and biofilm regulation by altering the cyclic diguanylate level. J Bacteriol **190**(19): 6439-47.

54. **McDowell, J. V., S. Y. Sung, M. Labandeira-Rey, J. T. Skare and R. T. Marconi.** 2001. Analysis of mechanisms associated with loss of infectivity of clonal populations of *Borrelia burgdorferi* B31MI. Infect Immun **69**(6): 3670-7.

55. **Motaleb, M. A., L. Corum, J. L. Bono, A. F. Elias, P. Rosa, D. S. Samuels and N. W. Charon.** 2000. *Borrelia burgdorferi* periplasmic flagella have both skeletal and motility functions. Proc Natl Acad Sci U S A **97**(20): 10899-904.

56. **Motaleb, M. A., M. R. Miller, C. Li, R. G. Bakker, S. F. Goldstein, R. E. Silversmith, R. B. Bourret and N. W. Charon.** 2005. CheX is a phosphorylated CheY phosphatase essential for *Borrelia burgdorferi* chemotaxis. J Bacteriol **187**(23): 7963-9.

57. **Motaleb, M. A., M. R. Miller, C. Li and N. W. Charon.** 2007. Phosphorylation assays of chemotaxis two-component system proteins in *Borrelia burgdorferi*. Methods Enzymol **422**: 438-47.

58. **Motaleb, M. A., S. Z. Sultan, M. R. Miller, C. Li and N. W. Charon.** 2011. CheY3 of *Borrelia burgdorferi* Is the Key Response Regulator Essential for Chemotaxis and Forms a Long-Lived Phosphorylated Intermediate. J Bacteriol **193**(13): 3332-3341.

59. **Ojaimi, C., C. Brooks, S. Casjens, P. Rosa, A. Elias, A. G. Barbour, A. Jasinskas, J. Benach, L. Katona, J. Radolf, M. Caimano, J. Skare, K. Swingle, D. Akins and I. Schwartz.** 2003. Profiling of temperature-induced changes in *Borrelia burgdorferi* gene expression by using whole genome arrays. Infect Immun **71**: 1689-1705.

60. **Ojaimi, C., V. Mulay, D. Liveris, R. Iyer and I. Schwartz.** 2005. Comparative transcriptional profiling of *Borrelia burgdorferi* clinical isolates differing in capacities for hematogenous dissemination. Infect Immun **73**(10): 6791-802.

61. **Ouyang, Z., J. S. Blevins and M. V. Norgard.** 2008. Transcriptional interplay among the regulators Rrp2, RpoN and RpoS in *Borrelia burgdorferi*. Microbiology **154**(Pt 9): 2641-58.

62. **Paul, K., V. Nieto, W. C. Carlquist, D. F. Blair and R. M. Harshey.** 2010. The c-di-GMP binding protein YcgR controls flagellar motor direction and speed to affect chemotaxis by a "backstop brake" mechanism. Mol Cell **38**(1): 128-39.

63. **Pitzer, J. E., S. Z. Sultan, Y. Hayakawa, G. Hobbs, M. R. Miller and M. A. Motaleb.** 2011. Analysis of the *Borrelia burgdorferi* cyclic-di-GMP binding protein PlzA reveals a role in motility and virulence. Infect Immun **79**: 1815-25.

64. **Policastro, P. F. and T. G. Schwan.** 2003. Experimental infection of Ixodes scapularis larvae (Acari: Ixodidae) by immersion in low passage cultures of *Borrelia burgdorferi*. J Med Entomol **40**(3): 364-70.

65. **Pratt, J. T., R. Tamayo, A. D. Tischler and A. Camilli.** 2007. PilZ domain proteins bind cyclic diguanylate and regulate diverse processes in *Vibrio cholerae*. J Biol Chem **282**(17): 12860-70.

66. **Purser, J. E., M. B. Lawrenz, M. J. Caimano, J. K. Howell, J. D. Radolf and S. J. Norris.** 2003. A plasmid-encoded nicotinamidase (PncA) is essential for infectivity of *Borrelia burgdorferi* in a mammalian host. Mol Microbiol **48**(3): 753-64.

67. **Purser, J. E. and S. J. Norris.** 2000. Correlation between plasmid content and infectivity in *Borrelia burgdorferi*. Proc Natl Acad Sci USA **97**: 13865-13870.

68. **Revel, A. T., A. M. Talaat and M. V. Norgard.** 2002. DNA microarray analysis of differential gene expression in *Borrelia burgdorferi*, the Lyme disease spirochete. Proc Natl Acad Sci **99**: 1562-1567.

69. **Rogers, E. A. and R. T. Marconi.** 2007. Delineation of species-specific binding properties of the CspZ protein (BBH06) of Lyme disease spirochetes: evidence for new contributions to the pathogenesis of *Borrelia* spp. Infect Immun **75**(11): 5272-81.

70. **Rogers, E. A., D. Terekhova, H. M. Zhang, K. M. Hovis, I. Schwartz and R. T. Marconi.** 2009. Rrp1, a cyclic-di-GMP-producing response regulator, is an important regulator of *Borrelia burgdorferi* core cellular functions. Mol Microbiol **71**(6): 1551-1573.

71. **Romling, U. and D. Amikam.** 2006. Cyclic di-GMP as a second messenger. Curr Opin Microbiol **9**(2): 218-28.

72. **Rosa, P. A., K. Tilly and P. E. Stewart.** 2005. The burgeoning molecular genetics of the Lyme disease spirochaete. Nat Rev Microbiol **3**(2): 129-43.

73. **Ross, P., H. Weinhouse, Y. Aloni, D. Michaeli, P. Weinberger-Ohana, R. Mayer, S. Braun, E. de Vroom, G. A. van der Marel, J. H. van Boom and M. Benziman.** 1987. Regulation of cellulose synthesis in *Acetobacter xylinum* by cyclic diguanylic acid. Nature **325**(6101): 279-81.

74. **Ruby, J. D. and N. W. Charon.** 1998. Effect of temperature and viscosity on the motility of the spirochete *Treponema denticola.* FEMS Microbiol Lett **169**(2): 251-4.

75. **Rudzinska, M. A., A. Spielman, S. Lewengrub, J. Piesman and S. Karakashian.** 1982. Penetration of the peritrophic membrane of the tick by *Babesia microti*. Cell Tissue Res **221**(3): 471-81.

76. **Ryjenkov, D. A., R. Simm, U. Romling and M. Gomelsky.** 2006. The PilZ domain is a receptor for the second messenger c-di-GMP: the PilZ domain protein YcgR controls motility in enterobacteria. J Biol Chem **281**(41): 30310-4.

77. **Ryjenkov, D. A., M. Tarutina, O. V. Moskvin and M. Gomelsky.** 2005. Cyclic diguanylate is a ubiquitous signaling molecule in bacteria: insights into biochemistry of the GGDEF protein domain. J Bacteriol **187**(5): 1792-8.

78. **Sagi, Y., S. Khan and M. Eisenbach.** 2003. Binding of the chemotaxis response regulator CheY to the isolated, intact switch complex of the bacterial flagellar motor: lack of cooperativity. J Biol Chem **278**(28): 25867-71.

79. **Samuels, D. S., K. Mach and C. F. Garon.** 1994. Genetic transformation of the Lyme disease agent *Borrelia burgdorferi* with coumarin-resistant *gyrB*. J Bacteriol **176**: 6045-6049.

80. **Samuels, D. S. and J. D. Radolf.** (2010). Borrelia: Molecular biology, host interaction and pathogenesis. Norfolk, Caister Academic Press.

81. **Schirmer, T. and U. Jenal.** 2009. Structural and mechanistic determinants of c-di-GMP signalling. Nat Rev Microbiol **7**(10): 724-35.

82. **Schmidt, A. J., D. A. Ryjenkov and M. Gomelsky.** 2005. The ubiquitous protein domain EAL is a cyclic diguanylate-specific phosphodiesterase: enzymatically active and inactive EAL domains. J Bacteriol **187**(14): 4774-81.

83. **Schneider, B. S., N. S. Zeidner, T. R. Burkot, G. O. Maupin and J. Piesman.** 2000. *Borrelia* isolates in Northern Colorado identified as *Borrelia bissettii*. J Clin Microbiol **38**(8): 3103-5.

84. **Shi, W., Z. Yang, Y. Geng, L. E. Wolinsky and M. A. Lovett.** 1998. Chemotaxis in *Borrelia burgdorferi*. J Bacteriol **180**(2): 231-5.

85. **Shu, C. J. and I. B. Zhulin.** 2002. ANTAR: an RNA-binding domain in transcription antitermination regulatory proteins. Trends Biochem Sci **27**(1): 3-5.

86. **Simm, R., M. Morr, A. Kader, M. Nimtz and U. Romling.** 2004. GGDEF and EAL domains inversely regulate cyclic di-GMP levels and transition from sessility to motility. Mol Microbiol **53**(4): 1123-34.

87. **Smith, K. D., S. V. Lipchock, T. D. Ames, J. Wang, R. R. Breaker and S. A. Strobel.** 2009. Structural basis of ligand binding by a c-di-GMP riboswitch. Nat Struct Mol Biol **16**(12): 1218-23.

88. **Steere, A. C.** 2001. Lyme disease. N Engl J Med **345**: 115-125.

89. **Steere, A. C., T. F. Broderick and S. E. Malawista.** 1978. Erythema chronicum migrans and Lyme arthritis: epidemiologic evidence for a tick vector. Am J Epidemiol **108**: 312-321.

90. **Steere, A. C., J. Coburn and L. Glickstein.** 2004. The emergence of Lyme disease. J Clin Invest **113**(8): 1093-101.

91. **Steere, A. C., R. L. Grodzicki, A. N. Kornblatt, J. E. Craft, A. G. Barbour, W. Burgdorfer, G. P. Schmid, E. Johnson and S. E. Malawista.** 1983. The spirochetal etiology of Lyme disease. N Engl J Med **308**: 733-740.

92. **Steere, A. C., S. E. Malawista, D. R. Snydman, R. E. Shope, W. A. Andiman, M. R. Ross and F. M. Steele.** 1977. Lyme arthritis: an epidemic of oligoarticular arthritis in children and adults in three Connecticut communities. Arthritis Rheum **20**: 7-17.

93. **Stewart, P. E., R. Thalken, J. L. Bono and P. Rosa.** 2001. Isolation of a circular plasmid region sufficient for autonomous replication and transformation of infectious *Borrelia burgdorferi*. Mol Microbiol **39**: 714-721.

94. **Stock, A. M., V. L. Robinson and P. N. Goudreau.** 2000. Two-component signal transduction. Annu Rev Biochem **69**: 183-215.

95. **Sudarsan, N., E. R. Lee, Z. Weinberg, R. H. Moy, J. N. Kim, K. H. Link and R. R. Breaker.** 2008. Riboswitches in eubacteria sense the second messenger cyclic di-GMP. Science **321**(5887): 411-3.

96. **Sultan, S. Z., J. E. Pitzer, T. Boquoi, G. Hobbs, M. R. Miller and M. A. Motaleb.** 2011. Analysis of the HD-GYP Domain Cyclic Dimeric GMP Phosphodiesterase Reveals a Role in Motility and the Enzootic Life Cycle of *Borrelia burgdorferi*. Infect Immun **79**(8): 3273-83.

97. **Sultan, S. Z., J. E. Pitzer, M. R. Miller and M. A. Motaleb.** 2010. Analysis of a *Borrelia burgdorferi* phosphodiesterase demonstrates a role for cyclic-di-guanosine monophosphate in motility and virulence. Mol Microbiol **77**(1): 128-42.

98. **Tamayo, R., J. T. Pratt and A. Camilli.** 2007. Roles of cyclic diguanylate in the regulation of bacterial pathogenesis. Annu Rev Microbiol **61**: 131-48.

99. **Tamayo, R., A. D. Tischler and A. Camilli.** 2005. The EAL domain protein VieA is a cyclic diguanylate phosphodiesterase. J Biol Chem **280**(39): 33324-30.

100. **Thomas, C., C. R. Andersson, S. R. Canales and S. S. Golden.** 2004. PsfR, a factor that stimulates psbAI expression in the cyanobacterium S*ynechococcus elongatus* PCC 7942. Microbiology **150**(Pt 4): 1031-40.

101. **Tischler, A. D. and A. Camilli.** 2004. Cyclic diguanylate (c-di-GMP) regulates *Vibrio cholerae* biofilm formation. Mol Microbiol **53**(3): 857-69.

102. **Tischler, A. D. and A. Camilli.** 2005. Cyclic diguanylate regulates *Vibrio cholerae* virulence gene expression. Infect Immun **73**(9): 5873-82.

103. **Tuckerman, J. R., G. Gonzalez and M. A. Gilles-Gonzalez.** 2011. Cyclic di-GMP activation of signal-dependent RNA processing. J Mol Biol **407**: 633-9.

104. **Wolfe, A. J. and K. L. Visick.** 2008. Get the message out: cyclic-Di-GMP regulates multiple levels of flagellum-based motility. J Bacteriol **190**(2): 463-75.

105. **Xu, H., M. J. Caimano, T. Lin, M. He, J. D. Radolf, S. J. Norris, F. Gheradini, A. J. Wolfe and X. F. Yang.** 2010. Role of acetyl-phosphate in activation of the Rrp2-RpoN-RpoS pathway in *Borrelia burgdorferi*. PLoS Pathog **6**(9).

106. **Yamamoto, K., K. Hirao, T. Oshima, H. Aiba, R. Utsumi and A. Ishihama.** 2005. Functional characterization in vitro of all two-component signal transduction systems from *Escherichia coli*. J Biol Chem **280**(2): 1448-1456.

107. **Yang, X. F., S. M. Alani and M. V. Norgard.** 2003. The response regulator Rrp2 is essential for the expression of major membrane lipoproteins in *Borrelia burgdorferi*. Proc Natl Acad Sci USA **100**: 11001-11006.

108. **Yound, J. D.** 1998. Underreporting of Lyme disease. N Engl J Med **338**: 1629.

109. **Zahler, M., R. Gothe and H. Rinder.** 1995. Diagnostic DNA amplification from individual tick eggs, larvae and nymphs. Exp Appl Acarol **19**(12): 731-6.

110. **Zhu, Z., L. Gern and A. Aeschlimann.** 1991. The peritrophic membrane of *Ixodes ricinus*. Parasitol Res **77**(7): 635-41.

APPENDIX A

Oligonucleotides used in this study.

Oligonucleotide	Sequence (5'➡3')
General primers	
KOverifyUp F (1)	CTTTAATGGGGCTTGGTATATGC
KOverifyDwn R (2)	GTTGATGCATCTGTTAAAATTG
Aad1-5'-R (3)	TCCTTGAAGCTCGGGTATTA
pKFSS1-3'F (4)	GGCGAGATCACCAAGGTAGTC
Kan-5'-R (5)	CAGCATCCATGTTGGAATTTAATCGC
Kan-3'-F (6)	GATATGAATAAATTGCAGTTTCATTTG
Kan pBSV2 F (7)	GCGATTAAATTCCAACATGGATGCTG
Kan pBSV2 R (8)	ACTCATCGAGCATCAAATGAAACTGC
FlaB F	CAGGTAACGGCACATATTCAGATGC
FlaB R	CTTGGTTTGCTCCAACATGAACTC
BB0419F_LIC	GACGACGACAAGATGGAAATGATAATTAAAGATAAAGC
BB0419R_LIC	GAGGAGAAGCCCGGTTTAATATCTAAACTGATTTCTTCCAG
BB0733F_LIC	GACGACGACAAGATTTTGTTTAGTATTTTTATATTCAAAAAAA GGAGAAAG
BB0733R_LIC	GAGGAGAAGCCCGGTTTAATTGAAATAATCATGGATCAACAT AGATAC
BB0733 KO >1kb upstr F (9)	GCTATCATTGCTCCTTCAGGCTGTGC
BB0733 KO >1kb downstr R (10)	CCTTTAATAGTACATGTTGATACGG
BB0374 F	AATTAGCTCTATTTCATTTTG
BB0374 R	ATGCAAAATTCTGAAAGCATTA
BB0374 KO >1kb upstr F (11)	GGACTAATGTCTTTATTCGCCCATGT
BB0374 KO >1kb downstr (12)	CCAAATATTATTCCCTGATCCCCTGCT
B31-*rrp1* KI construction	
BB0419F-1kb-upstr	GCCCATTAATGTTTTAATAGCTGA

Rev_419+AatII+AscI	GGCGCGCCTAGGACGTCTTAATATCTAAACTGATTTCTTCCAGAAAC
Fwd_KanR+1kbDNST419	GAGTTTTTCTAAATTTATATTTAATAGACTTTAGTATTTATAAGTTATAGACATTCC
Rev_1kbDNST419+AscI	GGCGCGCCCTTTCCCAAGATCAACAGAACTTAG
Fwd_KanR+AatII	GACGTCCTTTAATAAAACAATATGTTGCGATGATTAAGG
Rev_KanR+1kbDNST419	CTTATAAATACTAAAGTCTATTAAATATAAATTTAGAAAAACTCATCGAGCATCAAATG
B31-*rrp1* OV construction	
pFlaB+BamHI F	GTGGATCCTGAACTTAATACCTTGG
pFlaB+ClaI+SalI R	GTCGACATAATCGATTCCTCCATGATAAAATTTAAATTTC
419+ClaI F	ATCGATAATGATAATTAAAGATAAAGCTTTTG
419+SalI R	GTCGACCGCTTAATATCTAAACTGATTTCTTCC
B31-Δ*plzA* construction	
BB0733KO-UP F	CATTTGATACAACTTGGTTTAAAACTG
BB0733KO-UP R	ACCGGTCTAGACGTCAGCTTCAAATTGTTTTAAACAGTTTTAC
BB0733KO-DN F	GACGTCTCAAAGGATTGAAATTTTTCTTATGTGATTATG
BB0733KO-DN R	ACCGGTCAGAATATATTCCCAAAAGTGCCC
Spec/strep F	TGATTTGCTGGTTACGGTGA
Spec/strep R	ATTTGCCGACTACCTTGGTG
B31-*plzA* KI construction	
BB0733 KI F	GACGTCTTGTTTAGTATTTTTATATTCAAAAAAAGGAGAAAG
BB0733 KI R	CCTTGAAGCTCGGGTATTAGTTAATTGAAATAATCATGGATCAACATAGTATAC
PflgB-aphI-t7 (BB0733) KI F	GTATACTATGTTTAGCCATGATTATTTCAATTAACTAATACCCGAGCTTCAAGG
PflgB-aphI-T7 KI R	GACGTCCAGATCCGGATATAGTTCCTCCTTTC
B31-Δ*plzA::plzB* construction	
PlzB KI-UP F	CATTTGATACAACTTGGTTTAAAACTG
PlzB KI-UP R	TATCACACCGGTGACGTCAAACCTCTCCTTTCTCCTTTTTTTG
PlzB KI F	GACGTCATGGCAGTATCATCTAAAAAGATAAGAGAG
PlzB KI R	CTTCCTTGAAGCTCGGGTAGTCAGTCTTCAAAAAAATTAAAATAATTATG

Kan KI F	TATCACCCCGGGCTAATACCCGAGCTTCAAGGAAGA
Kan KI R	TATCACGACGTCTTAGAAAAACTCATCGAGCATCAAATGAAA C
B31-Δ*pdeB* construction	
BB0374KO-UP	CCGCAAGACTTTGCAAAAAAATAATTAAAC
BB0374KO-UP R	ACCGGTCTAGACGTCTTATTCCCTTGAAATTAAGCTCTATTA AC
BB0374KO-DN F	GACGTCAGACACTTAAAAGGAGAAAAAATATGATTTTG
BB0374KO-DN R	ACCGGTGTTATTGTTTTGTAATCAAGCCCATAATC
Spec/strep F	TGATTTGCTGGTTACGGTGA
Spec/strep R	ATTTGCCGACTACCTTGGTG
B31-*pdeB* KI construction	
BB0374 KI F	GACGTCATGAAAAATCCAAATGCAATTG
BB0374 KI R	GATTTTACATCAGTTTGATTTATAAGATCAACGCTAGCTTAAA TAGGTTCTGGTTTATGC
PflgB-Kan(BB0374) KI Fwd	GAAATAGAGCTAATTAAAAATAAATATTCTTTAATAGATATTA TATAACTAATACCCGAGCTTCAAGG
PflgB-aphI-T7 KI R	GACGTCCAGATCCGGATATAGTTCCTCCTTTC
Tick qPCR	
FlaB BB0147F-RT	CAGGTAACGGCACATATTCAGATGC
FlaB BB0147R-RT	CTTGGTTTGCTCCAACATGAACTC
Tick RIB-3 (ITS2)	CGGGATCCTTC(A,G)CTCGCCG(C,T)TACT
Tick RIB-4 (ITS2)	CCATCGATGTGAA(C,T)TGCAGGACA
RT-PCR	
Rrp1 BB0419F-RT	TTGAGGTTGCAACAAATGGA
Rrp1 BB0419R-RT	CGGGATCGCTTTTTAGCTTT
Eno BB0337F-RT	GCTTGAACTTGATGGCACCCCTAC
Eno BB0337R-RT	GTACGCTCCAAGATATTGATAAGG
BB0002F-RT	GCGGAGCAGACAAAGGGATTGATT
BB0002R-RT	ACATGCTCCATGGCCGGAAA
NagA BB0151F-RT	GCAGCTGGTGGAGTATTTACAGGA
NagA BB0151R-RT	GTGTGTCCCGCTTGAAGGTTTATG
NagB BB0152F-RT	GGGCGGCTAATCATGTAGCACAAA
NagB BB0152R-RT	CAATCGGAGAGCTTCCTGTTGGA

PtsG BB0645F-RT	AGAACTTGCTGCCCAAGGTACAGA
PtsG BB0645R-RT	CCGGGCAAACCAAACATCATGGTA
FliD BB0149F-RT	GTCAGGAAATTCTAGTAATAGCGAAG
FliD BB0149R-RT	CTTTCTTGCCAACTAAAAATATATAATCTCC
put fla BB0180F-RT	GAAATAGGACTTAAAGAGGTCGC
put fla BB0180R-RT	CCAATTTTCAATTTGTGTAGATAGTCG
FlgL BB0182F-RT	GAGCAAGCGGAACTTATGAATC
FlgL BB0182R-RT	CGCACCGTCTTTGCTTGTTTTGC
FliG-1 BB0221F-RT	GCAAAGAGAGTAAGGTCACAAAG
FliG-1 BB0221R-RT	CTTAGTAACTCTTCAAATTCTTTAATAATATGC
FlgD BB0284F-RT	GGTTAATCTTGGCAAGGATG
FlgD BB0284R-RT	GATGAAAGTTTTTCAAACGATCTACTC
FliI BB0288F-RT	GGTATGCGCAGAGGTTTTAG
FliI BB0288R-RT	CCTTTATTATCAATAGGTCTGCCAAG
FliF BB0291F-RT	CTTGTCAGAGAAGAGCTTGTG
FliF BB0291R-RT	GGCATAACAAGATTCACACTAACAG
FliE BB0292F-RT	CGATTACTGATGTCAACAAAAGCC
FliE BB0292R-RT	CTTGATAAGCCTTCACACCTC
FlgB BB0294F-RT	CTTAATTAAATCTAGTGATAAGCACCTG
FlgB BB0294R-RT	GTTTTGCACAAGTGCCTTAAC
CheW-2 BB0565F-RT	GTCAGTATCTTTTATTTAGTTTGGACG
CheW-2 BB0565R-RT	GAATATCAATTATTGGAACGATTTTGCC
CheA1 BB0567F-RT	GAGAGCTTATTGAAGGCGATGAAG
CheA1 BB0567R-RT	CTTTAACAGACTCTTCCAAAACCGAAC
CheY2 BB0570F-RT	GGAGTCTCAGAAGCAAAAGATGG
CheY2 BB0570R-RT	GATTGCTCAGATTCAGTGGTAAGAAC
Mcp-2 BB0596F-RT	CGACTAGGTACGACTATCGGTC
Mcp-2 BB0596R-RT	GCCCAATAGCAATTCTTTTAAACTTATG
Mcp-3 BB0597F-RT	GAGATAGCTATAGGTTTGGGATATTG
Mcp-3 BB0597R-RT	CCTTCAAGTGAATCTTCTGCTAAAG
CheX BB0671F-RT	CGGGCTTAAGTCGATAAATCAAAAG
CheX BB0671R-RT	CAGCAACCATCTCTTTTGTTTCTTC
CheY3 BB0672F-RT	GTTGATGACTCTGTTTTTACCGTAAAG
CheY3 BB0672R-RT	GACAAGTTATTCCATCCATTTTGG
Mcp-4 BB0680F-RT	GCTGTTGAGGATTATAGGCAAAAC

Mcp-4 BB0680R-RT	GCAAATATCCGGCCAAATACC
Mcp-5 BB0681F-RT	CTACGGCGGTTAAGGATAATAGTG
Mcp-5 BB0681R-RT	GGCATACCTATTAATATGTAAGGAATCTG
PlzA BB0733F-RT	CTGATAAAGCTTTTATCAAGTTTAATGGAG
PlzA BB0733R-RT	AGCGCAAAAACCTTTCCGCT
PlzB BBU_ZS7F20F-RT	TAGTATACTCAAGCGGGATATTACTC
PlzB BBU_ZS7F20R-RT	GGAATCCTTGATGAAGACATGG
PdeB BB0374F-RT	ATCTAGACGGAACTGGCTATCCT
PdeB BB0374R-RT	ATAGCAGAATAGGCACTAGCAGCG
pMAL-c4x constructs	
BB0419pMAL-BamHIF	CGGATCCGTGGAAATGATAATTAAAGATAAA
BB0419pMAL-SalIR	CCCGTCGACTTAATATCTAAACTGATTTCTTCC
BB0733pMAL-BamHIF	GGATCCTTGTTTAGTATTTTTATATTCAAAAAAAGGAGAAAG GAGAGGT
BB0733pMAL-SalIR	GTCGACTTAATTGAAATAATCATGGATCAACATAGTATACTC AAGTGGTA
PlzB pMAL-BamHIF	GGATCCATGGCAGTATCATCTAAAAAGATAAGAGAGTATAGA AA
PlzB pMAL-SalIR	GTCGACTCAGTCTTCAAAAAAATTAAAATAATTATGGATTATC ATAGTATACTCAA
WspR pTYB12 vector	
WspRpTyb12-BsmIF	GAATGCTATGCACAACCCTCATGAGAGCAAG
WspRpTyb12-EcoRIR	GAATTCTCAGCCCGCCGGGGCCGG

VITA

Jessica Lynn Kostick was born September 26, 1983 in Allentown, PA. She was raised in Emmaus, Pennsylvania and graduate from Emmaus High School in 2002. During the summer of 2005, she served as an Undergraduate Cancer Biology Fellow at Wayne State University Medical School located in Detroit, MI. Her fellowship work was entitled "p53, p16, and Rb inactivation combined with K-ras mutation promotes pancreatic tumor cell growth". In May of 2006, she received her Bachelor of Arts in Biological Sciences and Minor in Philosophy from the University of Delaware. A brief list of accomplishments performed during her graduate career is listed below.

Publications

Kostick, J.L, Szkotnicki, L.T., Rogers, E.A., Bocci, P., Raffaelli, N., and Marconi, R.T. The diguanylate cyclase, Rrp1, regulates critical steps in the enzootic cycle of the Lyme disease spirochetes. Mol Microbiol. 2011 July: 81(1):219-31.

Freedman, J.C., Rogers, E.A., **Kostick, J.L.,** Zhang, H., Iyer, R., Schwartz, I., and Marconi, R.T. Identification and molecular characterization of a cyclic-di-GMP effector protein, PlzA (BB0733): additional evidence for the existence of a functional cyclic-di-GMP regulatory network in the Lyme disease spirochete, *Borrelia burgdorferi*. FEMS Immunol Med Microbiol. 2010 Mar: 58(2):285-94.

Manuscripts in preparation and review

Kostick, J.L., Freedman, J.C., Szkotnicki, L.T., and Marconi, R.T. The c-di-GMP binding protein, PlzB, does not functionally complement the role of PlzA in the enzootic cycle of the Lyme disease spirochete, *Borrelia burgdorferi*.

Szkotnicki, L.T., **Kostick, J.L.**, Freedman, J.C, Bocci, P., Raffaelli, N., and Marconi, R.T. Metabolism of the second messenger, c-di-GMP, plays an integral role in virulence of the tick-borne relapsing fever spirochaete *Borrelia hermsii.*

Abstracts

Kostick, J.L. and Marconi, R.T. 2011. C-di-GMP regulates critical steps in the enzootic cycle of Lyme disease. Presentation to the 2011 IHII/McLaughlin Colloquium, Galveston, TX.

Kostick, J.L., Szkotnicki, L., Rogers, E.A., and Marconi, R.T. 2011. The *Borrelia burgdorferi* diguanylate cyclase, Rrp1, controls important steps in the enzootic cycle of Lyme disease spirochetes. Poster. Presentation to the Bacterial Locomotion & Signal Transduction XI Conference, New Orleans, LA.

Kostick, J.L., Szkotnicki, L., Rogers, E.A., and Marconi, R.T. 2010. The c-di-GMP producing, *Borrelia burgdorferi* response regulator protein 1 controls important steps in the enzootic cycle of the Lyme disease spirochetes. Poster. Presentation to the National Institutes of Health Graduate Research Festival, Bethesda, MD.

Kostick, J.L., Rogers, E.A., and Marconi, R.T. 2009. Analysis of the diguanylate cyclase Rrp1 and its role in *Borrelia burgdorferi* pathogenesis. Presentation to the Virginia Branch of the American Society for Microbiology Meeting, Richmond, VA.

Kostick, J.L., Rogers, E.A., and Marconi, R.T. 2009. Generation of a Pathogenic *Borrelia burgdorferi* Rrp1 Deletion Mutant. Poster. Presentation to the Summit on Systems Biology, Richmond, VA.

Kostick, J.L., Rogers, E.A., and Marconi, R.T. 2009. Generation of a Pathogenic *Borrelia burgdorferi* Rrp1 Deletion Mutant. Poster. Presentation to the 26th Annual Daniel T. Watts Research Poster Symposium, Richmond, VA.

Kostick, J.L., and Taylor, S.M. 2008. Poster. Replisome Protein Interactions and Global Methylation Dysregulation in Cancer. Presentation to the 25th Annual Daniel T. Watts Research Poster Symposium, Richmond, VA.